

THE CHEMICAL COMPOSITIONS OF THE 2 NEW HGMN STARS HD 30085 AND HD 30963. COMPARISON TO χ LUPI A, ν CAP AND HD 174567

R. MONIER¹

LESIA, UMR 8109, Observatoire de Paris et Université Pierre et Marie Curie Sorbonne Universités, place J. Janssen, Meudon, France.

E.GRIFFIN²

Dominion Astrophysical Observatory, 5071 West Saanich Road, Victoria, BC, V9E 2E7, Canada

M. GEBRAN³

Department of Physics and Astronomy, Notre Dame University-Louaize, PO Box 72, Zouk Mikael, Lebanon.

T. KILIÇOĞLU⁴

Department of Astronomy and Space Sciences, Faculty of Science, Ankara University, 06100, Turkey.

T.MERLE⁵

Institut d'Astronomie et d'Astrophysique, Université Libre de Bruxelles, CP 226, Boulevard du Triomphe, 1050 Brussels, Belgium

F. ROYER⁶

GEPI, Observatoire de Paris, place J. Janssen, Meudon, France.

ABSTRACT

We report on a detailed abundance study of the fairly bright slow rotators HD 30085 (A0 IV), HD 30963 (B9 III) and HD 174567 (A0 V), hitherto reported as normal stars and the sharp-lined χ Lupi A (B9 IV HgMn). In the spectra of HD 30085, HD 30963, the Hg II line at 3984 Å line is conspicuous and numerous lines of silicon, manganese, chromium, titanium, iron, strontium, yttrium and zirconium appear to be strong absorbers. A comparison of the mean spectra of HD 30085 and HD 30963 with a grid of synthetic spectra for selected unblended lines having reliable updated atomic data reveals large overabundances of phosphorus, titanium, chromium, manganese, strontium, yttrium, and zirconium, barium, platinum and mercury and underabundances of helium, magnesium, scandium, nickel. The surface abundances of χ Lupi A have been rederived on the same effective temperature scale and using the same atomic data for consistency and comparison for HD 30085 and HD 30963. For HD 174567, milder deficiencies and excesses are found. The abundances of sodium, magnesium and calcium have been corrected for NLTE effects. The effective temperatures, surface gravities, low projected rotational velocities and the peculiar abundance patterns of HD 30085 and HD 30963 show that these stars are 2 new HgMn stars and should be reclassified as such. HD 174567 is most likely a new marginally Chemically Peculiar star. A list of the identifications of lines absorbing more than 2 % in the spectrum of HD 30085 is also provided.

Keywords: stars: chemically peculiar — stars: individual (HD 30085, HD 30963, HD 174567)

1. INTRODUCTION

The fairly bright stars HD 30085 (HR 1510, A0 IV, V=6.3), HD 30963 (B9 III, V=7.2) and HD 174567 (HR 7098, A0V, V=6.63) have received little attention: only 30, 10 and 47 references respectively can be found in SIMBAD

for these stars. We have recently undertaken a spectroscopic survey of all apparently slowly rotating bright early A stars (A0-A1V) and late B stars (B8-B9V) observable from the northern hemisphere. This project addresses the fundamental questions of the physics of late-B and early-A stars: i) can we find new instances of rapid rotators seen pole-on (other than Vega) and study their physical properties (gradient of temperature across the disk, limb and gravity darkening), ii) is our census of Chemically Peculiar stars complete up to the magnitude limits we adopted ? If not, what are the physical properties of the newly found CP stars? HD 30085 and HD 174567 pertain to the sample of the 47 apparently slowly rotating A0-A1V stars in the northern hemisphere which satisfy $v_e \sin i \leq 60 \text{ km s}^{-1}$ and $\delta \geq -10^\circ$ analysed by Royer et al. (2014). An abundance analysis of selected lines outside the Balmer lines allowed to sort out these stars into 3 groups: 13 chemically peculiar stars were found (among which 4 are new CPs), 17 superficially normal stars and 17 spectroscopic binaries (Royer et al. 2014). Monier et al. (2015) reported on a first analysis of the abundances of Fe, Mn and Hg and showed that HD 30085, HD 18104, HD 32867 and HD 53588 are four new HgMn stars. Similarly HD 30963 is a slowly rotating B9 star which verifies similar criteria.

In this paper we report on the abundance analysis of 40 chemical elements from high resolution high quality échelle spectra of HD 30085, HD 30963 and HD 174567 in the optical range and one spectrum of the HgMn star χ Lupi A (χ Lupi = HD 141556 is a double-lined spectroscopic binary, we are only interested in the abundances of χ Lupi A, the HgMn star). We compare the elemental abundances we find in these four stars to those derived for ν Cap, a bona-fide normal late B-type star which we have recently analysed (Monier et al. 2018). Using model atmospheres and line synthesis, we derive for the first time the abundances of forty chemical elements in these four stars and find that they depart strongly from solar. The abundances of sodium, magnesium and calcium have been corrected for NLTE effects. The overabundances of Mn, Sr, Y, Zr, Pt and Hg and the underabundances of helium, magnesium, scandium, and nickel lead us to confirm that HD 30085 is indeed a new HgMn star and establish that HD 30963 is a new HgMn star. The superficially normal HD 174567 appears to be a new mild Chemically Peculiar star. We have also reanalysed the cool HgMn star χ Lupi A A on the same temperature scale and using the same atomic data and used it as a comparison star.

The paper is divided into 5 sections. The first section recapitulates what is known of HD 30085, HD 30963, HD 174567 and χ Lupi A, the second section describes new spectroscopic observations of HD 30085, HD 30963, HD 174567 and χ Lupi A. In the third section, we present the derivation of fundamental parameters and the spectral synthesis which we adopted to derive the abundances. In section 4, we discuss the determination of elemental abundances for each star in light of what is known of other HgMn stars. We also provide identifications of lines absorbing more than 2 % of the continuum in HD 30085. In the conclusion, we discuss the chemical peculiarity of the three new Chemically Peculiar stars in the light of what is known of other HgMn stars.

2. RECAP OF PREVIOUS SPECTROSCOPIC WORK ON HD 30085, HD 30963, HD 174567, ν CAP AND χ LUPI A

HD 30085 was ascribed a spectral type A0 IV by Cowley et al. (1969) in their survey of 1700 bright northern B9 to A9 stars with a prismatic dispersion of 125 \AA mm^{-1} around H_γ . At that time, Cowley et al. (1969) did not mention any peculiarity of the spectrum. In his study of helium-weak stars, Molnar (1972) classified HD 30085 as a B9 III from 63 \AA mm^{-1} plates centered on H_γ using slightly different MK criteria to assign the temperature and the luminosity class than Cowley et al. (1969) did. He did not comment on any peculiarity of the lines of Si, Sr and the metals in the spectrum of HD 30085 around H_γ . HD 30085 has been detected as a fairly bright UV source with TD1 (Jamar et al. 1976), its flux steadily rising towards shorter wavelength, suggesting the star is indeed a late B star rather than an early A star. Ramella et al. (1989) report on structures in the core of the Mg II doublet at 4481 \AA from 12.4 \AA mm^{-1} dispersion plates. More recently, Monier et al. (2015) have reported on the presence of the Hg II line at 3984 \AA and several strong Mn II in the high resolution spectra of HD 30085 and provided overabundances for Mn, Fe and Hg only based on the spectrum synthesis of a few lines which clearly established the HgMn nature of this star.

HD 30963 was ascribed a B9 III spectral type by Huang et al. (2010). HD 174567 has been used as a "normal comparison star" by Smith & Dworetsky (1993) in their abundance study of HgMn and superficially normal stars from IUE (International Ultraviolet Explorer) spectra. Their modelling of coadded IUE spectra of HD 174567 revealed abundances which are nearly solar confirming the superficially normal status for this star at that time.

The abundances of 22 elements in the atmosphere of χ Lupi A have been derived from optical spectra by Wahlgren et al. (1994) and they are collected in Table 6. The elemental abundances of ν Cap have been recently derived in Monier et al. (2018) which confirms its nearly solar abundances determined by Adelman (1991).

3. OBSERVATIONS

The high resolution spectra of HD 30085, HD 30963 and HD 174567 have been obtained at Observatoire de Haute Provence with SOPHIE, the échelle spectrograph in its high resolution mode ($R=75000$) yielding a full spectral coverage from 3820 Å to 6930 Å in 39 orders. A detailed technical description of SOPHIE is given in Perruchot et al. (2008). SOPHIE is a cross-dispersed, environmentally stabilized échelle spectrograph dedicated to high precision radial velocity. The spectra are extracted online from the detector images using a specific pipeline adapted from that of HARPS (High Accuracy Radial Velocity Planet Searcher¹). The sequence or reductions starts with the localization of the 39 orders on the 2D images, the optimal extraction of each order, the wavelength calibration and finally the correction for flat-field producing a two dimensional spectrum (e2ds). We have normalised each reduced order separately using a Chebychev polynomial fit with sigma clipping, rejecting points above or below 1σ of the local continuum. Normalized orders were then merged together, corrected by the blaze function and resampled into a constant wavelength step of about 0.02 Å (see Royer et al. 2014, for more details). The observing dates, exposure times and Signal to Noise ratios achieved for each observing run are collected in Table 1. For HD 30085 and HD 30963, the comparison of individual spectra taken at different epochs did not reveal any convincing radial velocity nor residual flux variations in the lines. We therefore coadded the individual orders into merged orders to enhance the signal-to-noise ratio up to 350. Complementary monoorder spectra of HD 30085 have been obtained at Dominion Astrophysical Observatory by EG with a lower resolving power $R=45000$. The three wavelengths intervals observed span from 3874 Å to 4020 Å, from 4038 Å to 4183 Å and from 4430 Å to 4560 Å. The H_ϵ and H_δ regions were observed in order to validate the fundamental parameters derived from the Strömgren's photometry (see section 4.1) and confirm the presence of the Hg II line at 3983.93 Å.

4. MODEL ATMOSPHERE ANALYSIS AND SYNTHETIC SPECTRA COMPUTATION

The abundances of forty chemical elements have been derived by iteratively adjusting synthetic spectra to the normalized spectra and looking for the best fit to carefully selected unblended lines. Specifically, synthetic spectra were computed assuming LTE using Hubeny & Lanz (1992) SYNSPEC49 code which calculates lines for elements up to $Z=99$. For selected lines of Na I, Mg I and Ca II, we have provided Non-LTE abundances.

4.1. Fundamental parameters

The fundamental data for HD 30085, HD 30963, ν Cap, HD 174567, and HD 141556 are collected in Table 2. The spectral type retrieved from SIMBAD appears in column 2 and the apparent magnitudes in column 3, the Strömgren indexes $b - y$, m_1 and c_1 in columns 4, 5, 6. The photometric data was taken from Hauck & Mermilliod (1998). The radial velocity of HD 30085, HD 174567 and ν Cap are those derived in Royer et al. (2014) using cross-correlation techniques, avoiding the Balmer lines and the atmospheric telluric lines. The normalized spectrum was cross-correlated with a synthetic template extracted from the POLLUX database² (Palacios et al. 2010) corresponding to the parameters $T_{\text{eff}} = 11000$ K, $\log g = 4$ and solar abundances. A parabolic fit of the upper part of the resulting cross-correlation function yields the Doppler shift, which is then used to shift spectra to rest wavelengths. The projected rotational velocities were derived from the position of the first zero of the Fourier transform of individual lines, they are taken from Royer et al. (2014). The radial velocity and projected equatorial velocity of HD 30085, HD 30963, ν Cap, HD 174567 and HD 141556 are collected in Table 2.

For the five stars, the effective temperature (T_{eff}) and surface gravity ($\log g$) were determined using the UVBY-BETA code developed by Napiwotzki et al. (1993) and appear in columns 7 and 8. This code is based on the Moon & Dworetsky (1985) grid, which calibrates the $uvby\beta$ photometry in terms of T_{eff} and $\log g$. The estimated errors on T_{eff} and $\log g$, are ± 125 K and ± 0.20 dex, respectively (see Sec. 4.2 in Napiwotzki et al. 1993).

4.1.1. Microturbulent velocity determinations

In order to derive the microturbulent velocity of HD 30085, HD 30963 and HD 174567, we have simultaneously derived the iron abundance [Fe/H] for fifty unblended Fe II lines and a set of microturbulent velocities ranging from 0.0 to 2.0 km s⁻¹. Figure 1 shows the standard deviation of the derived [Fe/H] as a function of the microturbulent velocity. The adopted microturbulent velocities are the values which minimize the standard deviations ie. for that value, all Fe II lines yield the same iron abundance. The microturbulent velocities of the three stars are collected in Table 2.

¹ <https://www.eso.org/sci/facilities/lasilla/instruments/harps.html>

² <http://pollux.graal.univ-montp2.fr>

Table 1. Log of the observed and archival spectra

Star ID	Date	instrument	R	Barycentric Julian Date	duration (s)	S/N
HD 30085	13/02/2012	SOPHIE	75000	2455971.36664683	800	216
HD 30085	10/12/2013	SOPHIE	75000	2456637.61970650	1200	269
HD 30085	07/02/2013	DAO	45000	2456331.255	3600	220
HD 30085	02/03/2013	DAO	45000	2456354.176	3600	220
HD 30085	03/03/2013	DAO	45000	2456355.136	3600	220
HD 30085	18/08/2015	DAO	45000	2457253.503	2500	250
HD 30085	19/08/2015	DAO	45000	2457254.507	2400	250
HD 30085	10/09/2015	DAO	45000	2457276.500	2100	240
HD 30085	11/09/2015	DAO	45000	2457277.478	3600	220
HD 30085	12/09/2015	DAO	45000	2457278.435	2700	250
HD 30085	21/10/2015	DAO	45000	2457317.459	2700	250
HD 30085	24/11/2015	DAO	45000	2457351.233	3600	220
HD 30085	24/11/2015	DAO	45000	2457351.261	1200	240
HD 30085	24/11/2015	DAO	45000	2457351.506	1800	240
HD 30085	24/11/2015	DAO	45000	2457351.527	1800	240
HD 30085	25/11/2015	DAO	45000	2457352.274	3600	220
HD 30085	25/11/2015	DAO	45000	2457352.501	3600	220
HD 30085	26/11/2015	DAO	45000	2457353.222	3600	220
HD 30085	26/11/2015	DAO	45000	2457353.476	3600	220
HD 30085	27/11/2015	DAO	45000	2457354.225	3600	220
HD 30085	25/12/2015	DAO	45000	2457382.278	3600	220
HD 30085	30/12/2015	DAO	45000	2457387.317	3600	220
HD 30085	31/12/2015	DAO	45000	2457388.274	3600	220
HD 30085	01/01/2016	DAO	45000	2457389.247	3600	220
HD 30085	23/01/2016	DAO	45000	2457411.159	3600	220
HD 30963	28/11/2015	SOPHIE	75000	2457354.49106071	2400	118
HD 30963	28/11/2015	SOPHIE	75000	2457355.48326524	1800	78
HD 30963	30/11/2015	SOPHIE	75000	2457356.51212353	1800	140
HD 30963	30/11/2015	SOPHIE	75000	2457357.46945236	1800	101
HD 30963	01/12/2015	SOPHIE	75000	2457358.43199975	1680	167
HD 30963	13/12/2016	SOPHIE	75000	2457736.46584169	900	129
HD 30963	13/12/2016	SOPHIE	75000	2457736.49875775	900	123
HD 30963	14/12/2016	SOPHIE	75000	2457737.44071886	1800	165
HD 174567	05/08/2009	SOPHIE	75000	2455049.36018803	1200	224
HD 141556	04/02/2013	FEROS	48000	2456327.37979	50	325

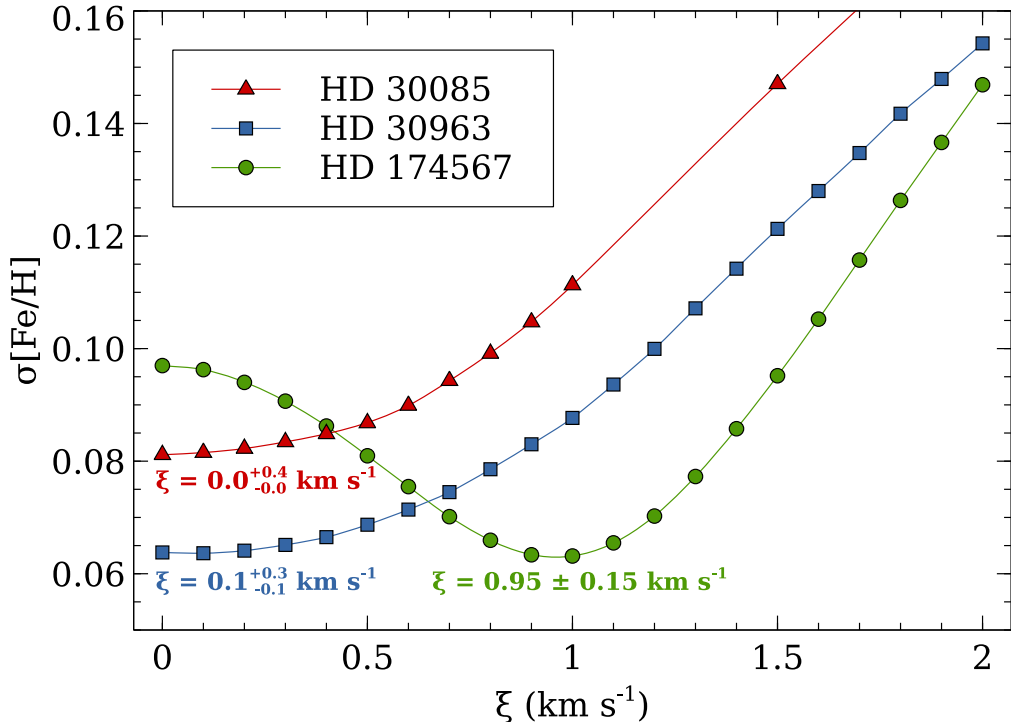
4.1.2. Location of the five stars in a log g ,log T_{eff} diagram

The locations of HD 30085, HD 30963, HD 174567, ν Cap, and χ Lupi in a theoretical gravity-temperature (log g , log T_{eff}) diagram are shown in Figure 2. Evolutionary tracks and isochrones from Bressan et al. (2012)³ are displayed for masses from 2.4 to $3.6 M_{\odot}$ with a step of $0.4 M_{\odot}$ and for $\log t$ (where t is in years) of 8.25 , 8.35 , 8.40 , 8.45 , and 8.50 . The evolutionary tracks are computed for a solar initial metallicity $Z=0.017$ including microscopic diffusion. The isochrones are retrieved for the current solar composition $Z=0.0152$. From this diagram, we have estimated masses, ages and fractional lifetimes on the Main Sequence which are collected in the last three rows of Table 2.

³ <http://stev.oapd.inaf.it/cgi-bin/cmd>

Table 2. Adopted fundamental parameters for HD 30085, HD 30963, ν Cap, HD 174567 and HD 141556

	HD 30085	HD 30963	ν Cap	HD 174567	HD 141556
Sp.T.	A0 IV	B9 III	B9 IV	A0 V	B9 IV
V	6.37	7.20	4.76	6.63	3.95
$b - y$	-0.038	-0.021	-0.021	0.008	-0.020
m_1	0.135	0.134	0.134	0.123	0.129
c_1	0.849	1.015	1.015	1.083	0.948
T_{eff} [K]	11300 ± 200	11476 ± 200	10300 ± 200	10200 ± 200	10608 ± 200
$\log g$ (cgs)	3.95 ± 0.20	3.66 ± 0.20	3.90 ± 0.20	3.55 ± 0.20	3.98 ± 0.20
$v_e \sin i$ [km s^{-1}]	26.0	37.0	24.0	10.5	2.0
$v_{\text{micr.}}$ [km s^{-1}]	$0.0^{+0.4}_{-0.0}$	$0.1^{+0.3}_{-0.1}$	0.50	0.95 ± 0.15	0.10
v_{rad} [km s^{-1}]	8.27	3.52	-11.39	-10.84	15.30
M [M_{\odot}]	3.1 ± 0.4	3.7 ± 0.4	2.8 ± 0.3	3.4 ± 0.4	2.8 ± 0.3
$\log t$ (t in yr.)	8.35 ± 0.05	8.27 ± 0.07	8.50 ± 0.06	8.37 ± 0.15	8.46 ± 0.10
t_{MS} (%)	64	85	69	86	63

**Figure 1.** Microturbulent velocity determinations for HD 30085, HD 30963 and HD 174567

4.2. Model atmospheres

The ATLAS9 code (Kurucz 1992) was used to compute a first model atmosphere for the effective temperature and surface gravity of each star assuming a plane parallel geometry, a gas in hydrostatic and radiative equilibrium and local thermodynamical equilibrium. The ATLAS9 model atmosphere contains 72 layers with a regular increase in $\log \tau_{Ross} = 0.125$ and was calculated assuming a solar chemical composition (Grevesse & Sauval 1998). It was converged up to $\log \tau = -5.00$ in order to attempt reproduce the cores of the Balmer lines. This ATLAS9 version uses the new opacity distribution function (ODF) of Castelli & Kurucz (2003) computed for that solar chemical composition. Once a first set of elemental abundances was derived using the ATLAS9 model atmosphere, the atmospheric structure

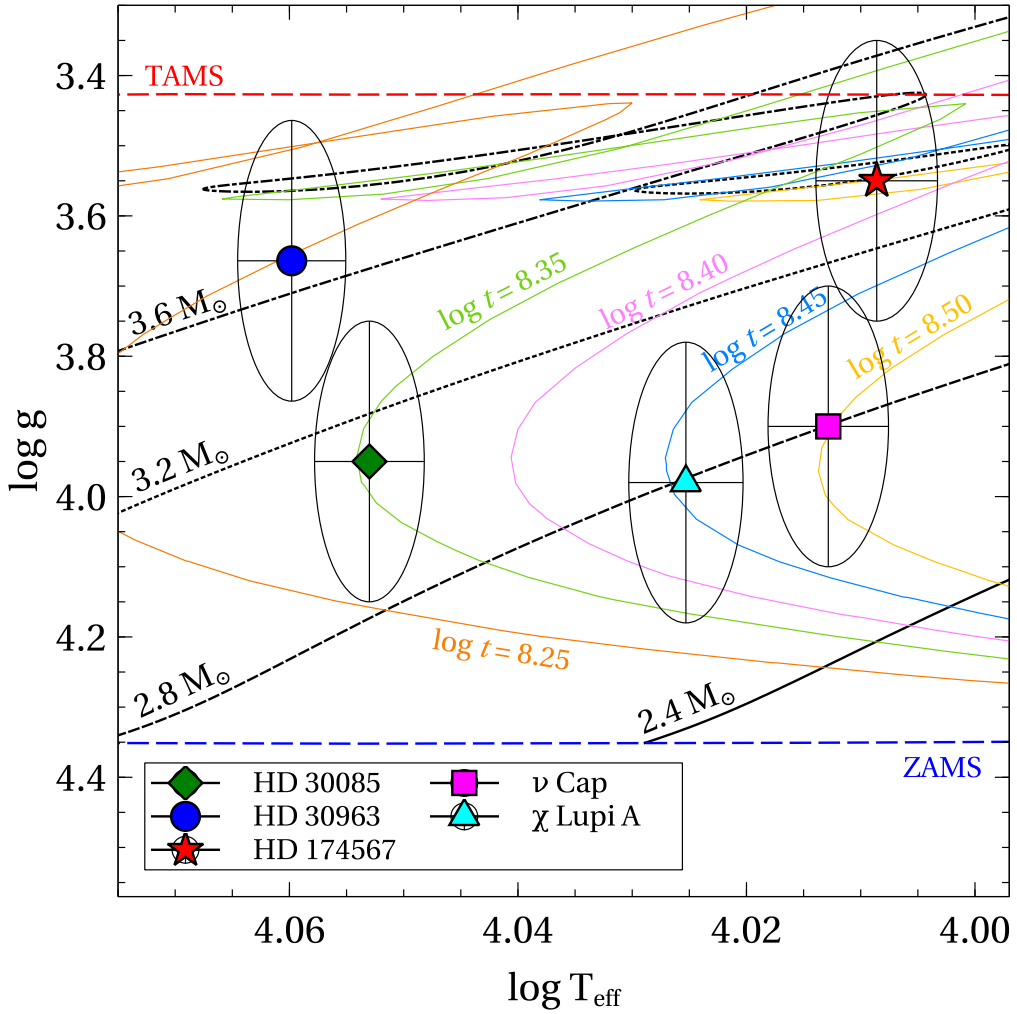


Figure 2. Location of HD 30085, HD 30963, χ Lupi A, ν Cap and HD 174567 in a gravity-temperature diagram.

was recomputed for these abundances using the Opacity sampling ATLAS12 code (Kurucz 2005, 2013). New slightly different abundances were then derived and a new ATLAS12 model recomputed until the abundances of iteration (n-1) differed of those of iteration (n) by less than ± 0.10 dex.

4.3. The linelist

Atomic linelists from Kurucz's database have provided the basis to construct our linelist⁴. These lists collect data mostly from the literature for light and heavy elements (usually critically evaluated transition probabilities from Martin et al. (1988) and Fuhr et al. (1988)) and computed data by Kurucz (1992) for the iron group elements. A first linelist was built from Kurucz's gfall21oct16.dat⁵ which includes hyperfine splitting levels. We then updated several oscillator strengths and damping parameters with more recent and accurate determinations when necessary. As a rule, we have preferred NIST⁶ and Wiese et al. (1996) oscillator strengths for CNO and also Nilsson et al. (2006). The H I lines are calculated using Vidal et al. (1973) tables upgraded by Schoening & Butler up to H 10. The He I lines are computed in SYNSPEC49 by using specific tables, either from Shamey (1969) or Dimitrijevic & Sahal-Brechot (1984).

We introduced hyperfine components for a few lines of Mn II (Holt et al. 1999), isotopic and hyperfine transitions for a few lines of Ga II (Nielsen et al. 2000a). To model the Hg II line at 3983.93 Å, we have included 9 hyperfine transitions from the various isotopes from Hg¹⁹⁶ up to Hg²⁰⁴ from Dolk et al. (2003).

⁴ <http://kurucz.harvard.edu/linelists/>

⁵ <http://kurucz.harvard.edu/linelists/gfnew/gfall21oct16.dat>

⁶ <http://physics.nist.gov/cgi-bin/AtData/linesform>

For the Rare Earths, we retrieved all relevant transitions from the DREAM database⁷. We also used specific publications reporting on laboratory measurements: Sm II (Lawler et al. 2006), Nd II (Den Hartog et al. 2003), Eu II (Lawler et al. 2001b), Tb II (Lawler et al. 2001a). In Kurucz's linelists, the damping constants are taken from the literature when available. For the iron group elements, they come from Kurucz's (1992) computations. Additional damping constants for a few Si II lines were taken from Lanz et al. (1988). When they are not available from the linelist, damping constants are actually computed in SYNSPEC49 using an approximate formula (Kurucz & Avrett 1981).

4.4. Spectrum synthesis

We have used only unblended lines to derive the abundances. For a given element, the final abundance is a weighted mean of the abundances derived for each transition (the weights are derived from the NIST grade assigned to that particular transition). For several elements, in particular the heaviest elements, only one unblended line was available and the abundance should be regarded as uncertain. For each modeled transition, the adopted abundance is that which provides the best fit calculated with SYNSPEC49 to the observed normalized profile. A grid of synthetic spectra was computed with SYNSPEC49 (Hubeny & Lanz 1992) to model each selected unblended line of the forty elements for the four stars. Computations were iterated varying the unknown abundance until minimization of the chi-square between the observed and synthetic spectrum was achieved. For HD 30085, the final synthetic spectrum has allowed the identification of most observed lines. The identifications of lines absorbing more than 2% of the continuum are collected in Table 10.

5. ABUNDANCE DETERMINATIONS

We discuss here the identifications of chemical elements, the lines selected for abundance determinations and the abundance determinations for each element. The abundances derived for each transition and the final abundances⁸ are collected with their errors in Table 8. We also provide non-LTE abundance corrections for three light elements, namely Na I, Mg I and Ca II. We use the Formato code (Merle et al., in prep.) to build simple model atoms, using atomic data from NIST (Kramida et al. 2018) for energy levels, from VALD (Ryabchikova et al. 2015) for radiative bound-bound transitions and from TOPbase (Cunto & Mendoza 1992) for radiative bound-free transitions. For inelastic collisions with electrons, we use the semi-empirical formula from Seaton (1962) for which a radiative counterpart exist and a collision strength of one for transitions with a forbidden radiative counterpart. For inelastic collisions with hydrogen, we use the formula from Drawin (1969) without scaling factor, excepted for Mg I where we implemented the mechanical quantum data from Guitou et al. (2015). The statistical equilibrium and the radiative transfer equation for each level and line in each model atom are consistently solved using the non-LTE 1D radiative transfer code MULTI (Carlsson 1986, 1992).

5.1. Helium

The strongest helium lines unambiguously detected are: λ 4026.19 Å, λ 4471.48 Å, λ 5875.621 Å. The others are either weak or embedded into blends. The least blended, λ 4471.48 Å, has been synthesized to derive the helium LTE abundance. Helium is underabundant in all stars, the deficiency is more important in the three HgMn stars. Figure 3 displays the best fit achieved to model the He I line at 4471.480 Å for HD 30085.

5.2. The light elements (C to Ti)

5.2.1. Carbon

Most of the expected C II lines are blended with more abundant species. The least blended is the high excitation C II triplet at 4267.26 Å which coincides with a 5 % line at 4267.18 Å in HD 30085 for instance. Carbon is underabundant in HD 30085, HD 174567 and χ Lupi A but solar in HD 30963. Sakhibullin (1987) has shown that the C II line at 4267.26 Å is prone to NLTE effects for B stars hotter than 15000 K. He suggests to use the C II lines at 3919 and 3921 Å less influenced by departures from LTE to derive carbon abundances. These lines yield the same carbon abundances.

5.2.2. Oxygen

For O I, the strongest expected allowed lines are those of multiplet 7 (NIST quality B+). The nine transitions of multiplet 7 dominate the opacity from 6155 Å to 6159 Å. Other lines of O I are blended with lines of iron-peak elements

⁷ <http://www.umh.ac.be/astro/dream.shtml>

⁸ We here refer to the absolute abundance in the star: $\log_{10} \left(\frac{X}{H} \right)_*$, where $\log_{10} (H) = 12.0$

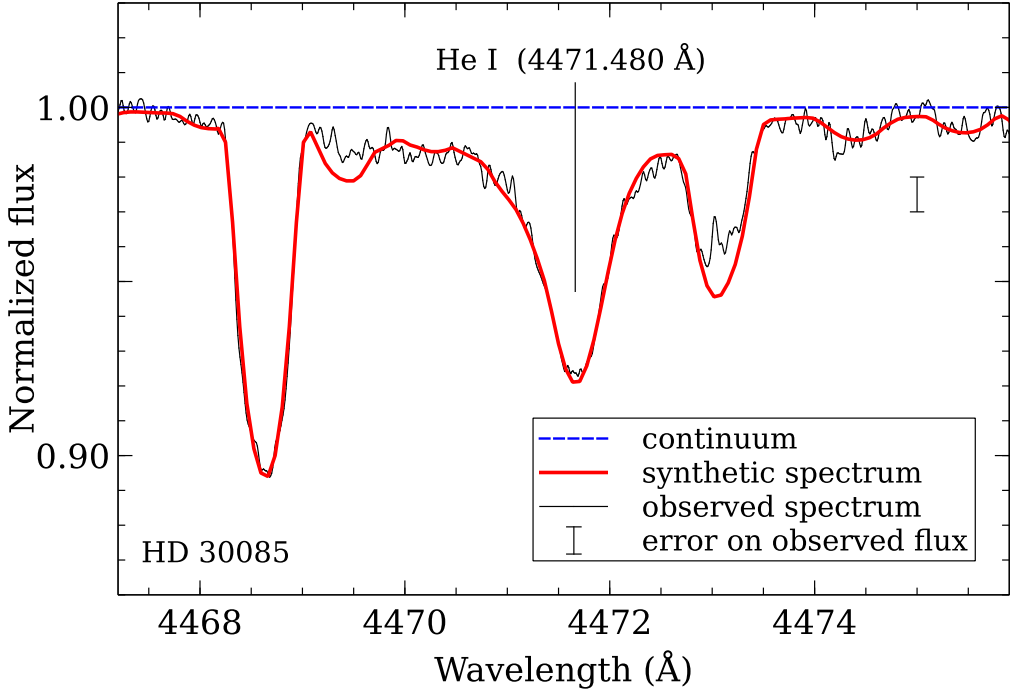


Figure 3. Synthesis of the He I line at 4471.480 Å for HD 30085.

and were therefore discarded to derive the oxygen abundance. Oxygen is underabundant in HD 30085 and χ Lupi A, solar in HD 30963 and slightly overabundant in HD 174567.

5.2.3. Sodium

We have used the 2 Na I lines at 4497.66 Å (NIST quality B+) and the resonance Na I lines at 5889.95 and 5895.92 Å (quality AA). The LTE overabundances of sodium derived from these lines are -4.97 for HD 30085 and -5.67 (ie. solar) upper limit for HD 30963 and HD 174567. The NLTE corrections for the resonance Na I lines at 5889.95 and 5895.92 Å are about -0.52 and -0.60 dex respectively which yields Non-LTE abundances of Na of -5.61 in HD 30085 and -6.27 for HD 30963 and HD 174567 and -5.57 for χ Lupi A, well below the LTE determinations. Sodium is underabundant in HD 30963 and HD 174567 and slightly overabundant in HD 30085 and χ Lupi A.

5.2.4. Magnesium

The unblended Mg II lines at 4390.514 Å and 4390.572 Å yield LTE abundances of -4.64, -4.57, -4.42 and -4.46 for HD 30085, HD 30963 and HD 174567 and χ Lupi A respectively. The unblended Mg I line at 5172.68 Å yields similar LTE abundances. We adopt the abundance derived from the unblended Mg I line at 5172.68 Å corrected with the NLTE correction of about -0.33 dex, which yields -4.42, -4.85, -4.59 and -5.02 respectively. Magnesium therefore appears to be underabundant in each star.

5.2.5. Aluminium

The synthesis of the unblended Al II line at 4663.056 Å shows that aluminium is severely depleted in the three Chemically Peculiar stars but not in the superficially normal HD 174567.

5.2.6. Silicon

The synthesis of strong and unblended lines of Si II shows that silicon is slightly overabundant in HD 30085, HD 30963 and HD 174567 and slightly depleted in χ Lupi A.

5.2.7. Phosphorus

The lines of P II expected strongest are λ 6024.18 Å and 6043.12 Å of multiplet 2. Phosphorus is overabundant in the four stars.

5.2.8. Sulfur

The lines of S II at 4162.67 Å, 4142.25 Å and 4153.06 Å of multiplet 4 are clearly present and unblended in the spectra of all stars. Sulfur is solar in HD 30085, overabundant in HD 30963 and χ Lupi A and underabundant in HD 30963.

5.2.9. Calcium

The synthesis of the unblended Ca II lines at 3933.66 Å and 5019.97 Å yields the calcium LTE abundances, respectively -5.64, -5.46, -5.64 and -5.83 in HD 30085, HD 30963, HD 174567 and χ Lupi A. The Non-LTE correction for the 3933.66 Å amounts to +0.37 dex, yielding final overabundances of -5.22 for HD 30085 and HD 174567 and -5.37 for HD 30963 and -5.46 for χ Lupi A respectively. Calcium therefore appears to be overabundant in all four stars.

5.2.10. Scandium

The line of multiplet 1 of Sc II at 4246.820 Å is the only unblended line (quality A' in NIST). Scandium appears to be overabundant in HD 30085, HD 30963 and HD 174567 but underabundant in χ Lupi A

5.2.11. Titanium

We have used ten unblended lines of Ti II listed in Table 8 to derive the mean titanium abundances. Titanium is overabundant in all four stars.

5.3. The iron-peak elements (V to Zn) and gallium

5.3.1. Vanadium

The vanadium abundance has been estimated using three lines of V II at 4005.705 Å, 4023.378 Å and 4036.78 Å. The adjustment of these lines suggests a significant underabundance of vanadium in HD 30085, overabundances for HD 30963 and HD 174567 and a nearly solar abundance for χ Lupi A.

5.3.2. Chromium

Several strong and unblended lines of Cr II could easily be found in the spectra of the four stars. Six unblended lines of Cr II were synthesized and yield chromium overabundances in the four stars. The three resonance lines of Cr I lines at 4245.35, 4274.82 and 4289.73 Å are also present and yield lower overabundances. The next lines of Cr I expected to contribute opacity are those of multiplet 3 but they are all blended. Lines of higher multiplets are expected too faint to be detectable even at an overabundance of -5.43. We have retained the overabundances from Cr II which is the dominant ionisation stage.

5.3.3. Manganese

The lines of Mn II are conspicuous in the spectra of HD 30085 and HD 30963. Two lines have hyperfine structures published by [Holt et al. \(1999\)](#). They yield overabundances in all stars, especially large for HD 30085 and HD 30963. The resonance lines of Mn I at 4030.753 Å and 4034.483 Å are properly reproduced by a lower manganese overabundance of about -5.13 for HD 30085 for instance. Three other lines at 4055.544 Å and 4526.530 Å and 4823.524 Å absorb a few % of the continuum and are properly reproduced by the same abundance. The other Mn I lines are very weak and blended.

5.3.4. Iron

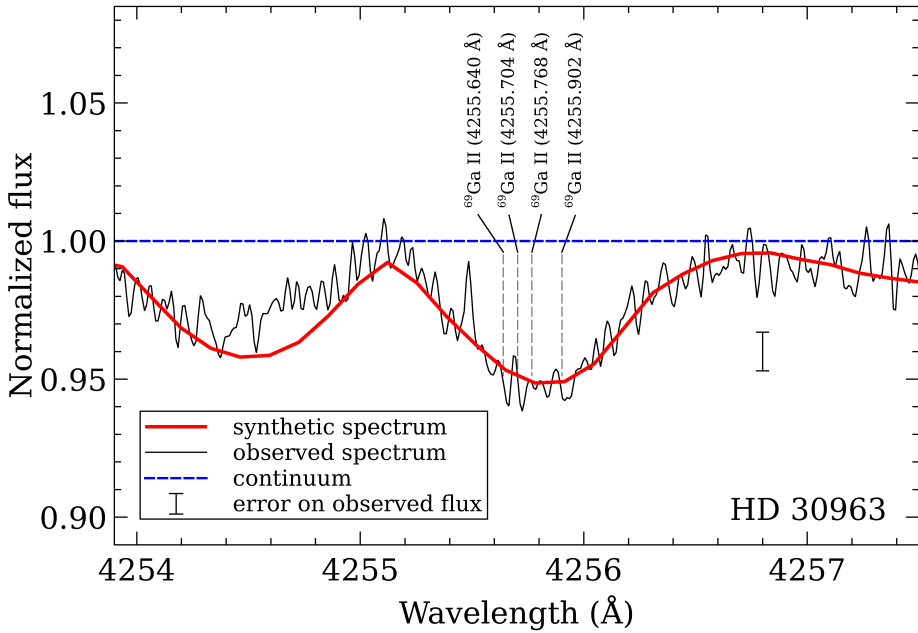
The abundance of iron was derived from the eleven Fe II lines, all of which are sensitive to small changes in $[\frac{Fe}{H}]$. Iron is overabundant in HD 30085, HD 30963 and HD 174567 and slightly underabundant for χ Lupi A. The ten lines of Fe I listed in [Castelli & Hubrig \(2004\)](#) are present, the strongest are 4045.812 Å and 4383.545 Å and are blended in all stars. The others range from 2 to 5 % absorption and are often blended. The only unblended Fe I line is 4383.545 Å, it is adjusted with a solar abundance of iron for all stars.

5.3.5. Nickel

The Ni II line at λ 4067.031 Å is weak in the spectra of HD 30085 and χ Lupi A, absorbing about 1% of the continuum and is properly fit with a pronounced underabundance of nickel in HD 30085 and in χ Lupi A. In HD 30963 and HD 174567, the line absorbs about 2% of the continuum and yields a nickel abundance of -6.75 and -5.27. Nickel appears to be underabundant in the three Chemically Peculiar star but slightly overabundant in the superficially normal HD 174567.

Table 3. The Ga II λ 6334.069 Å linelist

Wavelength (Å)	ion	$\log gf$	lower energy level (cm $^{-1}$)	EW (mÅ)
6333.930	Ga II	0.08	102944.595	14.7
6333.980	Ga II	0.21	102944.595	20.5
6333.990	Ga II	0.08	102944.595	14.6
6334.069	Ga II	0.10	102944.595	15.3
6334.080	Ga II	0.40	102944.595	26.5
6334.083	Ti II	-2.08	66521.008	0.0
6334.120	Ga II	0.02	102944.595	12.8
6334.200	Ga II	0.09	102944.595	20.9
6334.208	Cr II	-1.66	89812.422	0.0
6334.290	Ga II	0.01	102944.595	16.8
6334.368	Ni II	-2.36	120271.975	0.0

**Figure 4.** Synthesis of the Ga II 4255.77 Å blend in HD 30963 showing the contribution of hyperfine structure of gallium.

5.3.6. Gallium

We have used the high excitation Ga II line at λ 6334.069 Å with hyperfine splitting of the gallium isotopes. It is the strongest expected line of Ga II in this temperature regime. The eight transitions retrieved and modified from Nielsen et al. (2000a) are collected in Table 3.

In HD 30963, the line of Ga II at 6334.069 Å is clearly present. Other lines of Ga II are present at 4251.108 Å, 4254.032 Å, 4255.64 Å and 4261.995 Å and 5360.313 Å, 5363.353 Å and 5421.122 Å in the red part of the spectrum. The fits to the three lines of Ga II and their hyperfine structures at 4255.6 Å and 5360.3 Å are collected in Figure 4 and Figure 5 and consistently yield a large overabundance for HD 30963. In the other three stars, gallium is solar or underabundant.

5.4. The Sr-Y-Zr triad

5.4.1. Strontium

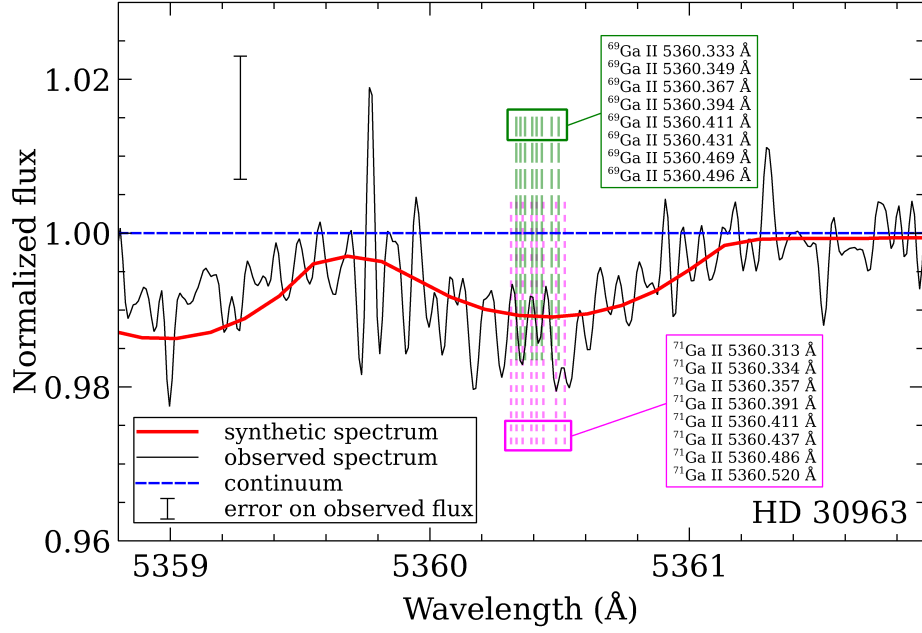


Figure 5. Synthesis of the Ga II 5360 Å blend in HD 30963 showing the hyperfine structure of gallium.

The two lines of Multiplet 2 have critical evaluation (NIST quality A and AA). The abundance of strontium was derived from the fit to the only unblended line of Sr II at 4215.52 Å. Strontium is significantly overabundant in HD 30085 and χ Lupi A and overabundant in HD 30963 and HD 174567.

5.4.2. Yttrium

The yttrium lines are conspicuous in the spectra of HD 30085 and HD 30963, most of them absorbing from a few % up to 10 %. The only unblended lines are the low excitation lines at 3982.592 Å and 5662.925 Å. Yttrium is very overabundant in each star.

5.4.3. Zirconium

The only two Zr II unblended lines are λ 4443.008 Å and λ 4457.431 Å. Zirconium is overabundant in all stars.

5.5. Barium

The two resonance lines of Ba II (Multiplet 1) at 4554.029 Å and 4934.076 Å and the low excitation line 6141.59 Å are present. The hyperfine structure of the various isotopes of barium we have used is collected in Table 4. Barium is overabundant by a factor of 10 in HD 30085, HD 30963 and HD 174567 and a factor of 5 in χ Lupi A.

5.6. The Rare Earths

We have searched for once ionized rare earths elements in the spectra of the four stars, namely La II, Ce II, Pr II, Nd II, Sm II, Eu II, Gd II, Tb II, Dy II, Ho II and Er II. As the twice ionised rare earths often are the dominant stages in these atmospheres of late B stars, we also looked for the twice ionized species, Pr III and Nd III, using the lines listed either in NIST or in DREAM and the linelists published in Ryabchikova et al. (2006) and Ryabchikova et al. (2007).

5.6.1. Lanthanum

The spectrum synthesis of the La II line at 4042.91 Å feature is consistent with one solar abundance upper limit for HD 30085 and an overabundance. Lanthanum is overabundant in HD 174567 and χ Lupi A. The line is blended in HD 30963.

For La III, the three lines λ 4499.064 Å, λ 5145.718 Å and λ 5148.391 Å retrieved from NIST are all blended with more abundant species in the three stars.

Table 4. The Ba II linelists

Wavelength (Å)	ion	$\log gf$	lower energy level (cm $^{-1}$)	EW (mÅ)
4553.934	Zr II	-0.57	19514.840	0.1
4553.995	Ba II	-1.57	0.000	0.1
4553.997	Ba II	-1.57	0.000	0.1
4553.998	Ba II	-1.99	0.000	0.0
4553.999	Ba II	-1.82	0.000	0.1
4554.001	Ba II	-1.82	0.000	0.1
4554.001	Ba II	-2.22	0.000	0.0
4554.011	Cr I	-0.73	33040.093	0.0
4554.029	Ba II	0.02	0.000	16.6
4554.029	Ba II	-1.45	0.000	1.3
4554.029	Ba II	-0.94	0.000	3.8
4554.046	Ba II	-1.38	0.000	0.3
4554.049	Ba II	-1.82	0.000	0.1
4554.049	Ba II	-1.15	0.000	0.6
4554.050	Ba II	-2.52	0.000	0.0
4554.051	Ba II	-1.57	0.000	0.1
4554.052	Ba II	-2.29	0.000	0.0
4934.005	Fe I	-0.61	33507.120	0.4
4934.074	Ba II	-3.12	0.000	0.0
4934.074	Ba II	-1.33	0.000	0.8
4934.075	Ba II	-3.15	0.000	0.0
4934.075	Ba II	-1.10	0.000	1.3
4934.076	Ba II	-1.77	0.000	0.3
4934.076	Ba II	-1.25	0.000	0.9
4934.077	Ba II	-0.29	0.000	7.0
4934.084	Fe I	-2.30	26627.608	0.1
6141.597	Fe I	-3.12	33765.304	0.0
6141.713	Ba II	-0.22	5674.824	2.4
6141.713	Ba II	-1.03	5674.824	0.4
6141.714	Ba II	-1.18	5674.824	0.3
6141.714	Ba II	-1.26	5674.824	0.2
6141.715	Ba II	-1.69	5674.824	0.1
6141.717	Ba II	-3.07	5674.824	0.0
6141.718	Ba II	-3.05	5674.824	0.0
6141.731	Fe I	-1.61	29056.322	0.1

5.6.2. Cerium

The synthesis of the unblended Ce II lines at 4133.80 Å and 4460.21 Å yields large overabundances of cerium in HD 30085 and χ Lupi A and a one solar upper limit for HD 30963 and HD 174567.

For Ce III, we find coincidences for seven out of ten low excitation lines listed in DREAM, however all of them are heavily blended in the spectra of the four stars.

5.6.3. Praseodymium

The lines of Pr III at 5284.69 and 5299.99 Å are unblended and provide large overabundances in HD 30085, HD 174567 and χ Lupi A. They are consistent with a solar abundance upper value for HD 30963.

5.6.4. *Neodymium*

For Nd III, the strongest expected lines in DREAM are the resonance lines λ 5265.019 Å and λ 5294.099 Å which correspond to structures absorbing respectively 3% and 5% of the local continuum inside complex blends. The synthesis of these lines yields moderate to large overabundances of Nd III in HD 30085, in HD 30963, HD 174567 and in χ Lupi A.

5.6.5. *Samarium*

The Sm II lines at 4280.79 Å and 4424.32 Å are unblended and are consistent with a 1 solar upper limit abundance of samarium in HD 30085, HD 30963, HD 174567 and an overabundance of 25 in χ Lupi A.

5.6.6. *Europium*

The Eu II resonance line at 4129.73 Å is unblended and consistent with a 1 solar upper limit abundance of europium in HD 30085, HD 30963, HD 174567 and a significant overabundance of about 100 in χ Lupi A.

5.6.7. *Gadolinium*

The Gd II line at 4037.32 Å is unblended and properly reproduced with large overabundances of about 100 in HD 30085, HD 174567 and χ Lupi A. It is blended in HD 30963.

5.6.8. *Terbium*

The Tb II line at 4005.47 Å is unblended in HD 30085 and HD 30963 and provides a 1 solar upper limit abundance. It is blended in HD 174567 and χ Lupi A.

5.6.9. *Dysprosium*

The Dy II line at 4000.45 Å is unblended in HD 30085, HD 174567 and χ Lupi A and provides a 1 solar upper limit for HD 30085 and an overabundance by a factor of 60 respectively for HD 174567 and χ Lupi A. This line is blended in HD 30963.

5.6.10. *Holmium*

The low excitation line of Ho II at 4152.62 Å is unblended and provides a 1 solar upper limit in HD 30085, HD 30963 and HD 174567 and an overabundance in χ Lupi A.

5.6.11. *Erbium*

For Er II , the line at 4142.91 Å is consistent with a 1 solar upper limit for HD 30085, is blended in HD 30963 and χ Lupi A and reproduced by a large overabundance of about 173 in HD 174567.

5.6.12. *Thulium*

The line at 4242.15 Å of Tm II is blended in HD 30085 and χ Lupi A and consistent with a 1 solar upper limit for HD 30963 and HD 174567.

5.6.13. *Ytterbium*

The Yb II line at 4135.095 Å provides a one solar upper limit for HD 30085, HD 174567 and χ Lupi A. It is blended in HD 30963.

5.6.14. *Hafnium*

The Hf II line at 3918.08 Å yields a 1 solar upper limit for HD 30085 and HD 174567 and is blended in HD 30963 and χ Lupi A.

5.7. *The very heavy elements Osmium, Platinum, Gold and Mercury*

5.7.1. *Osmium*

The Os II line at 4158.44 Å is consistent with a 1 solar upper limit in HD 30085, HD 174567 and χ Lupi A and is blended in HD 30963.

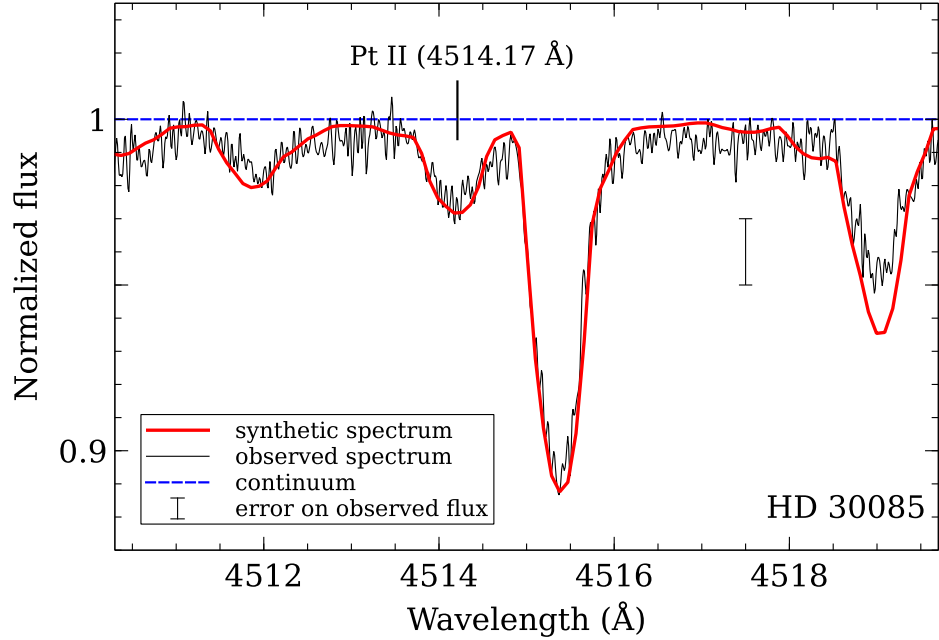


Figure 6. Synthesis of the Pt II 4514.17 Å line in HD 30085.

5.7.2. Platinum

The 4514.47 Å Pt II line is the only unblended line of platinum in the spectra of the four stars. It does not have any hyperfine structure published for the various isotopes of Pt. We therefore derived a crude estimate of the platinum overabundance. There are no other species at this wavelength which could account for the observed absorption as shows the spectrum synthesis without the Pt II line. The wavelength scale around the Pt II line was checked using the Fe II neighbouring control lines whose NIST wavelengths are accurate to within ± 0.001 Å.

The Pt II line at 4046.45 Å has hyperfine structure published (5 transitions), but it is blended with the 9 hyperfine transitions of the Hg I line at 4046.57 Å. Using the mercury abundance obtained in the following paragraph, the synthesis of this blend in the spectra of HD 30085 and HD 30963 also yields an overabundance similar to that derived from the 4514.47 Å line. The final adopted platinum abundance is that derived from the Pt II line at 4514.47 Å. It ranges from large overabundances of the order of 10^4 for 30085 and 10^3 in HD 30963 to a solar upper limit (-10.65) for HD 174567. This line is blended in χ Lupi A. The synthesis of the Pt II line at 4514.47 Å in HD 30085 is shown in Figure 6.

5.7.3. Gold

The only Au II line corresponding with weak features is λ 4052.790 Å but is blended with an Fe I line in the spectra of all four stars.

5.7.4. Mercury

The abundance of mercury has been derived from the low excitation Hg II line at 3983.93 Å only. This feature absorbs about 12 % of the continuum in HD 30085, HD 30963 and χ Lupi A and about 4 % in HD 174567. The other Hg II lines are all high excitation lines either weak or blended with more abundant species and were not synthesized. In particular Hg II 6149.4749 Å is blended with Fe II 6149.258 Å in HD 30085, HD 30963 and HD 174567 which precludes any conclusion on the mercury abundance. The blend is resolved in χ Lupi A and yields an overabundance which agrees from that found with the 3983.93 Å line.

To model the Hg II line at 3983.93 Å, we have included 9 transitions ie., all hyperfine structure from the various isotopes from Hg¹⁹⁶ and Hg²⁰⁴ listed in Dolk et al. (2003). These transitions are collected together with blending lines from Ti I, Fe I, Cr I and Cr II in Table 5.

The wavelength scale was checked by using four control lines on each side of the Hg II line: shortwards the Zr II line at 3982.0250 Å, the Y II line at 3982.59 Å and longwards the Zr II lines at 3984.718 Å and 3991.15 Å. Once corrected for the radial velocities of HD 30085 and HD 30963, the centers of these lines are found at their expected laboratory locations to within ± 0.02 Å which we will adopt as the accuracy of the wavelength scale in this spectral region. After

Table 5. The Hg II 3983.93 Å linelist

Wavelength (Å)	ion	$\log gf$	lower energy level (cm $^{-1}$)	EW (mÅ)
3983.771	Hg II	-4.50	35514.999	1.2
3983.827	Ti I	-1.46	17075.258	0.0
3983.832	Fe I	-4.81	24338.766	0.0
3983.839	Hg II	-3.00	35514.000	14.1
3983.844	Hg II	-3.13	35514.000	12.5
3983.851	Cr II	-4.31	81962.291	0.0
3983.853	Hg II	-3.00	35514.000	14.1
3983.874	Fe I	-2.70	34039.515	0.0
3983.899	Cr I	0.35	20520.904	3.2
3983.912	Hg II	-2.50	35514.000	19.2
3983.932	Hg II	-3.10	35514.000	12.9
3983.941	Hg II	-2.90	35514.000	15.3
3983.956	Fe I	-1.02	21999.129	2.5
3983.986	Cr II	-2.32	90512.561	0.0
3983.991	Cr II	-2.88	82362.188	0.0
3983.993	Hg II	-3.00	35514.000	14.2
3984.022	Cr I	-2.47	35397.971	0.0
3984.072	Hg II	-3.00	35514.000	14.4

rectification to the red wing of the H_{ϵ} line, the core of the Hg II lines of HF 30085 and HD 30963 are flat and extend from about 3983.90 ± 0.02 Å to 3984.07 ± 0.02 Å which roughly correspond to the positions of lines of the heaviest isotopes Hg²⁰⁰ and Hg²⁰⁴. The heavy isotopes of Hg thus contribute more to the absorption than the lighter isotopes in HD 30085 and HD 30963 as is the case in the coolest HgMn stars (Woolf & Lambert 1999, White et al. 1976). In χ Lupi A, the Hg II line center is at 3984.07 Å which corresponds to the line of the heaviest isotope.

First, we checked the influence of possible contaminant species to the Hg II line from 3983.50 Å up to 3984.50 Å which we estimate to be the maximum extension of the line wings. The only possible contaminants are three weak lines: Fe II λ 3983.737 Å, Cr I λ 3983.897 Å and Fe I λ 3983.956 Å. The equivalent widths of these lines were computed for the derived Fe and Cr abundances and the sum of their contributions, which amounts to about 4.9 mÅ, is by far insufficient to reproduced the equivalent width of the observed feature at 3983.93 Å (about 64 to 70 mÅ) of the Hg II in HD 30085, HD 30963 and χ Lupi A. Another test consisted in computing the flux without the Hg II transitions. This consistently resulted into a very weak absorption feature from 3983.50 Å to 3984.50 Å in the four stars. We can therefore conclude that the observed features at 3983.93 Å is indeed mostly due to the Hg II line and is almost free of blending.

Including the hyperfine structure of the seven isotopes from Table 2 of Dolk et al. (2003) significantly reduces the mercury abundance, for example to about 120000 \odot in HD 30085 (it would be of the order of $10^7 \odot$ if we include the single transition retrieved from VALD). In HD 30085 and HD 30963, the 12 % absorption at the core is reproduced but the synthetic profile is significantly offset to the blue by about -0.05 Å from the observed blue wing and + 0.10 Å from the observed red wing. In order to shift redwards the synthetic line core and give it a flat shape comparable to the observed one, we have iteratively altered the oscillator strengths of the individual hyperfine components until the overall observed line profile could be reproduced. We progressively decreased the oscillator strengths of the first 4 transitions of the three lightest isotopes Hg¹⁹⁶, Hg¹⁹⁸ and Hg¹⁹⁹ and increased those of 5 transitions of the heaviest Hg²⁰⁰, Hg²⁰¹, Hg²⁰² and Hg²⁰⁴ in order to redistribute the computed line opacity towards longer wavelengths. The final combination of oscillator strengths is recorded in Table 5.

We can give a very rough estimate of the contribution of each isotope in HD 30085 and HD 30963 by dividing the equivalent widths of its hyperfine components to the total equivalent width of the whole line. We thus find increasingly larger contributions as we move to heavier isotopes: Hg¹⁹⁶ 0.4 %, Hg¹⁹⁸ 9 %, Hg¹⁹⁹ 16 %, Hg²⁰⁰ 14 %, Hg²⁰¹ 20 %, Hg²⁰² 16 % and Hg²⁰⁴ 24 %.

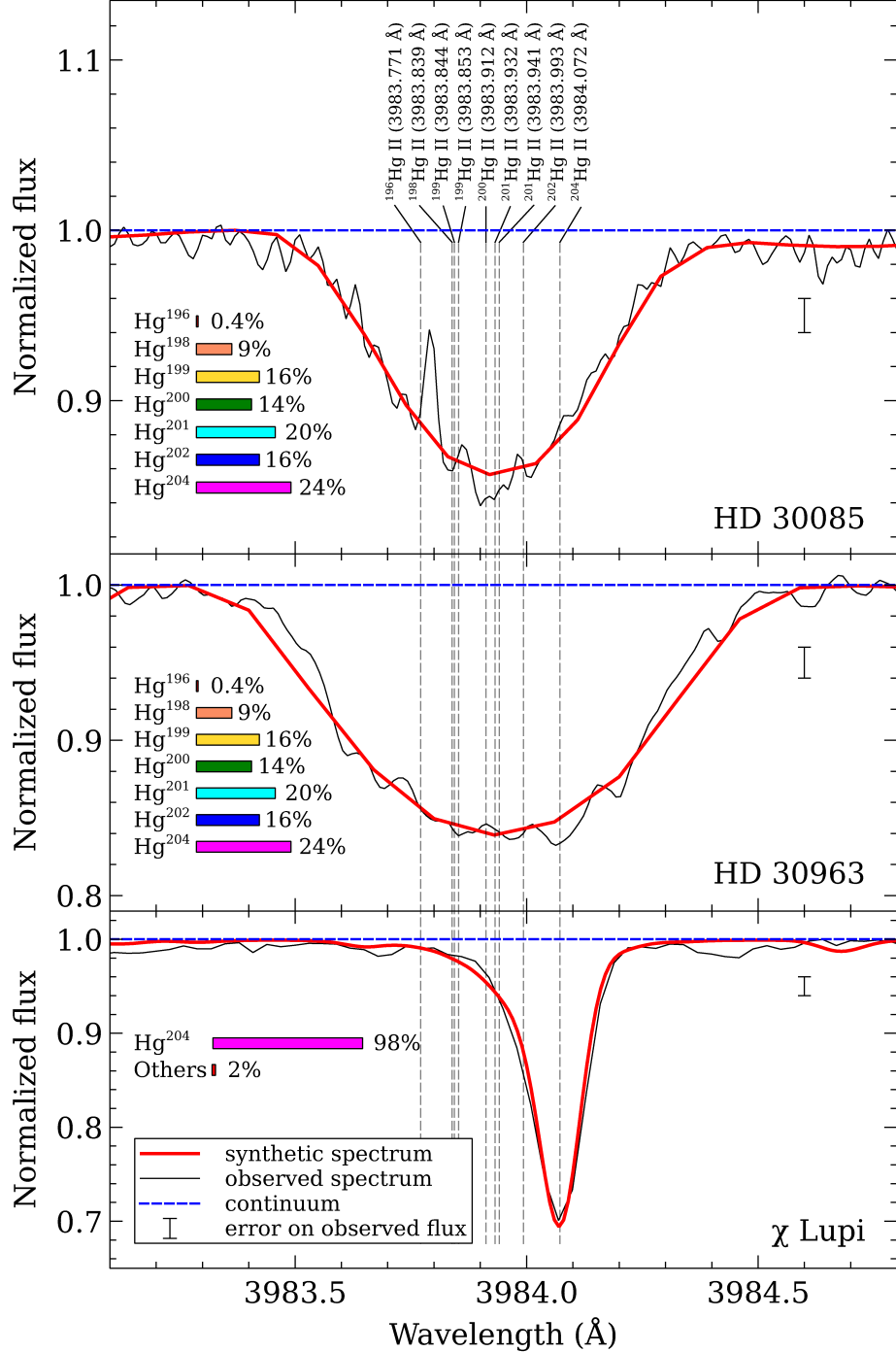


Figure 7. Synthesis of the Hg II 3983.87 Å blend in HD 30085, HD 30963 and χ Lupi A showing the contribution of hyperfine structure of various isotopes.

The final mercury abundances derived from the synthesis of the 3983.93 Å yield very large overabundances of about -5.83 in HD 30085 (see Figure 7), -5.31 in HD 30963, -5.91 for χ Lupi A and -7.61 in HD 174567. The observed Hg II line center in χ Lupi A is at about 3984.072 Å, which corresponds to the heaviest isotope of mercury only. The possible contribution of the various isotopes of mercury in HD 30085, HD 30963 and χ Lupi A is represented as histograms in Figure 8.

6. DISCUSSION

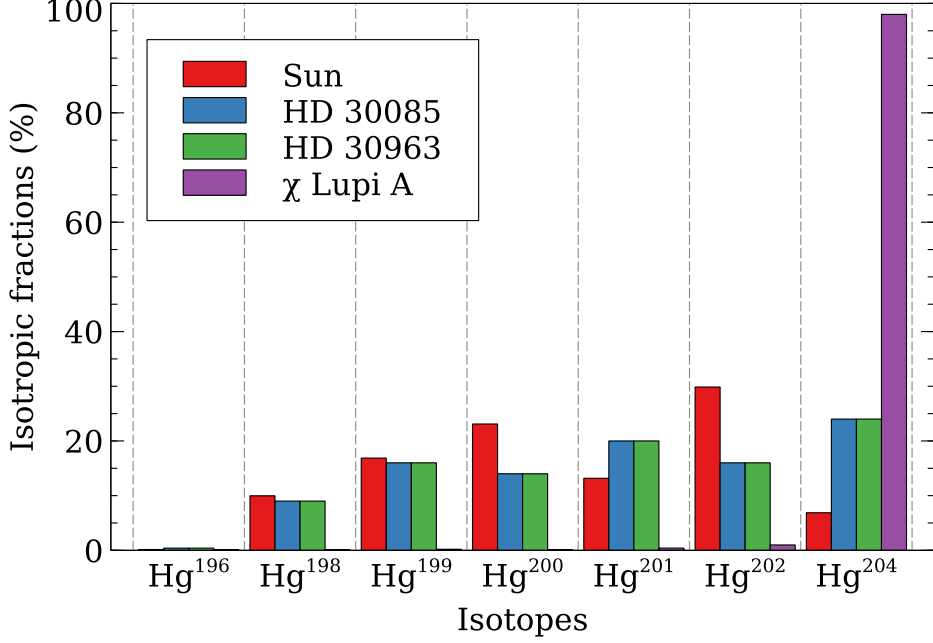


Figure 8. Possible contribution of the various isotopes of Hg to the 3983.93 Hg II line in each star.

In table 6 we compare the abundances we derived for χ Lupi A with those derived from high resolution spectra in the optical range by Wahlgren et al. (1994).

Table 6. Comparison between the abundances of χ Lupi A and the ones derived in Wahlgren et al. (1994)

Element	< log(X/H) >		Element	< log(X/H) >	
	This work	Wahlgren et al.		This work	Wahlgren et al.
He I	-1.67±0.23		C II	-3.76±0.34	-3.85
O I	-3.53±0.10		Na I		-4.97
Mg II	-4.66±0.15		Al II	-5.79±0.20	-5.85
Si II	-4.55±0.05		P II	-5.47±0.16	-
S II	-4.96±0.08		Ca II	-5.83±0.16	-5.70
Sc II	-10.13±0.14		Ti II	-6.73±0.06	-6.65±0.25
V II	-8.02±0.12		Cr II	-6.14±0.17	-5.96±0.27
Mn II	-6.13±0.04		Fe II	-4.57±0.16	-4.29±0.21
Ni II	-6.52±0.14		Ga II	-9.12	-
Sr II	-7.43±0.09		Y II	-8.06±0.16	-7.89±0.16
Zr II	-8.70±0.09		Ba II	-9.17±0.25	-8.80
La II	-9.13±0.13		Ce II	-8.90±0.25	-
Pr III	-9.09±0.13		Nd III	-8.80±0.25	-

Table 6 continued on next page

Table 6 (*continued*)

Element	< log(X/H) >		Element	< log(X/H) >	
	This work	Wahlgren et al.		This work	Wahlgren et al.
Sm II	-8.59±0.13	-	Eu II	-9.61±0.25	-
Gd II	-8.70±0.13	-	Dy II	-9.08±0.25	-
Ho II	-9.50±0.13	-	Yb II	-10.92±0.25	-
Os II	-10.55±0.13	-	Au II	-10.99±0.25	-7.49
Hg II	-5.91±0.13	-6.34			

Our abundance determinations for carbon, magnesium, aluminium, silicon, calcium, scandium, titanium, vanadium, chromium, manganese and zirconium agree within ± 0.20 dex (a representative error on our abundances) with those derived by Wahlgren et al. (1994). For the other nine elements common to both studies, the abundances differ by more than 0.20 dex. This probably comes from using different lines or different more recent atomic data for lines in common, different model atmospheres and different line synthesis codes.

From the list of identifications provided for the final composition of HD 30085 in table 10, we can conclude that the following species are present in the spectra of HD 30085 (and HD 30963 as well): C II, N II, O I, Na I, Mg II, Mg I, Mg II, Si II, P II, S II, Ca II, Sc II, Ti II, V II, Cr II, Cr I, Mn II, Fe II, Ni II, Ga II, Sr II, Y II, Zr II, Ba II, Pt II, Hg II. Among these species, Si II, Ti II, Cr II, Mn II, Fe II, Y II, Zr II, have numerous and strong lines and are important opacity sources. Lines from neutrals: Cr I, Mn I, Fe I are also observed and yield lower abundances than Cr II, Mn II and Fe II, indicating possibly departures from LTE. Gallium is present with a large overabundance in HD 30963.

In HD 30085, we only find evidence for overabundances of four Rare Earths from unblended lines of Ce II, Pr III and Nd III and Gd II. For the other Rare Earths, we find upper limits: the abundances must be solar or lower. In HD 30963, the blending is higher because of the larger $v_e \sin i$, we can conclude only that Nd III may be present and overabundant (evidence from one line only), all other lines are blended. In HD 174567, the low $v_e \sin i$ favors detection of weak unblended lines and evidence is found for overabundances of La II, Pr III, Nd III, Gd II, Dy II and Er II. The presence of once ionised Rare Earths is difficult to assess at these temperatures above 10000 K because they are not the dominant ionisation stage. In general, the abundances for the Rare Earths should be regarded as the least reliable ones in this study because they were usually inferred from the synthesis of one weak line of the once ionised specie only. The overabundances found for HD 30085 and HD 30963 run from very mild (2.0 \odot for Fe) up to quite large (10⁵ \odot for Hg). The underabundances run from mild -0.80 \odot for carbon to pronounced -0.02 \odot for nickel. Helium is quite underabundant in HD 30085, HD 30963 and χ Lupi A.

The abundance patterns of the five stars are compared in Figure 9. The comparison bona-fide normal late B star, ν Cap, has a nearly solar composition for all elements as already found by Monier et al. (2018) and Adelman (1991). For the other four stars, the overall trend is that the light elements (He through Mg) are most often deficient whereas elements heavier than Mn tend to be more and more overabundant as the atomic mass increases (with the exception of nickel). This pattern is most likely caused by radiative diffusion. In particular the overall shapes of the patterns of HD 30085 and HD 30963 compare well with that of χ Lupi A (HD 141556), even though differences for individual abundances exist. There are several similarities for the abundances of the elements lighter than Scandium between χ Lupi A and HD 30963, in particular for helium, magnesium, phosphorus, calcium. For elements heavier than scandium, the abundances of HD 30963 differ from that of χ Lupi A. For HD 30085, the carbon, magnesium, phosphorus, gallium, strontium, praseodymium abundances are similar to those of χ Lupi A. Overall, the chemical patterns of HD 30085 and HD 30963 follow that of χ Lupi A, which definitely confirms that these two star are new HgMn stars. Moreover the patterns of HD 30085 and HD 30963 also fall well within the general abundance pattern of confirmed HgMn stars in Fig. 1 of Ghazaryan & Alecian (2016) compilation. HD 30085 and HD 30963 are most likely classical HgMn stars.

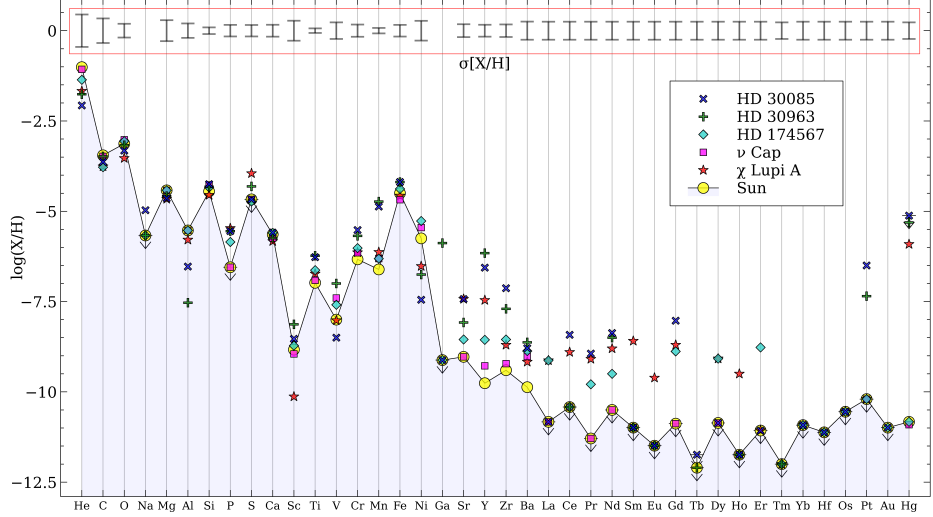


Figure 9. Comparison of the abundance patterns of HD 30085, HD 30963, χ Lupi A, HD 174567 and ν Cap

The pattern of HD 174567 is intermediate between that of ν Cap and that of the three HgMn stars. We therefore propose that HD 174567 is a new mild Chemically Peculiar star with overabundances of elements heavier than strontium less pronounced than in HD 30085 and HD 30963 but definitely larger than in ν Cap. The overabundances for Sr, Y, Zr, several Rare Earths and mercury suggest that HD 174567 could be a new cool and mild HgMn star. More observations of HD 174567 are foreseen in order to elucidate the nature of this interesting object.

7. CONCLUSION

With their characteristic underabundances of most light elements up to calcium and overabundances of manganese and elements heavier than strontium, in particular platinum and mercury, HD 30085 and HD 30963 are definitely two new HgMn stars. Their abundances differ from those of χ Lupi A possibly because their initial abundances differed slightly and because radiative diffusion operated in a slightly different manner in the younger and more massive stars HD 30085 and HD 30963. For HD 174567, the mild deficiencies for light elements and overabundances for strontium, yttrium and zirconium and several rare-earths and mercury suggest that this object should be reclassified as a mild Chemically Peculiar star. More observations of this interesting star will help elucidate its nature.

APPENDIX

A. DETERMINATION OF UNCERTAINTIES

For a representative line of a given element, six major sources are included in the uncertainty determinations: the uncertainty on the effective temperature ($\sigma_{T_{\text{eff}}}$), on the surface gravity ($\sigma_{\log g}$), on the microturbulent velocity (σ_{ξ_t}), on the apparent rotational velocity ($\sigma_{v_e \sin i}$), the oscillator strength ($\sigma_{\log g_f}$) and the continuum placement (σ_{cont}). These uncertainties are supposed to be independent, so that the total uncertainty σ_{tot_i} for a given transition (i) verifies:

$$\sigma_{\text{tot}_i}^2 = \sigma_{T_{\text{eff}}}^2 + \sigma_{\log g}^2 + \sigma_{\xi_t}^2 + \sigma_{v_e \sin i}^2 + \sigma_{\log g_f}^2 + \sigma_{\text{cont}}^2. \quad (\text{A1})$$

The mean abundance $\langle \frac{X}{H} \rangle$ is then computed as a weighted mean of the individual abundances $[X/H]_i$ derived for each transition (i):

$$\langle \frac{X}{H} \rangle = \frac{\sum_i ([\frac{X}{H}]_i / \sigma_{\text{tot}_i}^2)}{\sum_i (1 / \sigma_{\text{tot}_i}^2)} \quad (\text{A2})$$

and the total error, σ is given by:

$$\frac{1}{\sigma^2} = \sum_{i=1}^N (1 / \sigma_{\text{tot}_i}^2) \quad (\text{A3})$$

where N is the number of lines per element. The uncertainties σ for each element are collected in Tab. 7.

RM thanks Pr. Charles Cowley for his insightful comments during the analysis of HD 30085 and HD 174567. We thank the OHP night assistants for their helpful support during the three observing runs. This work has made use of the VALD database, operated at Uppsala University, the Institute of Astronomy RAS in Moscow, and the University of Vienna. We have also used the NIST Atomic Spectra Database (version 5.4) available <http://physics.nist.gov/asd>. We also acknowledge the use of the ELODIE archive at OHP available at <http://atlas.obs-hp.fr/elodie/>.

REFERENCES

- Adelman, S. J. 1991, MNRAS, 252, 116
- Biémont, É., Blagoev, K., Engström, L., et al. 2011, MNRAS, 414, 3350
- Biémont, E., Grevesse, N., Faires, L. M., Marsden, G., & Lawler, J. E. 1989, A&A, 209, 391, (BGF)
- Bressan, A., Marigo, P., Girardi, L., et al. 2012, MNRAS, 427, 127
- Butler, K. & Zeippen, C. J. 1991, J. Phys. IV France, 01, C1
- Carlsson, M. 1986, Uppsala Astronomical Observatory Reports, 33
- Carlsson, M. 1992, in Astronomical Society of the Pacific Conference Series, Vol. 26, Cool Stars, Stellar Systems, and the Sun, ed. M. S. Giampapa & J. A. Bookbinder, 499
- Castelli, F. & Hubrig, S. 2004, A&A, 425, 263
- Castelli, F. & Kurucz, R. L. 2003, in IAU Symposium, Vol. 210, Modelling of Stellar Atmospheres, ed. N. Piskunov, W. W. Weiss, & D. F. Gray, A20
- Cowley, A., Cowley, C., Jaschek, M., & Jaschek, C. 1969, AJ, 74, 375
- Cunto, W. & Mendoza, C. 1992, RMxAA, 23
- Davidson, M. D., Snoek, L. C., Volten, H., & Doenszelmann, A. 1992, A&A, 255, 457
- Den Hartog, E. A., Lawler, J. E., Sneden, C., & Cowan, J. J. 2003, ApJS, 148, 543
- Den Hartog, E. A., Lawler, J. E., Sneden, C., & Cowan, J. J. 2006, ApJS, 167, 292
- Dimitrijevic, M. S. & Sahal-Brechot, S. 1984, A&A, 136, 289
- Dolk, L., Wahlgren, G. M., & Hubrig, S. 2003, A&A, 402, 299
- Drake, G. 2006, Springer Handbook of Atomic, Molecular, and Optical Physics, ed. G. Drake (New York, NY: Springer New York), 199–219
- Drawin, H. W. 1969, Zeitschrift fur Physik, 225, 483
- Dworetsky, M. M., Jomaron, C. M., & Smith, C. A. 1998, A&A, 333, 665
- Fuhr, J. R., Martin, G. A., & Wiese, W. L. 1988, Journal of Physical and Chemical Reference Data, 17
- Ghazaryan, S. & Alecian, G. 2016, MNRAS, 460, 1912
- Grevesse, N. & Sauval, A. J. 1998, SSRv, 85, 161
- Guitou, M., Spielfiedel, A., Rodionov, D., et al. 2015, Chemical Physics, 462, 94 , inelastic Processes in Atomic, Molecular and Chemical Physics
- Hauck, B. & Mermilliod, M. 1998, A&AS, 129, 431
- Holt, R. A., Scholl, T. J., & Rosner, S. D. 1999, MNRAS, 306, 107
- Huang, W., Gies, D. R., & McSwain, M. V. 2010, ApJ, 722, 605
- Hubeny, I. & Lanz, T. 1992, A&A, 262, 501
- Jamar, C., Macau-Hercot, D., Monfils, A., et al. 1976, Ultraviolet bright-star spectrophotometric catalogue. A compilation of absolute spectrophotometric data obtained with the Sky Survey Telescope (S2/68) on the European Astronomical Satellite TD-1
- Kling, R., Schnabel, R., & Griesmann, U. 2001, The Astrophysical Journal Supplement Series, 134, 173
- Kramida, A., Ralchenko, Y., Reader, J., & NIST ASD Team. 2017, <http://physics.nist.gov/asd>, 5
- Kramida, A., Ralchenko, Y., Reader, J., & NIST ASD Team. 2018, <http://physics.nist.gov/asd>, 5
- Kurucz, R. L. 1992, RMxAA, 23
- Kurucz, R. L. 1993, (GUES)
- Kurucz, R. L. 2003, Robert L. Kurucz on-line database of observed and predicted atomic transitions
- Kurucz, R. L. 2005, Memorie della Societa Astronomica Italiana Supplimenti, 8, 14
- Kurucz, R. L. 2010, Robert L. Kurucz on-line database of observed and predicted atomic transitions
- Kurucz, R. L. 2013, ATLAS12: Opacity sampling model atmosphere program, Astrophysics Source Code Library
- Kurucz, R. L. & Avrett, E. H. 1981, SAO Special Report, 391
- Kurucz, R. L. & Peytremann, E. 1975, SAO Special Report, 362, 1, (KP)
- Lanz, T., Artru, M. C., Didelon, P., & Mathys, G. 1993, A&A, 272, 465
- Lanz, T., Dimitrijevic, M. S., & Artru, M.-C. 1988, A&A, 192, 249
- Lawler, J. E., Den Hartog, E. A., Sneden, C., & Cowan, J. J. 2006, ApJS, 162, 227
- Lawler, J. E., Sneden, C., & Cowan, J. J. 2004, ApJ, 604, 850
- Lawler, J. E., Sneden, C., Cowan, J. J., Ivans, I. I., & Den Hartog, E. A. 2009, Astrophys. J. Suppl. Ser., 182, 51, (LSCI)
- Lawler, J. E., Sneden, C., Cowan, J. J., et al. 2008, ApJS, 178, 71
- Lawler, J. E., Wickliffe, M. E., Cowley, C. R., & Sneden, C. 2001a, ApJS, 137, 341
- Lawler, J. E., Wickliffe, M. E., den Hartog, E. A., & Sneden, C. 2001b, Astrophys. J., 563, 1075, (LWHS)
- Ljung, G., Nilsson, H., Asplund, M., & Johansson, S. 2006, A&A, 456, 1181
- Martin, G. A., Fuhr, J. R., & Wiese, W. L. 1988, Atomic transition probabilities. Scandium through Manganese
- Martin, W. C. 1960, J. Opt. Soc. Am., 50, 174
- Meggers, W. F., Corliss, C. H., & Scribner, B. F. 1975, Tables of spectral-line intensities. Part I, II - arranged by elements.
- Miles, B. M. & Wiese, W. L. 1969, Atomic Data, 1, 1
- Miller, M. H., Wilkerson, T. D., Roig, R. A., & Bengtson, R. D. 1974, PhRvA, 9, 2312, (MWRB)
- Molnar, M. R. 1972, ApJ, 175, 453
- Monier, R., Gebran, M., & Royer, F. 2015, A&A, 577, A96
- Monier, R., Gebran, M., Royer, F., Kilicoglu, T., & Frémat, Y. 2018, ApJ, 854, 50
- Moon, T. T. & Dworetsky, M. M. 1985, MNRAS, 217, 305
- Napiwotzki, R., Schoenberner, D., & Wenske, V. 1993, A&A, 268, 653
- Nielsen, K., Karlsson, H., & Wahlgren, G. M. 2000a, A&A, 363, 815
- Nielsen, K., Karlsson, H., & Wahlgren, G. M. 2000b, A&A, 363, 815

- Nilsson, H., Ljung, G., Lundberg, H., & Nielsen, K. E. 2006, *A&A*, 445, 1165
- Palacios, A., Gebran, M., Josselin, E., et al. 2010, *A&A*, 516, A13
- Palmeri, P., Quinet, P., Wyart, J., & Biémont, E. 2000, *Physica Scripta*, 61, 323, (PQWB)
- Perruchot, S., Kohler, D., Bouchy, F., et al. 2008, in Proc. SPIE, Vol. 7014, Ground-based and Airborne Instrumentation for Astronomy II, 70140J
- Pinnington, E. H., Berends, R. W., & Lumsden, M. 1995, *Journal of Physics B: Atomic, Molecular and Optical Physics*, 28, 2095
- Raassen, A. J. J. & Uylings, P. H. M. 1998, *Journal of Physics B Atomic Molecular Physics*, 31, 3137
- Ramella, M., Boehm, C., Gerbaldi, M., & Faraggiana, R. 1989, *A&A*, 209, 233
- Royer, F., Gebran, M., Monier, R., et al. 2014, *A&A*, 562, A84
- Ryabchikova, T., Piskunov, N., Kurucz, R. L., et al. 2015, *PhyS*, 90, 054005
- Ryabchikova, T., Ryabtsev, A., Kochukhov, O., & Bagnulo, S. 2006, *Astron. and Astrophys.*, 456, 329, (RRKB)
- Ryabchikova, T., Sachkov, M., Kochukhov, O., & Lyashko, D. 2007, *A&A*, 473, 907
- Ryabtsev, A. N. 2010, private communication, (ISAN)
- Sakhibullin, N. A. 1987, *Soviet Ast.*, 31, 151
- Sansonetti, C. J. & Nave, G. 2014, *The Astrophysical Journal Supplement Series*, 213, 28
- Sansonetti, C. J. & Reader, J. 2001, *Physica Scripta*, 63, 219
- Seaton, M. J. 1962, *Proceedings of the Physical Society*, 79, 1105
- Shamey, L. J. 1969, PhD thesis, UNIVERSITY OF COLORADO AT BOULDER.
- Shenstone, A. G. 1961, *Proceedings of the Royal Society of London A: Mathematical, Physical and Engineering Sciences*, 261, 153
- Smith, K. C. & Dworetsky, M. M. 1993, *A&A*, 274, 335
- Theodosiou, C. E. 1989, *PhRvA*, 39, 4880
- Vidal, C. R., Cooper, J., & Smith, E. W. 1973, *ApJS*, 25, 37
- Wahlgren, G. M., Adelman, S. J., & Robinson, R. D. 1994, *ApJ*, 434, 349
- White, R. E., Vaughan, Jr., A. H., Preston, G. W., & Swings, J. P. 1976, *ApJ*, 204, 131
- Wickliffe, M. E., Lawler, J. E., & Nave, G. 2000, *J. Quant. Spectrosc. Radiat. Transfer*, 66, 363, (WLN)
- Wiese, W. L., Fuhr, J. R., & Deters, T. M. 1996, *Atomic transition probabilities of carbon, nitrogen, and oxygen : a critical data compilation*
- Wood, M. P., Lawler, J. E., Den Hartog, E. A., Sneden, C., & Cowan, J. J. 2014, *ApJS*, 214, 18
- Woolf, V. M. & Lambert, D. L. 1999, *ApJ*, 521, 414
- Zhiguo, Z., Li, Z. S., Lundberg, H., et al. 2000, *Journal of Physics B Atomic Molecular Physics*, 33, 521, (ZLLZ)
- Zhiguo, Z., Zhongshan, L., & Zhankui, J. 1999, *The European Physical Journal D - Atomic, Molecular, Optical and Plasma Physics*, 7, 499

Table 7. Abundance uncertainties for the elements analysed in HD 30085, HD 30963, HD 174567 and HD 141556

		HeI	CII	OI	MgII	AlIII	SiII	PII	SII	CaII
ΔT_{eff}	+200 K	-0.30	0.00	0.05	0.047	0.075	-0.017	0.00	0.00	0.109
$\Delta \log g$	0.15 dex	0.079	0.24	-0.06	-0.052	0.118	-0.017	-0.12	-0.12	-0.032
$\Delta \xi_t$	+0.20 km s ⁻¹	0.00	0.00	0.00	0.00	0.075	-0.035	-0.05	-0.046	0.00
$\Delta \log gf$	+0.10	-0.30	-0.12	-0.16	-0.25	-0.028	-0.053	-0.07	-0.071	-0.105
$\Delta_{\text{continuum}}$		-0.12	0.21	0.075	0.13	0.25	0.062	0.06	0.061	0.058
$2\sigma_{[X/H]}$		0.45	0.34	0.19	0.29	0.20	0.092	0.160	0.159	0.165
		ScII	TiII	VII	CrII	MnII	FeII	NiII	SrII	YII
ΔT_{eff}	+200 K	0.22	0.041	0.028	0.057	0.00	0.079	0.176	0.138	0.146
$\Delta \log g$	0.15 dex	-0.079	0.015	-0.014	0.03	0.007	0.041	0.114	-0.058	
$\Delta \xi_t$	+0.20 km s ⁻¹	-0.038	-0.016	0.00	0.00	0.00	-0.095	0.00	-0.058	0.00
$\Delta \log gf$	+0.10	-0.13	-0.23	-0.046	-0.15	-0.015	-0.095	-0.155	-0.058	-0.05
$\Delta_{\text{continuum}}$		0.067	0.03	0.014	0.046	0.014	0.0126	0.079	0.051	0.041
$2\sigma_{[X/H]}$		0.276	0.064	0.23	0.169	0.076	0.162	0.273	0.178	0.165
		ZrII	BaII	LaII	CeII	PrIII	NdIII	SmII	EuII	GdII
ΔT_{eff}	+200 K	0.058	0.114	0.11	0.11	0.11	0.11	0.11	0.11	0.11
$\Delta \log g$	0.15 dex	0.046	-0.032	-0.125	-0.13	-0.13	-0.13	-0.13	-0.13	-0.13
$\Delta \xi_t$	+0.20 km s ⁻¹	0.00	-0.097	-0.09	-0.09	-0.09	-0.09	-0.09	-0.09	-0.09
$\Delta \log gf$	+0.10	-0.066	-0.125	-0.13	-0.13	-0.13	-0.13	-0.13	-0.13	-0.13
$\Delta_{\text{continuum}}$		0.146	-0.097	-0.09	-0.09	-0.09	-0.09	-0.09	-0.09	-0.09
$2\sigma_{[X/H]}$		0.173	0.251	0.25	0.25	0.25	0.25	0.25	0.25	0.25
		DyII	TbII	HoII	ErII	Tm II	YbII	HfII	OsII	PtII
ΔT_{eff}	+200 K	0.11	0.11	0.11	0.11	-0.155	0.11	0.11	0.11	0.11
$\Delta \log g$	0.15 dex	-0.13	-0.13	-0.13	-0.13	0.041	-0.13	-0.13	-0.13	-0.13
$\Delta \xi_t$	+0.20 km s ⁻¹	-0.09	-0.09	-0.09	-0.09	-0.097	-0.09	-0.09	-0.09	-0.09
$\Delta \log gf$	+0.10	-0.13	-0.13	-0.13	-0.13	-0.108	-0.13	-0.13	-0.13	-0.13
$\Delta_{\text{continuum}}$		-0.09	-0.09	-0.09	-0.09	0.079	-0.09	-0.09	-0.09	-0.09
$2\sigma_{[X/H]}$		0.25	0.25	0.25	0.25	0.23	0.25	0.25	0.25	0.25
		AuII	Hg II							
ΔT_{eff}	+200 K	0.11	-0.155							
$\Delta \log g$	0.15 dex	-0.13	0.041							
$\Delta \xi_t$	+0.20 km s ⁻¹	-0.09	-0.097							
$\Delta \log gf$	+0.10	-0.13	-0.108							
$\Delta_{\text{continuum}}$		-0.09	0.079							
$2\sigma_{[X/H]}$		0.25	0.23							

Table 8. Elemental Abundances from unblended lines for HD 30085, HD 30963, HD 174567 and HD 141556. References are defined in Tab. 5.

Element	λ (Å)	$\log gf$	Ref.	$< \log(X/H) >$				
				HD30085	HD30963	HD174567	Chi Lupi A	$\sigma_{[X/H]}$
He I	4471.470	-2.211	NIST/ASD	-2.07	-1.77	-1.37	-1.67	
He I	4471.474	-0.287	NIST/ASD	-2.07	-1.77	-1.37	-1.67	
He I	4471.474	-1.035	NIST/ASD	-2.07	-1.77	-1.37	-1.67	
He I	4471.485	-1.035	NIST/ASD	-2.07	-1.77	-1.37	-1.67	
He I	4471.489	-0.558	NIST/ASD	-2.07	-1.77	-1.37	-1.67	
He I	4471.683	-0.910	NIST/ASD	-2.07	-1.77	-1.37	-1.67	
He I	5875.598	-1.516	NIST/ASD	-2.05	-1.75	-1.35	-1.65	
He I	5875.613	-0.339	NIST/ASD	-2.05	-1.75	-1.35	-1.65	
He I	5875.615	0.409	NIST/ASD	-2.05	-1.75	-1.35	-1.65	
He I	5875.625	-0.339	NIST/ASD	-2.05	-1.75	-1.35	-1.65	
He I	5875.640	0.138	NIST/ASD	-2.05	-1.75	-1.35	-1.65	
He I	5875.966	-0.214	NIST/ASD	-2.05	-1.75	-1.35	-1.65	
$< \log(He/H) >$				-2.07	-1.76	-1.36	-1.67	± 0.23
$< [\frac{He}{H}] >$				-1.00	-0.69	-0.29	-0.60	± 0.23
C II	4267.001	0.563	NIST/ASD	-3.63	-3.48	-3.78	-3.78	
C II	4267.261	-0.584	NIST/ASD	-3.63	-3.48	-3.78	-3.78	
C II	4267.261	0.716	NIST/ASD	-3.63	-3.48	-3.78	-3.70	
$< \log(C/H) >$				-3.63	-3.48	-3.78	-3.76	± 0.17
$< [\frac{C}{H}] >$				-0.15	0.00	-0.30	-0.28	± 0.17
O I	6155.961	-1.363	NIST/ASD	-3.32	-3.17	-3.06	-3.63	
O I	6155.971	-1.011	NIST/ASD	-3.32	-3.17	-3.06	-3.63	
O I	6155.989	-1.120	NIST/ASD	-3.32	-3.17	-3.06	-3.63	
O I	6156.737	-1.487	NIST/ASD	-3.32	-3.17	-3.06	-3.47	
O I	6155.755	-0.898	NIST/ASD	-3.26	-3.11	-3.00	-3.47	
O I	6156.778	-0.694	NIST/ASD	-3.32	-3.17	-3.06	-3.47	
O I	6158.149	-1.841	NIST/ASD	-3.32	-3.17	-3.06	-3.63	
O I	6158.172	-0.995	NIST/ASD	-3.32	-3.17	-3.06	-3.63	
O I	6158.187	-0.409	NIST/ASD	-3.32	-3.17	-3.06	-3.63	
$< \log(O/H) >$				-3.32	-3.17	-3.06	-3.53	± 0.10

Table 8 continued on next page

Table 8 (*continued*)

Element	λ (Å)	$\log gf$	Ref.	< $\log(X/H)$ >				
				HD30085	HD30963	HD174567	Chi Lupi A	$\sigma_{[X/H]}$
$< \left[\frac{O}{H} \right] >$								
Na I	4497.657	-1.574	NIST/ASD	-4.97	-5.67 (u.l)	-5.67 (u.l)	-4.97	
Na I	4497.657	-2.528	NIST/ASD	-4.97	-5.67 (u.l)	-5.67 (u.l)	-4.97	
Na I	5889.950	0.108	NIST/ASD	-5.61	-6.27	-6.27	-5.57	
Na I	5895.924	-0.194	NIST/ASD	-5.61	-6.27	-6.27	-5.57	
$< \log(Na/H) >$								
$< \left[\frac{Na}{H} \right] >$								
Mg II	4390.572	-0.523	NIST/ASD	-4.64	-4.64	-4.42	-4.72	
Mg II	4427.994	-1.208	NIST/ASD	-4.64	-4.52	-4.42	-4.64	
Mg I	5172.684	-0.393	NIST/ASD	-4.97	-4.91	-4.75	-5.01	
$< \log(Mg/H) >$								
$< \left[\frac{Mg}{H} \right] >$								
Al II	4663.056	-0.244	NIST/ASD	-6.53	-7.53	-5.53	-5.79	
$< \log(Al/H) >$								
$< \left[\frac{Al}{H} \right] >$								
Si II	4128.054	0.359	NIST/ASD	-4.30	-4.37	-4.45	-4.57	
Si II	4130.894	0.552	NIST/ASD	-4.32	-4.45	-4.45	-4.57	
Si II	5041.024	0.029	NIST/ASD	-4.15	-4.27	-4.15	bl.	
Si II	5055.984	0.523	NIST/ASD	-4.30	-4.35	-4.35	-4.60	
Si II	5056.317	-0.492	NIST/ASD	-4.30	-4.35	-4.30	-4.45	
Si II	6371.37	-0.082	NIST/ASD	-4.15	-4.15	bl.	-4.55	
$< \log(Si/H) >$								
$< \left[\frac{Si}{H} \right] >$								
P II	6024.18	0.137	NIST/ASD	-5.55	-5.55	bl.	-5.47	
P II	6043.13	0.384	NIST/ASD	-5.55	-5.55	-5.85	-5.70	
$< \log(P/H) >$								
$< \left[\frac{P}{H} \right] >$								
S II	4153.06	0.395	NIST/ASD	-4.67	-4.19	-4.67	-4.27	
S II	4162.31	0.161	NIST/ASD	-4.67	-4.37	-4.76	-	

Table 8 continued on next page

Table 8 (*continued*)

Element	λ (Å)	$\log gf$	Ref.	$< \log(X/H) >$				
				HD30085	HD30963	HD174567	Chi Lupi A	$\sigma_{[X/H]}$
S II	4162.67	0.830	NIST/ASD	-4.67	-4.37	-4.76	-5.65	
		$< \log(S/H) >$		-4.67	-4.31	-4.73	-4.96	± 0.08
		$< [\frac{S}{H}] >$		0.00	0.36	-0.06	0.72	± 0.08
Ca II	3933.663	0.135	NIST/ASD	-5.54	-5.46	-5.56	-5.94	
Ca II	5019.971	-0.280	NIST/ASD	-5.64	-6.03	-5.64	-5.83	
		$< \log(Ca/H) >$		-5.59	-5.74	-5.60	-5.83	± 0.08
		$< [\frac{Ca}{H}] >$		0.05	-0.10	0.04	-0.19	± 0.08
Sc II	4246.822	0.242	NIST/ASD	-8.53	-8.13	-8.72	-10.13	
Sc II	5031.021	-0.400	NIST/ASD	bl.	bl.	bl.	—	
Sc II	5526.813	-0.77	NIST/ASD	bl.	bl.	bl.	no data	
		$< \log(Sc/H) >$		-8.53	-8.13	-8.72	-10.13	± 0.14
		$< [\frac{Sc}{H}] >$		0.30	0.70	0.11	-1.30	± 0.14
Ti II	4163.644	-0.128	NIST/ASD	-6.24	-6.20	-6.64	-6.58	
Ti II	4287.873	-2.020	NIST/ASD	-6.28	-6.50	-6.68	-6.68	
Ti II	4290.210	-0.848	NIST/ASD	-6.33	-6.28	—	-6.68	
Ti II	4300.042	-0.442	NIST/ASD	-6.03	-6.03	-6.44	—	
Ti II	4411.072	-0.6767	NIST/ASD	-6.20	-6.13	-6.50	-6.44	
Ti II	4468.492	-0.620	NIST/ASD	-6.24	-6.24	-6.68	-7.03	
Ti II	4563.758	-0.96	NIST/ASD	-6.20	-6.24	-6.58	-6.74	
Ti II	5129.156	-1.239	NIST/ASD	-6.38	-6.24	-6.75	-6.68	
Ti II	5188.687	-1.220	NIST/ASD	-6.38	-6.24	-6.72	-6.74	
Ti II	5336.780	-1.700	NIST/ASD	-6.44	-6.24	-6.75	-6.74	
		$< \log(Ti/H) >$		-6.27	-6.23	-6.63	-6.73	± 0.06
		$< [\frac{Ti}{H}] >$		0.71	0.75	0.35	0.25	± 0.06
V II	4005.71	-0.450	NIST/ASD	bl.	bl.	-7.66	-8.07	
V II	4023.39	-0.610	K10/BGF/WLDS	-8.70	-8.00 (u.l)	-7.50	-8.00	
V II	4036.78	-1.570	NIST/ASD	-8.30	-7.00	-7.60	-8.00	
		$< \log(V/H) >$		-8.50	-7.50	-7.59	-8.02	± 0.12
		$< [\frac{V}{H}] >$		-0.50	0.50	0.41	-0.02	± 0.12

Table 8 continued on next page

Table 8 (*continued*)

Element	λ (Å)	$\log gf$	Ref.	< $\log(X/H)$ >				
				HD30085	HD30963	HD174567	Chi Lupi A	$\sigma_{[X/H]}$
Cr II	4558.644	-0.660	NIST/ASD	-5.43	-5.55	-5.85	-6.13	
Cr II	4558.787	-2.460	SN14	-5.43	-5.55	-5.85	-6.13	
Cr II	5237.322	-1.160	NIST/ASD	-5.55	-5.85	-6.13	-6.23	
Cr II	5308.421	-1.810	NIST/ASD	-5.63	-5.85	-6.18	-6.15	
Cr II	5313.581	-1.650	NIST/ASD	-5.55	-5.63	-6.10	-6.15	
Cr II	5502.086	-1.990	NIST/ASD	-5.55	-5.68	-6.03	nd	
< $\log(Cr/H)$ >				-5.52	-5.68	-6.02	-6.14	± 0.09
$< [\frac{Cr}{H}] >$				0.81	0.65	0.31	0.19	± 0.09
Mn II	4206.368	hfs	NIST/ASD	-4.87	-4.76	-6.31	-6.13	
Mn II	4259.19	hfs	NIST/ASD	-4.87	-4.71	-6.31	-6.13	
< $\log(Mn/H)$ >				-4.87	-4.73	-6.31	-6.13	± 0.08
$< [\frac{Mn}{H}] >$				1.74	1.88	0.30	0.48	± 0.08
Fe II	4258.148	-3.500	NIST/ASD	bl.	bl.	bl.	-4.40	
Fe II	4273.326	-3.350	NIST/ASD	-4.32	-4.30	-4.38	-4.50	
Fe II	4296.566	-2.900	NIST/ASD	-4.20	-4.20	-4.38	-4.40	
Fe II	4491.397	-2.640	NIST/ASD	-4.20	-4.20	-4.38	-4.60	
Fe II	4508.280	-2.300	NIST/ASD	-4.20	-4.20	-4.40	-4.72	
Fe II	4515.333	-2.360	NIST/ASD	-4.20	-4.20	-4.38	-4.60	
Fe II	4520.218	-2.600	NIST/ASD	-4.16	-4.16	-4.35	-4.57	
Fe II	4923.921	-1.210	NIST/ASD	-4.10	-4.10	-4.38	-4.62	
Fe II	5275.997	-1.900	NIST/ASD	-4.20	-4.20	-4.38	-4.72	
Fe II	5316.609	-1.780	NIST/ASD	-4.15	-4.15	-4.38	-4.65	
Fe II	5506.199	0.860	NIST/ASD	-4.24	-4.20	-4.38	nd	
< $\log(Fe/H)$ >				-4.19	-4.19	-4.38	-4.57	± 0.08
$< [\frac{Fe}{H}] >$				0.31	0.31	0.12	-0.07	± 0.08
Ni II	4067.04	-1.834	K03	-7.45	-6.75	-5.27	-6.52	
< $\log(Ni/H)$ >				-7.45	-6.75	-5.27	-6.52	± 0.14
$< [\frac{Ni}{H}] >$				-1.70	-1.00	0.48	-0.77	± 0.14
Ga II	4251.108	hfs	Dwo98	-9.12 (u.l)	bl.	-9.12 (u.l)	-9.12 (u.l)	

Table 8 continued on next page

Table 8 (*continued*)

Element	λ (Å)	$\log g f$	Ref.	< $\log(X/H)$ >				
				HD30085	HD30963	HD174567	Chi Lupi A	$\sigma_{[X/H]}$
Ga II	4254.032	hfs	Dwo98	-9.12 (u.l)	bl.	-9.12 (u.l)	-9.12 (u.l)	
Ga II	4255.640	hfs	Dwo98	-9.12 (u.l)	-5.88	-9.12 (u.l)	-9.12 (u.l)	
Ga II	4261.995	hfs	Dwo98	-9.12 (u.l)	bl.	-9.12 (u.l)	-9.12 (u.l)	
Ga II	5360.313	hfs	Niel2000	-5.88	-5.88	-9.12 (u.l)	-9.12 (u.l)	
Ga II	5363.353	hfs	Niel2000	bl.	bl.	-9.12 (u.l)	-9.12 (u.l)	
Ga II	5421.122	hfs	Niel2000	bl.	bl.	-9.12 (u.l)	-9.12 (u.l)	
Ga II	6334.07	hfs	Lanz1993	-5.88	-5.88	-9.12 (u.l)	-9.12 (u.l)	
< $\log(Ga/H)$ >				-9.12	-5.88	-9.12	-9.12	-
< $[\frac{Ga}{H}]$ >				0.00	3.24	0.00	0.00	-
Sr II	4215.519	-1.610	NIST/ASD	-7.43	-8.08	-8.55	-7.43	
< $\log(Sr/H)$ >				-7.43	-8.08	-8.55	-7.43	± 0.09
< $[\frac{Sr}{H}]$ >				1.60	0.95	0.48	1.60	± 0.09
Y II	3982.592	-0.560	NIST/ASD	-6.56	-6.16	-8.56	-8.16	
Y II	5662.922	0.340	Bie11	-6.56	-6.16	-8.56	-7.98	
< $\log(Y/H)$ >				-6.56	-6.16	-8.56	-8.06	± 0.08
< $[\frac{Y}{H}]$ >				3.20	3.60	1.20	1.70	± 0.08
Zr II	3998.965	-0.520	L06	-7.10	bl.	-8.70	-8.70	
Zr II	4442.992	-0.420	L06	-7.10	bl.	-8.70	-8.70	
Zr II	4457.431	-1.220	L06	-7.40	bl.	-8.40	-8.40	
Zr II	5112.270	-0.850	L06	-6.92	-7.70	-8.40	bl.	
< $\log(Zr/H)$ >				-7.13	-7.70	-8.55	-8.70	± 0.09
< $[\frac{Zr}{H}]$ >				2.27	1.70	0.85	0.70	± 0.09
Ba II	4554.04	hfs	VALD??	-8.79	-8.69	-8.87	-9.17	
Ba II	4934.077	hfs	VALD??	-8.79	bl.	-8.87	-9.17	
Ba II	6141.713	hfs	VALD ??	-8.79	-8.57	-8.87	-9.17	
< $\log(Ba/H)$ >				-8.79	-8.63	-8.87	-9.17	± 0.13
< $[\frac{Ba}{H}]$ >				1.08	1.24	1.00	0.70	± 0.13
La II	4042.91	0.33	Zi99	-10.83 (u.l)	bl.	-9.13	-9.13	
< $\log(La/H)$ >				-10.83	-	-9.13	-9.13	± 0.13

Table 8 continued on next page

Table 8 (*continued*)

Element	λ (Å)	$\log gf$	Ref.	< $\log(X/H)$ >				
				HD30085	HD30963	HD174567	Chi Lupi A	$\sigma_{[X/H]}$
$< \left[\frac{La}{H} \right] >$								
Ce II	4133.80	0.72	LSCI	-8.42	-10.42 (u.l)	-10.42 (u.l)	bl.	
Ce II	4460.21	0.28	PQWB	-8.42	-10.42 (u.l)	-10.42 (u.l)	-8.90	
$< \log(Ce/H) >$								
$< \left[\frac{Ce}{H} \right] >$								
Pr III	5264.44	-0.66	ISAN	bl.	bl.	bl.	-9.09	
Pr III	5284.69	-0.59	ISAN	-8.99	bl.	-9.99	bl.	
Pr III	5299.99	-0.53	ISAN	-8.89	bl.	-9.59	bl.	
$< \log(Pr/H) >$								
$< \left[\frac{Pr}{H} \right] >$								
Nd III	5265.019	-0.66	RRKB	-8.65	bl.	-9.50 (u.l)	-8.80	
Nd III	5294.10	-0.65	RRKB	-8.10	-8.50	-9.50	* bl.	
$< \log(Nd/H) >$								
$< \left[\frac{Nd}{H} \right] >$								
Sm II	4280.79	-0.33	LA06	-10.99 (u.l)	-10.99 (u.l)	-10.99 (u.l)	bl.	
Sm II	4424.32	0.14	LA06	-10.99 (u.l)	-10.99 (u.l)	noisy	2.40	
$< \log(Sm/H) >$								
$< \left[\frac{Sm}{H} \right] >$								
Eu II	4129.70	0.19	LWHS	-11.49 (u.l)	-11.49 (u.l)	-11.49 (u.l)	-9.61	
$< \log(Eu/H) >$								
$< \left[\frac{Eu}{H} \right] >$								
Gd II	4037.32	-0.11	DH06	-8.03	bl.	-8.88	-8.70	
$< \log(Gd/H) >$								
$< \left[\frac{Gd}{H} \right] >$								
Tb II	4005.47	-0.02	LA01	-12.10 (u.l)	-12.10 (u.l)	bl.	bl.	
Tb II	4033.03	-0.01	LA01	bl.	bl.	bl.	bl.	
$< \log(Tb/H) >$								
$< \left[\frac{Tb}{H} \right] >$								

Table 8 continued on next page

Table 8 (*continued*)

Element	λ (Å)	$\log gf$	Ref.	< $\log(X/H)$ >					
				HD30085	HD30963	HD174567	Chi Lupi A	$\sigma_{[X/H]}$	
Dy II	4000.45	0.040	NIST	-10.86 (u.l)	bl.	-9.08	-9.08		
				-10.86	—	-9.08	-9.08	± 0.13	
				$< [\frac{Dy}{H}] >$	0.00	—	1.78	1.78	± 0.13
Ho II	4152.62	-0.93	LA04	-11.74 (u.l)	-11.74 (u.l)	-11.74 (u.l)	-9.50		
				-11.74	-11.74	-11.74	-9.50	± 0.13	
				$< [\frac{Ho}{H}] >$	0.00	0.00	0.00	2.24	± 0.13
Er II	4142.91	-0.72	LA08	-11.07 (u.l)	bl.	-8.77	bl.		
				-11.07	—	-8.77	bl.	—	
				$< [\frac{Er}{H}] >$	0.00	—	2.30	bl.	—
Tm II	4242.15	-0.95	NIST	bl.	-12.0 (u.l)	-12.00 (u.l)	bl.		
				—	-12.00	-12.00	bl.	—	
				$< [\frac{Tm}{H}] >$	—	0.00	0.00	bl.	—
Yb II	4135.095	-0.21	?	-10.92 (u.l)	bl.	-10.92 (u.l)	-10.92 (u.l)		
				-10.92	—	-10.92	-10.92	± 0.13	
				$< [\frac{Yb}{H}] >$	0.00	—	0.00	0.00	± 0.13
Hf II	3918.08	-1.140	?	-11.12 (u.l)	bl.	-11.12 (u.l)	bl.		
				-11.12	—	-11.12	bl.	—	
				$< [\frac{Hf}{H}] >$	0.00	—	0.00	bl.	—
Os II	4158.44	-2.68	?	-10.55 (u.l)	bl.	-10.55 (u.l)	-10.55 (u.l)*		
				-10.55	—	-10.55	-10.55	± 0.13	
				$< [\frac{Os}{H}] >$	0.00	—	0.00	0.00	± 0.13
Pt II	4514.17	-1.48	?	-6.50	-7.35	-10.20 (u.l)	bl.		
				-6.50	-7.35	-10.20	bl.	—	
				$< [\frac{Pt}{H}] >$	3.70	2.85	0.00	bl.	—
Au II	4052.79	-1.68	?	-10.99 (u.l)	bl.	-10.99 (u.l)	-10.99 (u.l)		
				-10.99	—	-10.99	-10.99	± 0.13	
				$< [\frac{Au}{H}] >$	0.00	—	0.00	0.00	± 0.13

Table 8 continued on next page

Table 8 (*continued*)

Element	λ (Å)	$\log g f$	Ref.	$< \log(X/H) >$				
				HD30085	HD30963	HD174567	Chi Lupi A	$\sigma_{[X/H]}$
Hg II	3983.931	hfs	Do03	-5.12	-5.31	-7.61	* -5.91	
		$< \log(Hg/H) >$		-5.12	-5.31	-7.61	-5.91	± 0.12
		$< [\frac{Hg}{H}] >$		5.75	5.56	3.26	5.00	± 0.12

Table 9. Bibliographical references for the atomic data.

Element	Bibliographical source
He I	Ma60= Martin (1960)
He I	DR2006= Drake (2006)
C II	NIST/ASD= Kramida et al. (2017)
O I	KZ91= Butler, K. & Zeippen, C. J. (1991)
O I	W96= Wiese et al. (1996)
O I	NIST/ASD= Kramida et al. (2017)
Mg II	NIST/ASD= Kramida et al. (2017)
Mg II	NIST/ASD= Kramida et al. (2017)
Al II	NIST/ASD= Kramida et al. (2017)
Al I	NIST/ASD= Kramida et al. (2017)
Si II	NIST/ASD= Kramida et al. (2017)
Si II	Sh61= Shenstone (1961)
S II	GUES= Kurucz (1993)
S II	KP= Kurucz & Peytremann (1975)
S II	MWRB= Miller et al. (1974)
Ca II	NIST= http://physics.nist.gov/PhysRefData/ASD/
Ca II	T89= Theodosiou (1989)
Sc II	NIST/ASD= Kramida et al. (2017)
Ti II	NIST/ASD= Kramida et al. (2017)
Ti II	NIST/ASD= Kramida et al. (2017)

Table 9 continued on next page

Table 9 (*continued*)

Element	Bibliographical source
Ti II	NIST/ASD= Kramida et al. (2017)
Ti II	NIST/ASD= Kramida et al. (2017)
V II	K10= Kurucz (2010)
V II	BGF= Biemont et al. (1989)
V II	WLDSC= Wood et al. (2014)
Cr II	SN14= Sansonetti & Nave (2014)
Mn II	KL01= Kling et al. (2001)
Fe II	NIST/ASD= Kramida et al. (2017)
Fe II	RU98= Raassen & Uylings (1998)
Ni II	K03= Kurucz (2003)
Ga II	Dwo98= Dworetsky et al. (1998)
Ga II	Niel2000= Nielsen et al. (2000b)
Ga II	Lanz1993= Lanz et al. (1993)
Sr II	PBL95= Pinnington et al. (1995)
Y II	Bie11= Biémont et al. (2011)
Y II	MCS75= Meggers et al. (1975)
Zr II	L06= Ljung et al. (2006)
Ba II	NBS= Miles & Wiese (1969)
Ba II	DSVD92= Davidson et al. (1992)
La II	Zi99= Zhiguo et al. (1999)
Ce II	LSCI= Lawler et al. (2009)
Ce II	PQWB= Palmeri et al. (2000)
Pr III	ISAN= Ryabtsev (2010)
Nd III	RRKB= Ryabchikova et al. (2006)
Sm II	LA06= Lawler et al. (2006)
Eu II	LWHS= Lawler et al. (2001b)
Eu II	ZLLZ= Zhiguo et al. (2000)
Gd II	DH06= Den Hartog et al. (2006)
Dy II	WLN= Wickliffe et al. (2000)
Dy II	MC= Meggers et al. (1975)
Gd II	DH06= Den Hartog et al. (2006)
Tb II	LA01= Lawler et al. (2001a)

Table 9 continued on next page

Table 9 (*continued*)

Element	Bibliographical source
Ho II	LA04= Lawler et al. (2004)
Er II	LA08= Lawler et al. (2008)
Hg II	SR01= Sansonetti & Reader (2001)
Hg II	Do03= Dolk et al. (2003)

Table 10. Identifications of lines absorbing more than 2 % for HD 30085

λ_{obs} (Å)	λ_{lab} (Å)	Species	$\log gf$	E_{low}	Ref.
3920.738	3920.627	Fe II	-1.330	60628.698	NIST/VALD
3920.801	3920.690	C II	-0.230	131735.525	NIST/VALD
3922.121	3922.010	Fe II	-1.110	73606.162	NIST/VALD
3923.571	3923.460	S II	0.440	130641.115	NIST/VALD
3924.953	3924.842	Fe II	-1.100	78138.990	NIST/VALD
3926.527	3926.416	Mn II	-1.600	55757.109	NIST/VALD
3930.407	3930.296	Fe I	-1.490	704.007	NIST/VALD
3930.417	3930.306	Fe II	-4.300	13671.099	NIST/VALD
3931.063	3930.952	Mn II	-2.040	52651.876	NIST/VALD
3932.120	3932.009	Ti II	-1.640	9118.285	NIST/VALD
3933.379	3933.267	S II	0.570	131187.190	NIST/VALD
3934.206	3934.094	Zr II	-1.160	2572.210	NIST/VALD
3934.903	3934.791	Zr II	-0.900	5752.920	NIST/VALD
3936.054	3935.942	Fe II	-1.720	44915.056	NIST/VALD
3938.401	3938.289	Fe II	-4.100	13474.447	NIST/VALD
3939.081	3938.969	Fe II	-1.930	47674.729	NIST/VALD
3941.343	3941.231	Mn II	-2.430	43852.362	NIST/VALD
3943.710	3943.598	Mn II	-2.250	48336.810	NIST/VALD
3943.970	3943.858	Mn II	-2.260	43699.122	NIST/VALD
3945.323	3945.211	Fe II	-4.400	13673.205	NIST/VALD
3947.402	3947.290	O I	-2.100	73768.202	NIST/VALD

Table 10 continued on next page

Table 10 (*continued*)

λ_{obs} (Å)	λ_{lab} (Å)	Species	$\log gf$	E_{low}	Ref.
3947.592	3947.480	O I	-2.240	73768.202	NIST/VALD
3950.461	3950.349	Y II	-0.490	838.817	NIST/VALD
3952.530	3952.418	Mn II	-1.500	62564.430	NIST/VALD
3954.412	3954.300	Si II	-1.080	101020.939	NIST/VALD
3954.615	3954.503	Si II	-0.920	101029.008	NIST/VALD
3958.342	3958.230	Zr II	-0.310	4248.300	NIST/VALD
3961.021	3960.909	Fe II	-1.560	58628.442	NIST/VALD
3961.632	3961.520	Al I	-0.330	112.061	NIST/VALD
3966.245	3966.133	Fe II	-3.440	36125.574	NIST/VALD
3966.740	3966.628	Fe I	-0.320	25898.463	NIST/VALD
3967.784	3967.672	Y II	0.190	33334.894	NIST/VALD
3968.114	3968.001	Mn II	-2.730	43852.362	NIST/VALD
3969.370	3969.257	Fe I	-0.430	11976.239	NIST/VALD
3969.487	3969.374	Fe II	-5.230	13671.099	NIST/VALD
3969.512	3969.399	Fe II	-4.110	13477.524	NIST/VALD
3969.856	3969.743	Cr I	0.570	20523.900	NIST/VALD
3970.348	3970.235	Mn II	-2.440	44142.727	NIST/VALD
3971.435	3971.322	Fe I	-0.970	21715.733	NIST/VALD
3974.273	3974.160	Fe II	-4.000	21812.044	NIST/VALD
3975.131	3975.018	Fe II	-2.360	48038.381	NIST/VALD
3975.856	3975.743	Mn II	-1.360	62572.494	NIST/VALD
3977.678	3977.565	Si II	0.590	131678.076	NIST/VALD
3979.618	3979.505	Cr II	-0.860	45731.640	NIST/VALD
3982.705	3982.592	Y II	-0.490	1048.521	NIST/VALD
3983.951	3983.838	Hg II	-3.000	35514.000	NIST/VALD
3983.957	3983.844	Hg II	-3.130	35514.000	NIST/VALD
3983.966	3983.853	Hg II	-3.000	35514.000	NIST/VALD
3984.025	3983.912	Hg II	-2.500	35514.000	NIST/VALD
3984.045	3983.932	Hg II	-3.100	35514.000	NIST/VALD
3984.054	3983.941	Hg II	-2.900	35514.000	NIST/VALD
3984.106	3983.993	Hg II	-2.400	35514.000	NIST/VALD
3984.185	3984.072	Hg II	-1.700	35514.000	NIST/VALD

Table 10 continued on next page

Table 10 (*continued*)

λ_{obs} (Å)	λ_{lab} (Å)	Species	$\log gf$	E_{low}	Ref.
3986.694	3986.581	Mn II	-2.520	44142.727	NIST/VALD
3991.265	3991.152	Zr II	-0.250	6111.700	NIST/VALD
3991.893	3991.780	Si II	0.710	131920.044	NIST/VALD
3994.232	3994.119	Mn II	-1.170	65564.806	NIST/VALD
3995.430	3995.317	Mn II	-2.510	43392.628	NIST/VALD
3999.067	3998.954	Zr II	-0.390	4505.500	NIST/VALD
4000.145	4000.032	Mn II	-1.210	62588.626	NIST/VALD
4002.653	4002.540	Fe II	-2.070	48038.381	NIST/VALD
4003.397	4003.283	Cr II	-0.720	52296.993	NIST/VALD
4004.270	4004.156	Fe II	-3.240	36125.574	NIST/VALD
4005.356	4005.242	Fe I	-0.610	12560.934	NIST/VALD
4012.498	4012.384	Ti II	-1.840	4628.657	NIST/VALD
4012.610	4012.496	Cr II	-1.080	45667.110	NIST/VALD
4015.588	4015.474	Ni II	-2.410	32520.274	NIST/VALD
4018.482	4018.368	Zr II	-0.990	7736.020	NIST/VALD
4024.531	4024.417	Zr II	-0.970	8058.160	NIST/VALD
4024.666	4024.552	Fe II	-2.400	36252.930	NIST/VALD
4026.305	4026.191	He I	group	169086.800	NIST
4028.452	4028.338	Ti II	-0.960	15257.553	NIST/VALD
4029.798	4029.684	Zr II	-0.600	5752.920	NIST/VALD
4030.874	4030.760	Mn I	-0.480	0.000	NIST/VALD
4031.559	4031.445	Fe II	-3.160	38166.155	NIST/VALD
4032.893	4032.779	S II	0.240	131028.854	NIST/VALD
4033.054	4032.940	Fe II	-2.570	36254.622	NIST/VALD
4033.184	4033.070	Mn I	-0.620	0.000	NIST/VALD
4034.604	4034.490	Mn I	-0.810	0.000	NIST/VALD
4038.086	4037.972	Cr II	-0.680	52321.189	NIST/VALD
4041.475	4041.360	Mn I	0.280	17052.289	NIST/VALD
4044.124	4044.009	Fe II	-2.670	44933.149	NIST/VALD
4044.691	4044.576	P II	0.670	107360.463	NIST/VALD
4045.753	4045.638	Zr II	-0.600	5724.380	NIST/VALD
4045.927	4045.812	Fe I	0.280	11976.239	NIST/VALD

Table 10 continued on next page

Table 10 (*continued*)

λ_{obs} (Å)	λ_{lab} (Å)	Species	$\log gf$	E_{low}	Ref.
4048.795	4048.680	Zr II	-0.340	6467.610	NIST/VALD
4048.946	4048.831	Fe II	-2.380	44917.017	NIST/VALD
4049.212	4049.097	Cr II	-1.030	52296.993	NIST/VALD
4050.431	4050.316	Zr II	-1.000	5752.920	NIST/VALD
4052.045	4051.930	Cr II	-2.360	25035.451	NIST/VALD
4053.936	4053.821	Ti II	-1.130	15265.700	NIST/VALD
4054.194	4054.079	Cr II	-2.600	25046.715	NIST/VALD
4057.570	4057.455	Fe II	-1.680	58668.776	NIST/VALD
4063.709	4063.594	Fe I	0.060	12560.934	NIST/VALD
4067.146	4067.031	Ni II	-1.830	32496.075	NIST/VALD
4070.955	4070.840	Cr II	-0.930	52321.189	NIST/VALD
4071.853	4071.738	Fe I	-0.020	12968.554	NIST/VALD
4072.676	4072.561	Cr II	-2.460	29955.432	NIST/VALD
4075.566	4075.450	Si II	-1.400	79355.019	NIST/VALD
4076.896	4076.780	Si II	-1.700	79338.502	NIST/VALD
4077.830	4077.714	Sr II	0.150	0.000	NIST/VALD
4081.559	4081.443	Mn II	-2.190	49288.543	NIST/VALD
4085.160	4085.044	Mn II	-2.480	43336.173	NIST/VALD
4085.506	4085.390	Mn II	-2.520	44747.641	NIST/VALD
4085.512	4085.396	Mn II	-2.100	43395.394	NIST/VALD
4090.651	4090.535	Zr II	-1.010	6111.700	NIST/VALD
4093.330	4093.214	Fe II	-2.510	54063.344	NIST/VALD
4094.523	4094.407	Mn II	-2.580	43392.628	NIST/VALD
4096.726	4096.610	Zr II	-1.560	4505.500	NIST/VALD
4097.216	4097.100	Ca II	-1.000	60533.018	NIST/VALD
4097.609	4097.493	Fe II	-1.610	61725.611	NIST/VALD
4098.521	4098.405	Cr II	-1.710	42989.353	NIST/VALD
4100.121	4100.005	Mn II	-1.170	65564.806	NIST/VALD
4102.132	4102.016	Mn II	-3.430	43392.628	NIST/VALD
4105.095	4104.979	Mn II	-1.310	49425.654	NIST/VALD
4109.937	4109.820	Ca II	-0.740	60611.279	NIST/VALD
4110.731	4110.614	Mn II	-1.480	49465.982	NIST/VALD

Table 10 continued on next page

Table 10 (*continued*)

λ_{obs} (Å)	λ_{lab} (Å)	Species	$\log gf$	E_{low}	Ref.
4111.107	4110.990	Cr II	-2.250	30310.315	NIST/VALD
4111.120	4111.003	Cr II	-2.700	25035.451	NIST/VALD
4111.994	4111.877	Fe II	-2.670	48038.381	NIST/VALD
4113.333	4113.216	Cr II	-2.740	25046.715	NIST/VALD
4122.755	4122.638	Fe II	-3.300	20830.553	NIST/VALD
4124.910	4124.793	Fe II	-4.200	20516.953	NIST/VALD
4128.187	4128.070	Si II	0.360	79338.502	NIST/VALD
4128.240	4128.123	Mn II	-2.900	14325.865	NIST/VALD
4128.852	4128.735	Fe II	-3.600	20830.553	NIST/VALD
4130.989	4130.872	Si II	-0.780	79355.019	NIST/VALD
4131.007	4130.890	Si II	0.550	79355.019	NIST/VALD
4137.019	4136.902	Mn II	-1.250	49514.374	NIST/VALD
4140.557	4140.440	Mn II	-2.500	44899.850	NIST/VALD
4142.373	4142.256	S II	0.240	127825.085	NIST/VALD
4143.985	4143.868	Fe I	-0.510	12560.934	NIST/VALD
4145.185	4145.067	S II	0.440	127976.340	NIST/VALD
4145.898	4145.780	Cr II	-0.900	42900.629	NIST/VALD
4149.335	4149.217	Zr II	-0.030	6467.610	NIST/VALD
4151.104	4150.986	Zr II	-0.990	6467.610	NIST/VALD
4151.111	4150.993	Cr II	-2.070	42989.353	NIST/VALD
4153.182	4153.064	S II	0.620	128233.197	NIST/VALD
4156.394	4156.276	Zr II	-0.780	5724.380	NIST/VALD
4161.331	4161.213	Zr II	-0.720	5752.920	NIST/VALD
4161.914	4161.796	Sr II	-0.470	23715.189	NIST/VALD
4162.783	4162.665	S II	0.780	128599.162	NIST/VALD
4163.762	4163.644	Ti II	-0.130	20891.790	NIST/VALD
4171.151	4171.033	Mn II	-2.340	49425.654	NIST/VALD
4171.630	4171.512	Mn II	-2.120	49820.865	NIST/VALD
4172.021	4171.903	Cr II	-2.940	25043.517	NIST/VALD
4172.022	4171.904	Ti II	-0.290	20951.754	NIST/VALD
4173.568	4173.450	Fe II	-2.160	20830.553	NIST/VALD
4174.383	4174.265	S II	0.800	140319.232	NIST/VALD

Table 10 continued on next page

Table 10 (*continued*)

λ_{obs} (Å)	λ_{lab} (Å)	Species	$\log gf$	E_{low}	Ref.
4174.436	4174.318	Mn II	-3.510	14590.570	NIST/VALD
4177.648	4177.530	Y II	-0.160	3298.808	NIST/VALD
4177.804	4177.686	Fe II	-3.450	20518.744	NIST/VALD
4178.581	4178.463	P II	-0.440	77711.525	NIST/VALD
4178.973	4178.855	Fe II	-2.440	20830.553	NIST/VALD
4179.539	4179.421	Cr II	-1.800	30866.837	NIST/VALD
4179.926	4179.807	Zr II	-0.780	13428.500	NIST/VALD
4183.478	4183.359	Si II	-0.830	108779.995	NIST/VALD
4184.573	4184.454	Mn II	-1.950	49893.458	NIST/VALD
4186.791	4186.672	Zr II	-0.580	14162.900	NIST/VALD
4187.247	4187.128	Si II	-1.140	103553.528	NIST/VALD
4187.270	4187.151	Si II	-1.260	103553.528	NIST/VALD
4190.826	4190.707	Si II	-0.330	108820.317	NIST/VALD
4198.252	4198.133	Si II	-0.600	108779.995	NIST/VALD
4199.214	4199.095	Fe I	0.160	24574.655	NIST/VALD
4199.603	4199.484	Fe II	-0.330	89922.758	NIST/VALD
4200.388	4200.269	Mn II	-1.730	49885.389	NIST/VALD
4200.637	4200.518	Fe II	-0.410	90067.932	NIST/VALD
4200.777	4200.658	Si II	-0.890	101023.046	NIST/VALD
4201.017	4200.898	Si II	-0.730	101024.349	NIST/VALD
4202.634	4202.515	Fe II	-2.360	54902.163	NIST/VALD
4205.494	4205.375	Mn II	-3.450	14593.834	NIST/VALD
4205.708	4205.589	Fe II	-0.420	90390.556	NIST/VALD
4206.487	4206.368	Mn II	-1.540	43528.661	NIST/VALD
4209.096	4208.977	Zr II	-0.460	5752.920	NIST/VALD
4212.026	4211.907	Zr II	-1.080	4248.300	NIST/VALD
4213.629	4213.510	Fe II	-1.840	62693.478	NIST/VALD
4215.644	4215.524	Sr II	-0.170	0.000	NIST/VALD
4218.500	4218.380	Mn II	-1.970	55757.109	NIST/VALD
4222.501	4222.381	Zr II	-0.900	9742.800	NIST/VALD
4223.251	4223.131	N I	-1.090	83364.615	NIST/VALD
4224.980	4224.860	Cr II	-1.250	42989.353	NIST/VALD

Table 10 continued on next page

Table 10 (*continued*)

λ_{obs} (Å)	λ_{lab} (Å)	Species	$\log gf$	E_{low}	Ref.
4227.546	4227.426	Fe I	0.270	26874.550	NIST/VALD
4233.283	4233.163	Fe II	-1.810	20830.553	NIST/VALD
4233.363	4233.243	Cr II	-1.940	31165.263	NIST/VALD
4238.912	4238.792	Mn II	-3.590	14784.143	NIST/VALD
4238.930	4238.810	Fe I	-0.230	27394.692	NIST/VALD
4239.306	4239.186	Mn II	-2.240	43311.972	NIST/VALD
4240.510	4240.390	Mn II	-2.040	49820.865	NIST/VALD
4242.453	4242.333	Mn II	-1.260	49820.865	NIST/VALD
4242.484	4242.364	Cr II	-1.170	31221.723	NIST/VALD
4242.568	4242.448	Mg II	-1.070	93310.590	NIST/VALD
4242.662	4242.542	Mg II	-1.230	93311.112	NIST/VALD
4244.366	4244.246	Mn II	-2.200	43339.453	NIST/VALD
4246.060	4245.940	Mn II	-2.300	43131.511	NIST/VALD
4246.940	4246.820	Sc II	0.240	2540.950	NIST/VALD
4250.550	4250.429	Fe II	-1.720	61974.931	NIST/VALD
4251.838	4251.717	Mn II	-1.060	49885.389	NIST/VALD
4252.753	4252.632	Cr II	-1.810	31116.871	NIST/VALD
4253.084	4252.963	Mn II	-1.140	49893.458	NIST/VALD
4253.146	4253.025	Mn II	-2.280	43392.628	NIST/VALD
4253.233	4253.112	Mn II	-2.050	49893.458	NIST/VALD
4254.642	4254.521	Cr II	-1.290	47352.811	NIST/VALD
4258.169	4258.048	Zr II	-1.130	4505.500	NIST/VALD
4258.276	4258.155	Fe II	-3.500	21812.044	NIST/VALD
4259.312	4259.191	Mn II	-1.440	43537.186	NIST/VALD
4260.588	4260.467	Mn II	-4.210	14905.127	NIST/VALD
4260.595	4260.474	Fe I	0.080	19350.891	NIST/VALD
4262.034	4261.913	Cr II	-1.340	31165.263	NIST/VALD
4263.982	4263.861	Fe II	-1.690	62048.230	NIST/VALD
4267.121	4267.000	C II	0.560	145549.272	NIST/VALD
4267.304	4267.183	C II	0.720	145550.705	NIST/VALD
4267.381	4267.260	C II	0.720	145550.705	NIST/VALD
4267.880	4267.759	S II	0.290	129858.175	NIST/VALD

Table 10 continued on next page

Table 10 (*continued*)

λ_{obs} (Å)	λ_{lab} (Å)	Species	$\log gf$	E_{low}	Ref.
4269.398	4269.277	Cr II	-2.020	31084.610	NIST/VALD
4271.881	4271.760	Fe I	-0.160	11976.239	NIST/VALD
4273.438	4273.317	Fe II	-3.300	21812.044	NIST/VALD
4275.688	4275.567	Cr II	-1.520	31116.871	NIST/VALD
4278.272	4278.151	Fe II	-3.950	21712.445	NIST/VALD
4278.735	4278.614	Mn II	-2.430	43311.972	NIST/VALD
4282.070	4281.949	Mn II	-2.440	43336.173	NIST/VALD
4282.611	4282.490	Mn II	-1.660	44521.806	NIST/VALD
4283.891	4283.770	Mn II	-2.040	43336.173	NIST/VALD
4284.309	4284.188	Cr II	-1.670	31084.610	NIST/VALD
4284.549	4284.428	Mn II	-1.970	43311.323	NIST/VALD
4286.392	4286.270	Fe II	-1.710	62169.219	NIST/VALD
4290.337	4290.215	Ti II	-0.850	9395.802	NIST/VALD
4292.355	4292.233	Mn II	-1.540	43395.394	NIST/VALD
4293.392	4293.270	Mn II	-0.400	85960.620	NIST/VALD
4294.216	4294.094	Ti II	-1.110	8744.341	NIST/VALD
4294.246	4294.124	Fe I	-1.110	11976.239	NIST/VALD
4294.520	4294.398	S II	0.580	130134.156	NIST/VALD
4296.689	4296.567	Fe II	-2.900	21812.044	NIST/VALD
4300.164	4300.042	Ti II	-0.440	9518.152	NIST/VALD
4302.044	4301.922	Ti II	-1.150	9363.743	NIST/VALD
4303.290	4303.168	Fe II	-2.610	21812.044	NIST/VALD
4305.569	4305.447	Sr II	-0.110	24516.650	NIST/VALD
4307.988	4307.866	Ti II	-1.070	9395.802	NIST/VALD
4308.024	4307.902	Fe I	-0.070	12560.934	NIST/VALD
4308.275	4308.153	Mn II	-1.900	43696.217	NIST/VALD
4309.036	4308.914	Zr II	-0.800	11984.460	NIST/VALD
4309.744	4309.622	Y II	-0.750	1451.798	NIST/VALD
4310.822	4310.700	Mn II	-0.200	86057.625	NIST/VALD
4312.982	4312.860	Ti II	-1.100	9518.152	NIST/VALD
4313.102	4312.980	Fe II	-1.560	62943.509	NIST/VALD
4314.424	4314.302	Fe II	-3.600	21583.397	NIST/VALD

Table 10 continued on next page

Table 10 (*continued*)

λ_{obs} (Å)	λ_{lab} (Å)	Species	$\log gf$	E_{low}	Ref.
4315.093	4314.971	Ti II	-1.100	9363.743	NIST/VALD
4315.107	4314.985	Fe II	-3.190	38166.155	NIST/VALD
4317.834	4317.712	Mn II	-1.890	55757.109	NIST/VALD
4318.298	4318.176	Fe II	-1.880	63556.492	NIST/VALD
4318.651	4318.529	Mn II	-2.420	43537.810	NIST/VALD
4319.524	4319.402	Fe II	-1.990	61725.611	NIST/VALD
4319.795	4319.673	Fe II	-1.640	63274.196	NIST/VALD
4321.073	4320.950	Ti II	-1.800	9395.802	NIST/VALD
4321.427	4321.304	Fe II	-1.740	63467.773	NIST/VALD
4325.170	4325.047	Mn II	-1.120	43528.661	NIST/VALD
4325.555	4325.432	Fe II	-2.380	49506.310	NIST/VALD
4325.657	4325.534	Fe II	-2.360	49103.030	NIST/VALD
4325.885	4325.762	Fe I	0.010	12968.554	NIST/VALD
4326.767	4326.644	Mn II	-1.370	43537.186	NIST/VALD
4332.076	4331.953	Mg II	-1.150	93799.750	NIST/VALD
4333.375	4333.252	Zr II	-0.600	19433.239	NIST/VALD
4337.106	4336.983	Mn II	-2.750	43852.362	NIST/VALD
4337.737	4337.614	Zr II	-1.000	14298.640	NIST/VALD
4338.037	4337.914	Ti II	-1.130	8710.567	NIST/VALD
4338.468	4338.345	Mn II	-2.070	43850.340	NIST/VALD
4338.819	4338.696	Fe II	-4.330	21712.445	NIST/VALD
4339.678	4339.555	Zr II	-1.700	6467.610	NIST/VALD
4341.195	4341.072	Cr II	-1.650	45731.640	NIST/VALD
4341.479	4341.356	Ti II	-2.280	8997.787	NIST/VALD
4341.764	4341.641	C I	-1.490	64086.924	NIST/VALD
4342.705	4342.582	Mn II	-1.950	44747.641	NIST/VALD
4343.396	4343.273	Fe II	-2.210	49506.310	NIST/VALD
4344.106	4343.983	Mn II	-1.110	43528.661	NIST/VALD
4344.404	4344.281	Ti II	-2.090	8744.341	NIST/VALD
4345.716	4345.593	Mn II	-2.180	43537.810	NIST/VALD
4346.514	4346.391	Mn II	-1.550	52716.400	NIST/VALD
4348.519	4348.396	Mn II	-1.800	43696.217	NIST/VALD

Table 10 continued on next page

Table 10 (*continued*)

λ_{obs} (Å)	λ_{lab} (Å)	Species	$\log gf$	E_{low}	Ref.
4351.885	4351.762	Cr I	-0.430	8307.575	NIST/VALD
4351.886	4351.763	Fe II	-2.080	21812.044	NIST/VALD
4354.456	4354.333	Fe II	-1.350	61725.611	NIST/VALD
4356.744	4356.620	Mn II	-2.050	43699.122	NIST/VALD
4357.695	4357.571	Fe II	-2.010	49100.956	NIST/VALD
4358.848	4358.724	Y II	-1.320	838.817	NIST/VALD
4359.844	4359.720	Zr II	-0.460	9968.650	NIST/VALD
4361.376	4361.252	Fe II	-2.260	49506.310	NIST/VALD
4363.379	4363.255	Mn II	-1.890	44900.887	NIST/VALD
4365.341	4365.217	Mn II	-1.340	53014.822	NIST/VALD
4367.776	4367.652	Ti II	-0.860	20891.790	NIST/VALD
4368.366	4368.242	O I	-1.960	76794.977	NIST/VALD
4368.374	4368.250	O I	-2.190	76794.977	NIST/VALD
4369.524	4369.400	Fe II	-3.600	22409.818	NIST/VALD
4371.071	4370.947	Zr II	-0.860	9742.800	NIST/VALD
4375.057	4374.933	Y II	0.160	3298.808	NIST/VALD
4377.093	4376.969	Si II	-0.900	103553.528	NIST/VALD
4377.118	4376.994	Si II	-1.020	103553.528	NIST/VALD
4377.891	4377.767	Mn II	-2.180	43852.362	NIST/VALD
4379.793	4379.669	Mn II	-1.870	43852.362	NIST/VALD
4379.866	4379.742	Zr II	-0.360	12359.661	NIST/VALD
4383.669	4383.545	Fe I	0.200	11976.239	NIST/VALD
4384.213	4384.089	Fe II	-2.580	50216.076	NIST/VALD
4384.437	4384.313	Fe II	-3.700	21430.357	NIST/VALD
4384.761	4384.637	Mg II	-0.780	80619.500	NIST/VALD
4385.503	4385.379	Fe II	-2.600	22409.818	NIST/VALD
4386.971	4386.847	Ti II	-0.960	20951.754	NIST/VALD
4388.054	4387.930	He I	-0.887	171134.897	NIST
4390.638	4390.514	Mg II	-1.480	80650.022	NIST/VALD
4390.688	4390.564	Mg II	-0.520	80650.022	NIST/VALD
4393.510	4393.385	Mn II	-1.460	44139.032	NIST/VALD
4395.156	4395.031	Ti II	-0.660	8744.341	NIST/VALD

Table 10 continued on next page

Table 10 (*continued*)

λ_{obs} (Å)	λ_{lab} (Å)	Species	$\log gf$	E_{low}	Ref.
4398.135	4398.010	Y II	-1.000	1048.521	NIST/VALD
4399.890	4399.765	Ti II	-1.190	9975.999	NIST/VALD
4403.004	4402.879	Fe II	-2.600	49506.924	NIST/VALD
4403.637	4403.512	Mn II	-1.820	53014.822	NIST/VALD
4404.875	4404.750	Fe I	-0.140	12560.934	NIST/VALD
4404.875	4404.750	Zr II	-1.400	14733.370	NIST/VALD
4406.468	4406.343	Fe II	0.580	109465.565	NIST/VALD
4407.906	4407.781	Fe II	0.780	109473.634	NIST/VALD
4409.650	4409.525	Fe II	0.950	109489.771	NIST/VALD
4411.197	4411.072	Ti II	-0.670	24961.191	NIST/VALD
4413.725	4413.600	Fe II	-4.200	21581.615	NIST/VALD
4416.943	4416.818	Fe II	-2.600	22409.818	NIST/VALD
4417.839	4417.714	Ti II	-1.430	9395.802	NIST/VALD
4419.066	4418.941	Fe II	-1.850	64088.814	NIST/VALD
4419.721	4419.596	Fe III	-2.210	66468.153	NIST/VALD
4420.835	4420.710	P II	-0.330	88893.219	NIST/VALD
4422.710	4422.585	Y II	-1.270	838.817	NIST/VALD
4422.716	4422.591	Y II	-1.270	840.213	NIST/VALD
4428.120	4427.994	Mg II	-1.210	80619.500	NIST/VALD
4431.722	4431.596	Fe II	-1.790	64040.422	NIST/VALD
4434.116	4433.990	Mg II	-0.910	80650.022	NIST/VALD
4434.193	4434.067	Mn II	-1.510	53014.822	NIST/VALD
4435.867	4435.741	Mn II	-2.580	44142.727	NIST/VALD
4436.612	4436.486	Mg II	-0.820	93310.590	NIST/VALD
4436.724	4436.598	Mg II	-0.980	93311.112	NIST/VALD
4442.122	4441.996	Mn II	-2.210	44139.032	NIST/VALD
4443.134	4443.008	Zr II	-0.330	11984.460	NIST/VALD
4443.927	4443.801	Ti II	-0.720	8710.567	NIST/VALD
4444.662	4444.536	Fe II	-2.640	50159.621	NIST/VALD
4449.736	4449.610	Fe II	-1.700	63948.803	NIST/VALD
4450.608	4450.482	Ti II	-1.520	8744.341	NIST/VALD
4451.668	4451.542	Fe II	-1.910	49506.924	NIST/VALD

Table 10 continued on next page

Table 10 (*continued*)

λ_{obs} (Å)	λ_{lab} (Å)	Species	$\log gf$	E_{low}	Ref.
4455.387	4455.261	Fe II	-2.000	50216.076	NIST/VALD
4457.557	4457.431	Zr II	-0.800	9553.100	NIST/VALD
4461.838	4461.711	Fe II	-2.100	50212.834	NIST/VALD
4465.858	4465.731	Cr II	-1.280	52321.189	NIST/VALD
4468.619	4468.492	Ti II	-0.620	9118.285	NIST/VALD
4471.607	4471.480	He I	group	169086.800	NIST
4473.048	4472.921	Fe II	-3.500	22939.352	NIST/VALD
4475.387	4475.260	P II	0.440	105549.673	NIST/VALD
4478.764	4478.637	Mn II	-0.940	53595.541	NIST/VALD
4480.818	4480.691	Fe II	-2.560	50216.076	NIST/VALD
4481.257	4481.130	Mg II	0.750	71490.190	NIST/VALD
4481.277	4481.150	Mg II	-0.550	71490.190	NIST/VALD
4481.454	4481.327	Mg II	0.590	71491.058	NIST/VALD
4488.452	4488.325	Ti II	-0.510	25192.965	NIST/VALD
4489.312	4489.185	Fe II	-3.000	22810.345	NIST/VALD
4491.527	4491.400	Fe II	-2.640	23031.283	NIST/VALD
4493.652	4493.525	Fe II	-1.560	63876.325	NIST/VALD
4494.545	4494.418	Zr II	-0.480	19433.239	NIST/VALD
4497.108	4496.980	Zr II	-0.860	5752.920	NIST/VALD
4498.069	4497.941	Mn II	-2.600	43529.741	NIST/VALD
4498.988	4498.860	Mn II	-2.300	48433.592	NIST/VALD
4499.812	4499.684	Fe II	-1.680	62048.230	NIST/VALD
4500.671	4500.543	Mn II	-2.040	48336.810	NIST/VALD
4501.398	4501.270	Ti II	-0.770	8997.787	NIST/VALD
4503.329	4503.201	Mn II	-2.140	48320.677	NIST/VALD
4507.219	4507.091	Fe II	-1.760	62693.478	NIST/VALD
4508.408	4508.280	Fe II	-2.300	23031.283	NIST/VALD
4515.462	4515.334	Fe II	-2.360	22939.352	NIST/VALD
4519.084	4518.956	Mn II	-1.310	53595.541	NIST/VALD
4519.368	4519.240	Mn II	-2.570	43537.810	NIST/VALD
4520.349	4520.221	Fe II	-2.600	22637.195	NIST/VALD
4522.756	4522.628	Fe II	-1.990	22939.352	NIST/VALD

Table 10 continued on next page

Table 10 (*continued*)

λ_{obs} (Å)	λ_{lab} (Å)	Species	$\log gf$	E_{low}	Ref.
4525.075	4524.947	S II	0.030	121530.021	NIST/VALD
4525.454	4525.326	Mn II	-2.120	48433.592	NIST/VALD
4534.089	4533.960	Ti II	-0.770	9975.999	NIST/VALD
4534.295	4534.166	Fe II	-3.400	23031.283	NIST/VALD
4534.408	4534.279	Mg II	-1.050	93799.630	NIST/VALD
4534.433	4534.304	Mg II	-0.940	93799.750	NIST/VALD
4541.647	4541.518	Fe II	-3.000	23031.283	NIST/VALD
4549.326	4549.197	Fe II	-1.770	47674.729	NIST/VALD
4549.596	4549.467	Fe II	-1.730	22810.345	NIST/VALD
4549.751	4549.622	Ti II	-0.100	12774.817	NIST/VALD
4554.162	4554.033	Ba II	0.140	0.000	NIST/VALD
4555.118	4554.989	Cr II	-1.370	32836.653	NIST/VALD
4556.017	4555.888	Fe II	-2.250	22810.345	NIST/VALD
4558.773	4558.644	Cr II	-0.660	32854.249	NIST/VALD
4563.886	4563.757	Ti II	-0.960	9851.014	NIST/VALD
4565.864	4565.735	Cr II	-2.110	32603.349	NIST/VALD
4572.101	4571.971	Ti II	-0.320	12677.106	NIST/VALD
4576.458	4576.328	Fe II	-2.920	22939.352	NIST/VALD
4579.651	4579.521	Fe II	-2.340	50216.076	NIST/VALD
4580.183	4580.053	Fe II	-3.900	20833.301	NIST/VALD
4582.965	4582.835	Fe II	-3.060	22939.352	NIST/VALD
4583.959	4583.829	Fe II	-1.740	22637.195	NIST/VALD
4588.170	4588.040	P II	0.570	103339.144	NIST/VALD
4588.328	4588.198	Cr II	-0.640	32836.653	NIST/VALD
4589.990	4589.860	P II	0.400	103165.615	NIST/VALD
4590.077	4589.947	Ti II	-1.780	9975.999	NIST/VALD
4592.182	4592.052	Cr II	-1.220	32854.941	NIST/VALD
4596.138	4596.008	Fe II	-1.960	50212.834	NIST/VALD
4598.615	4598.485	Fe II	-1.540	62945.045	NIST/VALD
4602.210	4602.080	P II	0.740	103667.860	NIST/VALD
4616.755	4616.624	Cr II	-1.290	32844.706	NIST/VALD
4618.938	4618.807	Cr II	-1.110	32854.941	NIST/VALD

Table 10 continued on next page

Table 10 (*continued*)

λ_{obs} (Å)	λ_{lab} (Å)	Species	$\log gf$	E_{low}	Ref.
4619.753	4619.622	Fe II	-1.960	62169.219	NIST/VALD
4620.644	4620.513	Fe II	-3.190	22810.345	NIST/VALD
4621.551	4621.420	Si II	-0.610	101023.046	NIST/VALD
4621.851	4621.720	Si II	-0.450	101024.349	NIST/VALD
4626.029	4625.898	Fe II	-2.550	48038.381	NIST/VALD
4628.910	4628.779	Fe II	-1.700	63272.980	NIST/VALD
4629.421	4629.290	Ti II	-2.250	9518.152	NIST/VALD
4629.463	4629.332	Fe II	-2.260	22637.195	NIST/VALD
4634.204	4634.073	Cr II	-1.240	32844.706	NIST/VALD
4635.449	4635.318	Fe II	-1.580	48039.109	NIST/VALD
4638.172	4638.040	Fe II	-1.540	62169.219	NIST/VALD
4640.934	4640.802	Fe II	-1.740	62171.625	NIST/VALD
4657.113	4656.981	Fe II	-3.570	23317.635	NIST/VALD
4663.188	4663.056	Al II	-0.240	85481.348	NIST/VALD
4663.836	4663.704	Fe II	-3.890	23317.488	NIST/VALD
4666.876	4666.744	Fe II	-3.400	22810.345	NIST/VALD
4670.302	4670.170	Fe II	-4.100	20830.553	NIST/VALD
4673.389	4673.256	Si II	-0.640	103556.025	NIST/VALD
4673.417	4673.284	Si II	-0.790	103556.156	NIST/VALD
4689.679	4689.546	Mn II	-2.410	49425.654	NIST/VALD
4702.866	4702.733	Mn II	-2.270	49820.865	NIST/VALD
4716.401	4716.267	S II	-0.370	109831.595	NIST/VALD
4717.398	4717.264	Mn II	-1.840	52716.400	NIST/VALD
4727.975	4727.841	Mn II	-1.950	43311.972	NIST/VALD
4730.530	4730.396	Mn II	-2.020	43336.173	NIST/VALD
4731.573	4731.439	Fe II	-3.100	23317.635	NIST/VALD
4734.270	4734.136	Mn II	-2.720	43336.173	NIST/VALD
4738.434	4738.300	Mn II	-1.870	43395.394	NIST/VALD
4739.722	4739.588	Mg II	-0.660	93310.590	NIST/VALD
4739.846	4739.712	Mg II	-0.820	93311.112	NIST/VALD
4749.247	4749.112	Mn II	-1.960	49893.458	NIST/VALD
4755.862	4755.727	Mn II	-1.220	43529.741	NIST/VALD

Table 10 continued on next page

Table 10 (*continued*)

λ_{obs} (Å)	λ_{lab} (Å)	Species	$\log gf$	E_{low}	Ref.
4762.515	4762.380	Mn I	0.430	23296.670	NIST/VALD
4762.924	4762.789	Mn II	-2.500	43529.741	NIST/VALD
4764.863	4764.728	Mn II	-1.330	43537.810	NIST/VALD
4770.486	4770.351	Mn II	-2.260	43537.810	NIST/VALD
4780.115	4779.979	Ti II	-1.370	16515.936	NIST/VALD
4783.556	4783.420	Mn I	0.040	18531.640	NIST/VALD
4784.761	4784.625	Mn II	-1.500	53014.822	NIST/VALD
4791.918	4791.782	Mn II	-1.680	49885.389	NIST/VALD
4805.229	4805.093	Ti II	-1.120	16625.244	NIST/VALD
4806.996	4806.860	Mn II	-1.840	43696.217	NIST/VALD
4811.759	4811.623	Mn II	-2.360	43699.122	NIST/VALD
4812.169	4812.033	Mn II	-2.290	49885.389	NIST/VALD
4812.480	4812.344	Cr II	-1.800	31168.575	NIST/VALD
4815.686	4815.549	S II	0.070	110268.595	NIST/VALD
4820.965	4820.828	Fe II	-0.720	83136.510	NIST/VALD
4823.657	4823.520	Mn I	0.140	18705.370	NIST/VALD
4824.268	4824.131	Cr II	-1.230	31219.331	NIST/VALD
4826.820	4826.683	Fe II	-0.500	82978.717	NIST/VALD
4830.197	4830.060	Mn II	-1.850	49820.865	NIST/VALD
4836.367	4836.230	Cr II	-2.250	31117.325	NIST/VALD
4839.873	4839.736	Mn II	-1.870	49893.458	NIST/VALD
4842.462	4842.325	Mn II	-2.070	49885.389	NIST/VALD
4847.745	4847.608	Mn II	-1.840	43852.362	NIST/VALD
4848.387	4848.250	Cr II	-1.130	31168.575	NIST/VALD
4851.208	4851.070	Mg II	-0.790	93799.630	NIST/VALD
4851.237	4851.099	Mg II	-0.680	93799.750	NIST/VALD
4851.675	4851.537	Mn II	-2.670	43852.362	NIST/VALD
4854.999	4854.861	Y II	-0.380	8001.020	NIST/VALD
4855.679	4855.541	Fe II	-4.440	21809.232	NIST/VALD
4856.328	4856.190	Cr II	-2.260	31082.883	NIST/VALD
4859.879	4859.741	Fe I	-0.760	23192.500	NIST/VALD
4860.340	4860.202	Cr II	-2.040	31221.723	NIST/VALD

Table 10 continued on next page

Table 10 (*continued*)

λ_{obs} (Å)	λ_{lab} (Å)	Species	$\log gf$	E_{low}	Ref.
4860.818	4860.680	Fe II	-0.380	82853.704	NIST/VALD
4864.464	4864.326	Cr II	-1.360	31116.871	NIST/VALD
4866.337	4866.199	Fe II	-0.670	83136.510	NIST/VALD
4871.407	4871.269	Fe II	-4.240	21809.232	NIST/VALD
4871.456	4871.318	Fe I	-0.360	23110.940	NIST/VALD
4874.148	4874.010	Ti II	-0.800	24961.191	NIST/VALD
4876.537	4876.399	Cr II	-1.460	31084.610	NIST/VALD
4876.627	4876.489	Cr II	-1.470	31168.575	NIST/VALD
4883.430	4883.292	Fe II	-0.600	82853.704	NIST/VALD
4883.820	4883.682	Y II	0.070	8743.050	NIST/VALD
4884.742	4884.604	Cr II	-2.080	31117.325	NIST/VALD
4891.631	4891.492	Fe I	-0.110	22996.675	NIST/VALD
4900.258	4900.119	Y II	-0.090	8331.707	NIST/VALD
4901.762	4901.623	Cr II	-1.140	52321.189	NIST/VALD
4908.284	4908.145	Fe II	-0.270	83308.242	NIST/VALD
4911.334	4911.195	Ti II	-0.610	25192.965	NIST/VALD
4912.601	4912.462	Cr II	-1.260	52296.993	NIST/VALD
4913.434	4913.295	Fe II	0.050	82978.717	NIST/VALD
4917.351	4917.212	S II	-0.380	112937.572	NIST/VALD
4920.576	4920.436	Mn II	-2.130	44142.727	NIST/VALD
4920.643	4920.503	Fe I	0.070	22845.870	NIST/VALD
4921.366	4921.226	Mn II	-1.630	53595.541	NIST/VALD
4924.062	4923.922	Fe II	-1.210	23317.635	NIST/VALD
4924.255	4924.115	S II	-0.340	109831.595	NIST/VALD
4925.487	4925.347	S II	-0.210	109560.686	NIST/VALD
4948.227	4948.087	Fe II	-0.220	83136.510	NIST/VALD
4948.931	4948.791	Fe II	-0.030	83459.720	NIST/VALD
4951.721	4951.581	Fe II	0.210	83136.510	NIST/VALD
4952.792	4952.652	Fe II	-0.620	83459.720	NIST/VALD
4954.119	4953.979	Fe II	-2.810	44933.149	NIST/VALD
4957.737	4957.596	Fe I	0.230	22650.416	NIST/VALD
4958.962	4958.821	Fe II	-0.760	83713.585	NIST/VALD

Table 10 continued on next page

Table 10 (*continued*)

λ_{obs} (Å)	λ_{lab} (Å)	Species	$\log gf$	E_{low}	Ref.
4969.497	4969.356	Fe II	-0.830	83558.566	NIST/VALD
4971.359	4971.218	Fe II	-0.500	83558.566	NIST/VALD
4977.139	4976.998	Mn II	-2.130	53700.393	NIST/VALD
4977.174	4977.033	Fe II	-0.040	83558.566	NIST/VALD
4978.060	4977.919	Fe II	-0.600	83308.242	NIST/VALD
4984.626	4984.485	Fe II	0.080	83308.242	NIST/VALD
4990.647	4990.506	Fe II	0.200	83308.242	NIST/VALD
4991.580	4991.438	Fe II	-0.590	82853.704	NIST/VALD
4993.497	4993.355	Fe II	-3.700	22637.195	NIST/VALD
4998.897	4998.755	Mn II	-2.050	53781.049	NIST/VALD
4999.325	4999.183	Fe II	-0.430	82853.704	NIST/VALD
5001.622	5001.480	Ca II	-0.520	60533.018	NIST/VALD
5002.095	5001.953	Fe II	0.920	82853.704	NIST/VALD
5004.330	5004.188	Fe II	0.500	82853.704	NIST/VALD
5006.982	5006.840	Fe II	-0.360	83713.585	NIST/VALD
5007.591	5007.449	Fe II	-0.460	83726.416	NIST/VALD
5007.876	5007.734	Fe II	-0.280	82978.717	NIST/VALD
5009.126	5008.984	Fe II	-0.530	83459.720	NIST/VALD
5009.706	5009.564	S II	-0.230	109831.595	NIST/VALD
5010.203	5010.061	Fe II	-0.690	83726.416	NIST/VALD
5012.126	5011.984	Fe II	-0.880	83459.720	NIST/VALD
5014.211	5014.069	S II	0.050	113461.537	NIST/VALD
5015.820	5015.678	He I	-0.820	166277.440	NIST
5015.894	5015.752	Fe II	-0.030	83459.720	NIST/VALD
5018.577	5018.435	Fe II	-1.350	23317.635	NIST/VALD
5019.606	5019.464	Fe II	-2.780	44917.017	NIST/VALD
5020.112	5019.970	Ca II	-0.280	60611.279	NIST/VALD
5020.156	5020.014	Fe II	-0.850	82978.717	NIST/VALD
5021.733	5021.591	Fe II	-0.190	82978.717	NIST/VALD
5022.560	5022.418	Fe II	-0.070	83459.720	NIST/VALD
5022.931	5022.789	Fe II	-0.090	82978.717	NIST/VALD
5026.941	5026.798	Fe II	-0.440	83136.510	NIST/VALD

Table 10 continued on next page

Table 10 (*continued*)

λ_{obs} (Å)	λ_{lab} (Å)	Species	$\log gf$	E_{low}	Ref.
5029.236	5029.093	Fe II	-0.630	83558.566	NIST/VALD
5029.519	5029.376	Mn II	-1.950	53805.244	NIST/VALD
5030.775	5030.632	Fe II	0.430	82978.717	NIST/VALD
5032.038	5031.895	Fe II	-0.830	83990.103	NIST/VALD
5032.590	5032.447	S II	0.190	110268.595	NIST/VALD
5032.846	5032.703	Fe II	0.080	83812.350	NIST/VALD
5034.147	5034.004	Fe II	-0.800	83558.566	NIST/VALD
5035.843	5035.700	Fe II	0.630	82978.717	NIST/VALD
5036.856	5036.713	Fe II	-0.560	83812.350	NIST/VALD
5040.893	5040.750	Fe II	-0.640	83558.566	NIST/VALD
5041.173	5041.030	Si II	0.030	81191.341	NIST/VALD
5045.250	5045.107	Fe II	0.000	83136.510	NIST/VALD
5047.775	5047.632	Fe II	-0.240	83136.510	NIST/VALD
5049.671	5049.528	Mn II	-2.050	53595.541	NIST/VALD
5052.313	5052.170	C I	-1.300	61981.822	NIST/VALD
5056.123	5055.980	Si II	0.520	81251.320	NIST/VALD
5056.460	5056.317	Si II	-0.490	81251.320	NIST/VALD
5060.392	5060.249	Fe II	-0.650	84266.595	NIST/VALD
5061.854	5061.710	Fe II	0.280	83136.510	NIST/VALD
5065.250	5065.106	Fe II	-0.550	84131.623	NIST/VALD
5068.034	5067.890	Fe II	-0.080	83308.242	NIST/VALD
5071.040	5070.896	Fe II	0.270	83136.510	NIST/VALD
5074.040	5073.896	Fe II	-0.720	84266.595	NIST/VALD
5074.195	5074.051	Fe II	-2.200	54904.243	NIST/VALD
5075.904	5075.760	Fe II	0.180	84326.965	NIST/VALD
5082.370	5082.226	Fe II	-0.130	83990.103	NIST/VALD
5083.646	5083.502	Fe II	-0.750	83459.720	NIST/VALD
5086.451	5086.307	Fe II	-0.420	83990.103	NIST/VALD
5087.444	5087.300	Fe II	-0.420	83713.585	NIST/VALD
5087.563	5087.419	Y II	-0.170	8743.050	NIST/VALD
5089.357	5089.213	Fe II	0.010	83308.242	NIST/VALD
5089.637	5089.493	Fe II	-0.410	84326.965	NIST/VALD

Table 10 continued on next page

Table 10 (*continued*)

λ_{obs} (Å)	λ_{lab} (Å)	Species	$\log gf$	E_{low}	Ref.
5093.603	5093.459	Fe II	-2.320	54869.899	NIST/VALD
5093.716	5093.572	Fe II	0.170	83713.585	NIST/VALD
5095.045	5094.901	Fe II	-0.720	84424.421	NIST/VALD
5097.050	5096.905	Fe II	-0.600	83726.416	NIST/VALD
5097.419	5097.274	Fe II	0.320	83713.585	NIST/VALD
5097.464	5097.319	Cr II	-2.630	29951.815	NIST/VALD
5098.827	5098.682	Fe II	-0.490	84268.805	NIST/VALD
5100.757	5100.612	Fe II	0.230	83726.416	NIST/VALD
5100.800	5100.655	Fe II	-4.200	22637.195	NIST/VALD
5100.879	5100.734	Fe II	0.720	83726.416	NIST/VALD
5100.999	5100.854	Fe II	-2.200	47674.729	NIST/VALD
5102.662	5102.517	Mn II	-1.900	48320.677	NIST/VALD
5106.251	5106.106	Fe II	-0.250	83308.242	NIST/VALD
5107.237	5107.092	Mn II	-1.470	59539.848	NIST/VALD
5107.253	5107.108	Fe II	-0.830	83459.720	NIST/VALD
5107.686	5107.541	Fe II	-0.640	83812.350	NIST/VALD
5112.299	5112.154	Fe II	-0.790	84326.965	NIST/VALD
5112.442	5112.297	Zr II	-0.590	13428.500	NIST/VALD
5113.144	5112.999	Fe II	-0.530	83812.350	NIST/VALD
5115.206	5115.061	Fe II	-0.500	84131.623	NIST/VALD
5117.176	5117.031	Fe II	-0.040	84131.623	NIST/VALD
5119.479	5119.334	Fe II	-0.670	83812.350	NIST/VALD
5121.242	5121.097	Fe II	0.360	104110.051	NIST/VALD
5122.014	5121.869	Fe II	0.400	103755.162	NIST/VALD
5123.355	5123.210	Y II	-0.830	8001.020	NIST/VALD
5123.471	5123.326	Mn II	-1.850	48336.810	NIST/VALD
5123.578	5123.433	Fe II	0.350	103706.771	NIST/VALD
5127.452	5127.307	Fe II	0.440	103755.162	NIST/VALD
5128.007	5127.862	Fe II	-2.450	44933.149	NIST/VALD
5129.301	5129.156	Ti II	-1.240	15257.553	NIST/VALD
5130.171	5130.026	Fe II	0.270	103771.300	NIST/VALD
5130.313	5130.168	Fe II	0.670	108392.853	NIST/VALD

Table 10 continued on next page

Table 10 (*continued*)

λ_{obs} (Å)	λ_{lab} (Å)	Species	$\log gf$	E_{low}	Ref.
5132.807	5132.661	Fe II	-4.100	22637.195	NIST/VALD
5134.219	5134.073	Fe II	0.290	104916.599	NIST/VALD
5134.346	5134.200	Fe II	0.390	105158.567	NIST/VALD
5139.583	5139.437	Fe II	0.430	103981.003	NIST/VALD
5139.639	5139.493	Fe II	0.350	103981.003	NIST/VALD
5141.523	5141.377	Fe II	-0.770	84424.421	NIST/VALD
5144.020	5143.874	Fe II	-0.200	84266.595	NIST/VALD
5144.498	5144.352	Fe II	0.310	84424.421	NIST/VALD
5145.876	5145.730	Fe II	-0.210	83990.103	NIST/VALD
5145.968	5145.822	Fe II	-0.140	83990.103	NIST/VALD
5146.264	5146.118	Fe II	-4.080	22809.360	NIST/VALD
5148.679	5148.533	Fe II	0.340	103835.807	NIST/VALD
5149.045	5148.899	Fe II	-0.420	83990.103	NIST/VALD
5149.376	5149.230	Fe II	0.410	103601.919	NIST/VALD
5149.608	5149.462	Fe II	0.550	84266.595	NIST/VALD
5150.627	5150.481	Fe II	-0.080	84266.595	NIST/VALD
5151.688	5151.542	Fe II	0.260	104206.833	NIST/VALD
5152.850	5152.704	Fe II	0.640	103601.919	NIST/VALD
5153.122	5152.976	Fe II	0.770	103618.046	NIST/VALD
5153.645	5153.499	Cr II	-2.500	30310.315	NIST/VALD
5153.928	5153.782	Fe II	0.760	103618.046	NIST/VALD
5154.647	5154.501	Fe II	0.410	103876.141	NIST/VALD
5154.887	5154.741	Fe II	-0.790	84296.883	NIST/VALD
5156.257	5156.111	Fe III	-1.990	69694.365	NIST/VALD
5156.601	5156.455	Fe II	0.510	103601.919	NIST/VALD
5157.409	5157.263	Fe II	0.380	103618.046	NIST/VALD
5157.429	5157.283	Fe II	-0.170	84326.965	NIST/VALD
5158.205	5158.059	Fe II	0.810	103972.934	NIST/VALD
5160.986	5160.840	Fe II	-2.600	44915.056	NIST/VALD
5161.448	5161.302	Fe II	0.500	105416.662	NIST/VALD
5163.161	5163.015	Fe II	0.490	103642.253	NIST/VALD
5163.718	5163.572	Fe II	0.900	103835.807	NIST/VALD

Table 10 continued on next page

Table 10 (*continued*)

λ_{obs} (Å)	λ_{lab} (Å)	Species	$\log gf$	E_{low}	Ref.
5165.076	5164.930	Fe II	0.560	108134.747	NIST/VALD
5165.788	5165.642	Fe II	0.590	108707.408	NIST/VALD
5165.878	5165.732	Fe II	0.450	103005.074	NIST/VALD
5166.343	5166.197	Fe II	0.930	108134.747	NIST/VALD
5166.697	5166.551	Fe II	-0.040	84326.965	NIST/VALD
5167.469	5167.322	Mg I	-0.870	21850.405	NIST/VALD
5167.673	5167.526	Fe II	-0.770	84526.899	NIST/VALD
5169.175	5169.028	Fe II	-0.870	23317.635	NIST/VALD
5170.251	5170.104	Fe II	0.730	105061.784	NIST/VALD
5170.923	5170.776	Fe II	-0.330	84326.965	NIST/VALD
5171.449	5171.302	Fe II	0.410	105295.683	NIST/VALD
5171.586	5171.439	Fe II	0.290	104069.717	NIST/VALD
5172.831	5172.684	Mg I	-0.390	21870.463	NIST/VALD
5173.276	5173.129	Fe II	0.460	105061.784	NIST/VALD
5176.858	5176.711	Fe II	0.350	103706.771	NIST/VALD
5177.165	5177.018	Fe II	-0.200	83713.585	NIST/VALD
5177.536	5177.389	Fe II	1.160	103642.253	NIST/VALD
5177.795	5177.648	Mn II	-1.750	48433.592	NIST/VALD
5177.941	5177.794	Fe II	0.650	108183.149	NIST/VALD
5178.521	5178.374	Fe II	-0.330	84131.623	NIST/VALD
5179.289	5179.142	Fe II	0.480	108578.360	NIST/VALD
5179.682	5179.535	Fe II	0.550	103706.771	NIST/VALD
5180.459	5180.312	Fe II	-0.090	83812.350	NIST/VALD
5183.751	5183.604	Mg I	-0.170	21911.178	NIST/VALD
5183.862	5183.715	Fe II	0.220	103755.162	NIST/VALD
5185.379	5185.232	Si II	0.530	131863.595	NIST/VALD
5185.588	5185.441	Fe II	0.400	105529.582	NIST/VALD
5185.667	5185.520	Si II	-0.300	103556.025	NIST/VALD
5185.702	5185.555	Si II	-0.460	103556.156	NIST/VALD
5186.049	5185.902	Ti II	-1.490	15265.700	NIST/VALD
5187.014	5186.867	Fe II	-0.190	84424.421	NIST/VALD
5188.834	5188.687	Ti II	-1.220	12758.260	NIST/VALD

Table 10 continued on next page

Table 10 (*continued*)

λ_{obs} (Å)	λ_{lab} (Å)	Species	$\log gf$	E_{low}	Ref.
5190.156	5190.009	Fe II	0.490	105400.535	NIST/VALD
5191.062	5190.915	Fe II	-0.480	84710.751	NIST/VALD
5191.557	5191.410	P II	-0.370	86743.961	NIST/VALD
5191.739	5191.592	Zr II	-0.710	14162.900	NIST/VALD
5192.762	5192.615	Fe II	0.200	103101.857	NIST/VALD
5192.898	5192.751	Fe II	0.700	103101.857	NIST/VALD
5193.007	5192.860	Si II	0.670	131992.620	NIST/VALD
5193.881	5193.734	Fe II	0.740	104190.707	NIST/VALD
5194.528	5194.381	Fe II	0.780	103706.771	NIST/VALD
5195.035	5194.888	Fe II	-0.110	84424.421	NIST/VALD
5195.402	5195.255	Fe II	0.440	104190.707	NIST/VALD
5196.083	5195.936	Fe II	0.920	104174.580	NIST/VALD
5196.587	5196.440	Fe II	-0.630	83713.585	NIST/VALD
5197.715	5197.568	Fe II	-2.050	26055.412	NIST/VALD
5199.266	5199.119	Fe II	0.120	83713.585	NIST/VALD
5200.557	5200.410	Y II	-0.570	8001.020	NIST/VALD
5200.945	5200.798	Fe II	-0.040	83812.350	NIST/VALD
5201.598	5201.451	Fe II	0.810	105594.111	NIST/VALD
5202.739	5202.591	Fe II	-0.720	83726.416	NIST/VALD
5202.812	5202.664	Si II	0.890	131863.595	NIST/VALD
5202.829	5202.681	Si II	0.870	132162.012	NIST/VALD
5203.782	5203.634	Fe II	-0.110	83812.350	NIST/VALD
5205.870	5205.722	Y II	-0.340	8331.707	NIST/VALD
5210.698	5210.550	Fe II	0.790	103166.386	NIST/VALD
5211.679	5211.531	Ti II	-1.170	20891.790	NIST/VALD
5212.771	5212.623	S II	0.320	121530.021	NIST/VALD
5212.979	5212.831	Fe II	-0.300	84844.864	NIST/VALD
5213.682	5213.534	Fe II	-0.760	84870.912	NIST/VALD
5214.100	5213.952	Fe II	-0.260	84527.806	NIST/VALD
5214.151	5214.003	Fe II	0.860	104069.717	NIST/VALD
5214.203	5214.055	Fe II	-0.600	83713.585	NIST/VALD
5214.638	5214.490	Fe II	-0.590	84710.751	NIST/VALD

Table 10 continued on next page

Table 10 (*continued*)

λ_{obs} (Å)	λ_{lab} (Å)	Species	$\log gf$	E_{low}	Ref.
5215.332	5215.184	Fe II	1.120	108336.392	NIST/VALD
5215.495	5215.347	Fe II	0.000	83713.585	NIST/VALD
5215.907	5215.759	Fe II	-1.610	65693.858	NIST/VALD
5215.994	5215.846	Fe II	-0.160	83726.416	NIST/VALD
5217.007	5216.859	Fe II	0.670	84527.806	NIST/VALD
5217.007	5216.859	Fe II	0.480	84710.751	NIST/VALD
5218.990	5218.842	Fe II	-0.170	83726.416	NIST/VALD
5220.068	5219.920	Fe II	-0.550	84870.912	NIST/VALD
5221.183	5221.035	Fe II	0.410	104481.066	NIST/VALD
5222.500	5222.352	Fe II	-0.280	84844.864	NIST/VALD
5223.337	5223.189	Fe II	0.450	103876.141	NIST/VALD
5223.408	5223.260	Fe II	-0.170	83812.350	NIST/VALD
5223.952	5223.804	Fe II	-0.500	83713.585	NIST/VALD
5224.552	5224.404	Fe II	-0.430	83990.103	NIST/VALD
5225.362	5225.214	Fe II	0.980	105287.615	NIST/VALD
5225.491	5225.343	Fe II	0.710	103190.571	NIST/VALD
5225.524	5225.376	Fe II	0.760	105529.582	NIST/VALD
5226.111	5225.963	Fe II	-0.440	83812.350	NIST/VALD
5226.213	5226.065	Fe II	0.800	103876.141	NIST/VALD
5226.686	5226.538	Ti II	-1.290	12628.845	NIST/VALD
5227.244	5227.096	Fe II	-2.450	54063.344	NIST/VALD
5227.465	5227.317	Fe II	0.190	84844.864	NIST/VALD
5227.634	5227.486	Fe II	0.850	84296.883	NIST/VALD
5227.730	5227.582	Fe II	-2.200	54063.355	NIST/VALD
5227.909	5227.761	Fe II	-0.500	84296.883	NIST/VALD
5228.781	5228.633	Fe II	0.900	108779.995	NIST/VALD
5229.040	5228.892	Fe II	-0.300	84266.595	NIST/VALD
5232.060	5231.912	Fe II	-0.650	84938.264	NIST/VALD
5232.644	5232.496	Cr II	-2.360	32834.831	NIST/VALD
5232.929	5232.781	Fe II	-0.080	83726.416	NIST/VALD
5233.088	5232.940	Fe I	-0.060	23711.456	NIST/VALD
5234.427	5234.279	Fe II	0.980	104118.119	NIST/VALD

Table 10 continued on next page

Table 10 (*continued*)

λ_{obs} (Å)	λ_{lab} (Å)	Species	$\log gf$	E_{low}	Ref.
5234.772	5234.624	Fe II	-2.210	25981.646	NIST/VALD
5236.769	5236.621	Fe II	-0.680	84326.965	NIST/VALD
5237.470	5237.322	Cr II	-1.160	32854.249	NIST/VALD
5238.098	5237.949	Fe II	0.100	84266.595	NIST/VALD
5239.538	5239.389	Fe II	0.860	104319.754	NIST/VALD
5239.956	5239.807	Fe II	-0.480	84326.965	NIST/VALD
5241.203	5241.054	Fe II	-0.580	83812.350	NIST/VALD
5241.328	5241.179	Fe II	0.550	103876.141	NIST/VALD
5243.329	5243.180	Fe II	-1.700	66612.660	NIST/VALD
5245.219	5245.070	Fe II	0.870	108465.440	NIST/VALD
5245.603	5245.454	Fe II	-0.540	84326.965	NIST/VALD
5246.922	5246.773	Cr II	-2.460	29951.815	NIST/VALD
5248.104	5247.955	Fe II	0.550	84938.264	NIST/VALD
5249.489	5249.340	Fe II	-0.590	83990.103	NIST/VALD
5249.584	5249.435	Cr II	-2.620	30307.366	NIST/VALD
5251.359	5251.210	Fe II	-0.660	84325.265	NIST/VALD
5251.374	5251.225	Fe II	0.420	84844.864	NIST/VALD
5251.464	5251.315	Fe II	0.630	105400.535	NIST/VALD
5251.972	5251.823	Mn II	-1.820	56886.287	NIST/VALD
5253.669	5253.520	P II	0.320	88893.219	NIST/VALD
5253.797	5253.648	Fe II	-0.130	84296.883	NIST/VALD
5254.550	5254.401	Fe II	-0.460	84685.247	NIST/VALD
5255.069	5254.920	Fe II	-3.340	26051.708	NIST/VALD
5257.081	5256.932	Fe II	-4.180	23317.488	NIST/VALD
5257.268	5257.119	Fe II	0.160	84685.247	NIST/VALD
5258.042	5257.893	Fe II	-0.530	84326.965	NIST/VALD
5260.403	5260.254	Fe II	1.090	84035.172	NIST/VALD
5262.462	5262.313	Fe II	-0.370	85048.655	NIST/VALD
5264.169	5264.020	Fe II	-0.440	84685.247	NIST/VALD
5264.328	5264.179	Fe II	0.300	84710.751	NIST/VALD
5264.364	5264.215	Mg II	-0.370	93310.590	NIST/VALD
5264.517	5264.368	Mg II	-0.530	93311.112	NIST/VALD

Table 10 continued on next page

Table 10 (*continued*)

λ_{obs} (Å)	λ_{lab} (Å)	Species	$\log gf$	E_{low}	Ref.
5264.950	5264.801	Fe II	-3.230	26055.412	NIST/VALD
5270.181	5270.032	Fe II	-0.200	84710.751	NIST/VALD
5272.562	5272.413	Fe II	-2.010	48039.109	NIST/VALD
5275.115	5274.965	Cr II	-1.560	32834.831	NIST/VALD
5276.147	5275.997	Fe II	-1.900	25805.326	NIST/VALD
5278.346	5278.196	Fe II	-1.600	66524.608	NIST/VALD
5279.089	5278.939	Fe II	-2.680	47675.430	NIST/VALD
5280.028	5279.878	Cr II	-2.100	32854.249	NIST/VALD
5280.204	5280.054	Cr II	-2.320	32859.027	NIST/VALD
5283.233	5283.083	Fe II	0.340	104319.754	NIST/VALD
5284.242	5284.092	Fe II	-3.200	23317.635	NIST/VALD
5288.071	5287.921	Fe II	0.370	105239.223	NIST/VALD
5290.238	5290.088	Fe II	0.500	105763.481	NIST/VALD
5291.811	5291.661	Fe II	0.540	84527.806	NIST/VALD
5294.480	5294.330	Mn II	-0.040	79540.929	NIST/VALD
5295.534	5295.384	Mn II	0.340	79542.406	NIST/VALD
5295.550	5295.400	Mn II	0.360	79544.708	NIST/VALD
5296.227	5296.077	P II	-0.050	87124.006	NIST/VALD
5297.150	5297.000	Mn II	-0.240	79550.458	NIST/VALD
5297.178	5297.028	Mn II	0.400	79550.458	NIST/VALD
5297.210	5297.060	Mn II	0.620	79550.502	NIST/VALD
5299.007	5298.857	Fe II	-0.400	84844.864	NIST/VALD
5299.452	5299.302	Mn II	-0.440	79558.533	NIST/VALD
5299.480	5299.330	Mn II	0.380	79558.533	NIST/VALD
5299.520	5299.370	Mn II	0.830	79558.560	NIST/VALD
5302.552	5302.402	Mn II	0.200	79566.596	NIST/VALD
5302.590	5302.440	Mn II	1.000	79569.219	NIST/VALD
5303.543	5303.393	Fe II	-1.530	66016.482	NIST/VALD
5305.572	5305.422	Fe II	0.860	109054.227	NIST/VALD
5306.003	5305.853	Cr II	-2.160	30866.837	NIST/VALD
5306.332	5306.182	Fe II	0.040	84870.912	NIST/VALD
5307.501	5307.351	Mn II	-2.060	56886.287	NIST/VALD

Table 10 continued on next page

Table 10 (*continued*)

λ_{obs} (Å)	λ_{lab} (Å)	Species	$\log gf$	E_{low}	Ref.
5308.503	5308.352	Fe II	0.550	104118.119	NIST/VALD
5308.572	5308.421	Cr II	-1.810	32836.653	NIST/VALD
5310.781	5310.630	Fe II	-0.610	84527.806	NIST/VALD
5310.843	5310.692	Cr II	-2.270	32844.706	NIST/VALD
5313.251	5313.100	Fe II	-0.720	84844.864	NIST/VALD
5313.732	5313.581	Cr II	-1.650	32854.941	NIST/VALD
5315.231	5315.080	Fe II	-0.420	85048.655	NIST/VALD
5315.712	5315.561	Fe II	-1.460	66379.429	NIST/VALD
5316.221	5316.070	P II	-0.290	86743.961	NIST/VALD
5316.365	5316.214	Fe II	0.340	84035.172	NIST/VALD
5316.761	5316.610	Fe II	-1.780	25428.789	NIST/VALD
5316.928	5316.777	Fe II	-2.800	25981.646	NIST/VALD
5318.206	5318.055	Fe II	-0.230	84527.806	NIST/VALD
5318.890	5318.739	Fe II	-0.540	84035.172	NIST/VALD
5320.883	5320.732	S II	0.430	121530.021	NIST/VALD
5322.013	5321.862	Fe II	0.670	106021.587	NIST/VALD
5322.387	5322.236	Fe II	-0.550	84326.965	NIST/VALD
5325.694	5325.543	Fe II	-3.260	25981.646	NIST/VALD
5329.251	5329.100	O I	-1.590	86625.757	NIST/VALD
5329.831	5329.680	O I	-1.470	86627.777	NIST/VALD
5329.841	5329.690	O I	-1.270	86627.777	NIST/VALD
5330.841	5330.690	Fe II	0.520	103601.919	NIST/VALD
5330.886	5330.735	O I	-1.570	86631.453	NIST/VALD
5330.891	5330.740	O I	-0.980	86631.453	NIST/VALD
5335.020	5334.869	Cr II	-1.830	32842.898	NIST/VALD
5337.873	5337.722	Fe II	-3.790	26051.708	NIST/VALD
5337.923	5337.772	Cr II	-2.300	32859.027	NIST/VALD
5339.339	5339.188	Ca II	-0.330	68057.061	NIST/VALD
5339.339	5339.188	Ca II	-0.450	68057.061	NIST/VALD
5339.745	5339.594	Fe II	0.520	84296.883	NIST/VALD
5340.453	5340.302	Fe II	0.920	109392.978	NIST/VALD
5344.260	5344.108	Fe II	-0.760	84938.264	NIST/VALD

Table 10 continued on next page

Table 10 (*continued*)

λ_{obs} (Å)	λ_{lab} (Å)	Species	$\log gf$	E_{low}	Ref.
5344.902	5344.750	P II	-0.390	86597.549	NIST/VALD
5347.010	5346.858	Fe II	-0.570	84326.965	NIST/VALD
5347.339	5347.187	Fe II	-0.270	85172.826	NIST/VALD
5353.406	5353.254	Fe II	-0.580	84710.751	NIST/VALD
5355.573	5355.421	Fe II	-0.500	84685.247	NIST/VALD
5359.024	5358.872	Fe II	-0.610	84685.247	NIST/VALD
5359.399	5359.247	Fe II	-0.670	84710.751	NIST/VALD
5360.632	5360.480	Fe II	-0.580	85048.655	NIST/VALD
5362.903	5362.751	Fe II	-0.190	84710.751	NIST/VALD
5363.013	5362.861	Fe II	-2.620	25801.677	NIST/VALD
5363.122	5362.970	Fe II	-0.210	84685.247	NIST/VALD
5366.361	5366.209	Fe II	-0.200	84710.751	NIST/VALD
5370.114	5369.962	Fe I	0.540	35257.323	NIST/VALD
5370.429	5370.277	Fe II	-0.570	84266.595	NIST/VALD
5370.468	5370.316	Fe II	-0.780	84710.751	NIST/VALD
5370.586	5370.434	Fe II	-0.770	84326.965	NIST/VALD
5371.429	5371.277	Fe II	-0.700	85048.655	NIST/VALD
5375.994	5375.842	Fe II	-0.330	84296.883	NIST/VALD
5375.994	5375.842	Fe II	-0.700	85048.655	NIST/VALD
5383.522	5383.369	Fe I	0.650	34782.420	NIST/VALD
5387.216	5387.063	Fe II	0.500	84863.380	NIST/VALD
5388.180	5388.027	Fe II	-0.690	84296.883	NIST/VALD
5391.018	5390.865	Cr II	1.100	87140.138	NIST/VALD
5393.993	5393.840	Fe II	-0.250	84296.883	NIST/VALD
5395.904	5395.751	Cr II	0.990	86978.837	NIST/VALD
5396.008	5395.855	Fe II	0.280	85495.368	NIST/VALD
5396.690	5396.537	Cr II	0.720	86736.859	NIST/VALD
5397.958	5397.805	Cr II	0.860	86849.779	NIST/VALD
5398.092	5397.939	Fe II	-0.740	84870.912	NIST/VALD
5399.715	5399.562	Fe II	-0.750	84870.912	NIST/VALD
5401.674	5401.521	Mg II	-0.450	93799.630	NIST/VALD
5401.709	5401.556	Mg II	-0.340	93799.750	NIST/VALD

Table 10 continued on next page

Table 10 (*continued*)

λ_{obs} (Å)	λ_{lab} (Å)	Species	$\log gf$	E_{low}	Ref.
5402.211	5402.058	Fe II	0.470	85184.772	NIST/VALD
5402.928	5402.775	Y II	-0.630	14832.536	NIST/VALD
5403.046	5402.893	Fe II	-0.590	85172.826	NIST/VALD
5404.304	5404.151	Fe I	0.520	35767.564	NIST/VALD
5405.245	5405.092	Fe II	-0.430	85172.826	NIST/VALD
5405.814	5405.661	Fe II	-0.440	84870.912	NIST/VALD
5407.757	5407.604	Cr II	-2.150	30866.837	NIST/VALD
5408.968	5408.815	Fe II	-2.660	48038.381	NIST/VALD
5411.526	5411.373	Fe II	-0.050	85495.368	NIST/VALD
5412.123	5411.970	Fe II	-0.570	85172.826	NIST/VALD
5412.896	5412.743	Fe II	-0.600	84870.912	NIST/VALD
5414.243	5414.089	Fe II	-3.480	25981.646	NIST/VALD
5415.006	5414.852	Fe II	-0.320	84863.380	NIST/VALD
5415.353	5415.199	Fe I	0.640	35379.208	NIST/VALD
5421.079	5420.925	Cr II	-2.360	30307.366	NIST/VALD
5422.072	5421.918	Mn II	-2.100	49425.654	NIST/VALD
5424.222	5424.068	Fe I	0.520	34843.153	NIST/VALD
5425.423	5425.269	Fe II	-3.400	25805.326	NIST/VALD
5426.064	5425.910	P II	0.180	87124.598	NIST/VALD
5427.972	5427.818	Fe II	-1.580	54232.199	NIST/VALD
5428.821	5428.667	S II	-0.180	109560.686	NIST/VALD
5430.141	5429.987	Fe II	0.430	85462.908	NIST/VALD
5432.468	5432.314	Fe II	0.530	104763.356	NIST/VALD
5432.969	5432.815	S II	0.200	109831.595	NIST/VALD
5433.116	5432.962	Fe II	-3.530	26350.134	NIST/VALD
5435.934	5435.780	O I	-1.540	86627.777	NIST/VALD
5437.014	5436.860	O I	-1.400	86631.453	NIST/VALD
5439.854	5439.700	Fe II	-2.380	54273.053	NIST/VALD
5442.513	5442.359	Fe II	-0.310	85048.655	NIST/VALD
5443.598	5443.444	Fe II	-0.600	84527.806	NIST/VALD
5444.541	5444.387	Fe II	-0.170	85495.368	NIST/VALD
5444.771	5444.617	Mn II	-2.320	52385.713	NIST/VALD

Table 10 continued on next page

Table 10 (*continued*)

λ_{obs} (Å)	λ_{lab} (Å)	Species	$\log gf$	E_{low}	Ref.
5445.955	5445.801	Fe II	-0.110	85048.655	NIST/VALD
5449.146	5448.992	Mn II	-2.280	49465.982	NIST/VALD
5450.250	5450.095	Fe II	-0.090	85679.757	NIST/VALD
5451.472	5451.317	Fe II	-0.650	84685.247	NIST/VALD
5453.983	5453.828	S II	0.440	110268.595	NIST/VALD
5456.085	5455.930	Fe II	-0.510	84527.806	NIST/VALD
5456.597	5456.442	Si II	0.650	134218.733	NIST/VALD
5457.877	5457.722	Fe II	-0.140	85728.844	NIST/VALD
5462.300	5462.145	Si II	-1.020	103860.741	NIST/VALD
5466.087	5465.932	Fe II	0.350	85679.757	NIST/VALD
5466.519	5466.364	Fe II	0.710	104626.240	NIST/VALD
5466.585	5466.430	Si II	-0.240	101023.046	NIST/VALD
5467.049	5466.894	Si II	-0.080	101024.349	NIST/VALD
5467.067	5466.912	Fe II	-1.870	54902.288	NIST/VALD
5469.606	5469.451	Si II	-0.760	103885.252	NIST/VALD
5470.933	5470.778	Mn II	-1.990	52385.713	NIST/VALD
5473.009	5472.854	Fe II	-0.720	84685.247	NIST/VALD
5473.775	5473.620	S II	-0.230	109560.686	NIST/VALD
5475.981	5475.826	Fe II	-0.080	84685.247	NIST/VALD
5478.247	5478.092	Si II	-1.160	101024.349	NIST/VALD
5478.520	5478.365	Cr II	-1.970	33697.843	NIST/VALD
5479.554	5479.399	Fe II	-0.350	85172.826	NIST/VALD
5481.112	5480.957	Fe II	-0.490	84870.912	NIST/VALD
5481.426	5481.271	Fe II	-0.280	85462.908	NIST/VALD
5482.460	5482.305	Fe II	0.410	85184.772	NIST/VALD
5487.774	5487.618	Fe II	0.290	85462.908	NIST/VALD
5488.931	5488.775	Fe II	-0.400	85462.908	NIST/VALD
5492.234	5492.078	Fe II	0.090	85679.757	NIST/VALD
5492.554	5492.398	Fe II	-0.100	84685.247	NIST/VALD
5493.987	5493.831	Fe II	0.260	84685.247	NIST/VALD
5497.562	5497.406	Y II	-0.580	14098.572	NIST/VALD
5498.730	5498.574	Fe II	-0.340	85495.368	NIST/VALD

Table 10 continued on next page

Table 10 (*continued*)

λ_{obs} (Å)	λ_{lab} (Å)	Species	$\log gf$	E_{low}	Ref.
5499.886	5499.730	P II	-0.300	87124.598	NIST/VALD
5501.239	5501.083	Mn II	-1.710	52377.644	NIST/VALD
5502.241	5502.085	Cr II	-1.990	33618.936	NIST/VALD
5502.826	5502.670	Fe II	-0.190	85184.772	NIST/VALD
5503.368	5503.212	Cr II	-2.370	33415.550	NIST/VALD
5503.371	5503.215	Fe II	-0.120	84685.247	NIST/VALD
5503.515	5503.359	Fe II	-0.510	85495.368	NIST/VALD
5504.049	5503.893	Fe II	-0.730	84870.912	NIST/VALD
5506.355	5506.199	Fe II	0.860	84863.380	NIST/VALD
5507.226	5507.070	Fe II	-0.060	84870.912	NIST/VALD
5508.779	5508.623	Cr II	-2.120	33521.091	NIST/VALD
5509.874	5509.718	S II	-0.170	109831.595	NIST/VALD
5510.051	5509.895	Y II	-1.010	8001.020	NIST/VALD
5510.119	5509.963	Mn II	-1.770	52385.713	NIST/VALD
5510.795	5510.639	Fe II	-0.680	85184.772	NIST/VALD
5510.939	5510.783	Fe II	0.100	85184.772	NIST/VALD
5511.243	5511.087	Fe II	-0.380	85728.844	NIST/VALD
5511.708	5511.552	Mn II	-1.850	52377.644	NIST/VALD
5525.274	5525.117	Fe II	-3.940	26352.767	NIST/VALD
5529.209	5529.052	Fe II	-0.260	84870.912	NIST/VALD
5530.094	5529.937	Fe II	-1.810	54273.656	NIST/VALD
5530.494	5530.337	Fe II	-0.650	85048.655	NIST/VALD
5532.243	5532.086	Fe II	-0.100	84870.912	NIST/VALD
5534.996	5534.839	Fe II	-2.900	26170.181	NIST/VALD
5535.051	5534.894	Fe II	-0.440	85048.655	NIST/VALD
5544.358	5544.201	Fe II	-0.230	85679.757	NIST/VALD
5544.915	5544.758	Fe II	0.140	84863.380	NIST/VALD
5548.388	5548.231	Fe II	-0.540	85679.757	NIST/VALD
5549.157	5549.000	Fe II	-0.190	84870.912	NIST/VALD
5555.067	5554.910	Fe II	-0.460	85680.279	NIST/VALD
5556.675	5556.517	Mn II	-2.350	49820.865	NIST/VALD
5559.205	5559.047	Mn II	-1.310	49885.389	NIST/VALD

Table 10 continued on next page

Table 10 (*continued*)

λ_{obs} (Å)	λ_{lab} (Å)	Species	$\log gf$	E_{low}	Ref.
5561.296	5561.138	Fe II	-0.580	84863.380	NIST/VALD
5561.590	5561.432	Mn II	-2.420	49893.458	NIST/VALD
5561.682	5561.524	Fe II	-0.560	85048.655	NIST/VALD
5563.546	5563.388	Fe II	-0.550	85728.844	NIST/VALD
5567.993	5567.835	Fe II	-1.870	54283.234	NIST/VALD
5569.232	5569.074	Cr II	0.860	87688.592	NIST/VALD
5569.775	5569.617	Cr II	0.710	87946.692	NIST/VALD
5570.697	5570.539	Mn II	-1.430	49820.865	NIST/VALD
5578.070	5577.912	Fe II	-0.110	85462.908	NIST/VALD
5578.166	5578.008	Fe II	-0.620	85495.368	NIST/VALD
5578.284	5578.126	Mn II	-1.400	49893.458	NIST/VALD
5578.381	5578.223	Cr II	0.600	87946.692	NIST/VALD
5580.084	5579.926	Fe II	-0.500	85728.844	NIST/VALD
5581.783	5581.625	Fe II	-0.520	85495.368	NIST/VALD
5587.000	5586.842	Cr II	0.930	88003.158	NIST/VALD
5587.218	5587.060	Fe II	0.460	106900.723	NIST/VALD
5587.272	5587.114	Fe II	-1.990	54275.649	NIST/VALD
5588.191	5588.033	Fe II	-0.740	85495.368	NIST/VALD
5588.379	5588.221	Fe II	0.160	85462.908	NIST/VALD
5592.417	5592.258	Mn II	-2.430	49893.458	NIST/VALD
5606.310	5606.151	S II	0.120	110766.562	NIST/VALD
5615.802	5615.643	Fe I	0.050	26874.550	NIST/VALD
5620.790	5620.631	Cr II	-1.390	52321.189	NIST/VALD
5639.637	5639.477	Si II	-0.130	117176.229	NIST/VALD
5639.844	5639.684	Fe II	-0.650	85679.757	NIST/VALD
5640.132	5639.972	S II	0.260	113461.537	NIST/VALD
5640.493	5640.333	S II	-0.040	110508.706	NIST/VALD
5644.029	5643.869	Fe II	-1.350	61726.068	NIST/VALD
5645.550	5645.390	Fe II	0.190	85184.772	NIST/VALD
5646.387	5646.227	Fe II	-0.580	85679.757	NIST/VALD
5649.060	5648.900	Fe II	-0.170	85184.772	NIST/VALD
5651.684	5651.524	Fe II	-0.610	85728.844	NIST/VALD

Table 10 continued on next page

Table 10 (*continued*)

λ_{obs} (Å)	λ_{lab} (Å)	Species	$\log gf$	E_{low}	Ref.
5651.735	5651.575	Fe II	-0.580	85728.806	NIST/VALD
5655.507	5655.347	Fe II	-0.550	85728.844	NIST/VALD
5658.981	5658.821	Fe II	-0.720	85188.279	NIST/VALD
5660.145	5659.985	S II	-0.220	110313.403	NIST/VALD
5660.301	5660.141	Fe II	-0.420	85728.844	NIST/VALD
5663.085	5662.924	Y II	0.200	15679.418	NIST/VALD
5669.721	5669.560	Si II	0.290	114529.145	NIST/VALD
5675.413	5675.252	Fe II	-0.580	85495.368	NIST/VALD
5688.971	5688.810	Si II	0.130	114414.585	NIST/VALD
5691.157	5690.996	Fe II	-0.180	86124.348	NIST/VALD
5701.532	5701.370	Si II	-0.060	114327.152	NIST/VALD
5706.582	5706.420	Si II	-0.240	114264.567	NIST/VALD
5726.715	5726.553	Fe II	-0.040	86416.369	NIST/VALD
5738.055	5737.892	Fe II	-0.310	86599.791	NIST/VALD
5746.729	5746.566	Fe II	-0.400	85728.844	NIST/VALD
5748.037	5747.874	Fe II	-2.950	44933.149	NIST/VALD
5751.649	5751.486	Fe II	-0.610	85728.844	NIST/VALD
5752.393	5752.230	Mn II	-1.930	53700.393	NIST/VALD
5780.292	5780.128	Fe II	0.420	86124.348	NIST/VALD
5780.499	5780.335	Fe II	-0.330	86416.369	NIST/VALD
5783.787	5783.623	Fe II	0.370	86416.369	NIST/VALD
5784.609	5784.445	Fe II	0.150	86599.791	NIST/VALD
5790.824	5790.660	Hg I	0.710	54068.780	NIST/VALD
5800.618	5800.454	Si II	-0.100	116982.652	NIST/VALD
5802.936	5802.771	Fe II	-0.450	86124.348	NIST/VALD
5806.896	5806.731	Si II	-0.110	116861.685	NIST/VALD
5811.799	5811.634	Fe II	-0.610	86124.348	NIST/VALD
5813.834	5813.669	Fe II	-2.700	44929.533	NIST/VALD
5813.979	5813.814	Fe II	-1.840	62689.872	NIST/VALD
5826.453	5826.288	Mn II	-1.760	53781.049	NIST/VALD
5830.509	5830.344	Fe II	-0.200	86710.909	NIST/VALD
5835.661	5835.496	Fe II	-2.700	47674.729	NIST/VALD

Table 10 continued on next page

Table 10 (*continued*)

λ_{obs} (Å)	λ_{lab} (Å)	Species	$\log gf$	E_{low}	Ref.
5839.155	5838.989	Fe II	-0.600	87471.787	NIST/VALD
5842.461	5842.295	Fe II	-0.330	86599.791	NIST/VALD
5852.654	5852.488	Ne I	-0.450	135888.715	NIST/VALD
5854.354	5854.188	Fe II	-0.110	86599.791	NIST/VALD
5859.778	5859.612	Fe II	-0.660	86599.759	NIST/VALD
5867.594	5867.428	Si II	-0.040	116982.652	NIST/VALD
5868.610	5868.444	Si II	0.410	117176.229	NIST/VALD
6024.351	6024.180	P II	0.140	86743.961	NIST/VALD
6034.211	6034.040	P II	-0.220	86597.549	NIST/VALD
6040.531	6040.360	Mn II	-2.140	55700.654	NIST/VALD
6043.291	6043.120	P II	0.420	87124.598	NIST/VALD
6045.640	6045.469	Fe II	-2.500	50075.919	NIST/VALD
6049.612	6049.440	Fe II	-0.370	86416.369	NIST/VALD
6053.640	6053.468	Cr II	-2.150	38269.568	NIST/VALD
6061.140	6060.968	Fe II	-1.690	62945.045	NIST/VALD
6069.841	6069.669	Fe II	-0.500	86416.369	NIST/VALD
6071.592	6071.420	Fe II	-0.250	86416.369	NIST/VALD
6074.510	6074.338	Ne I	-0.480	134459.290	NIST/VALD
6084.276	6084.103	Fe II	-3.900	25805.326	NIST/VALD
6089.804	6089.631	Cr II	-1.450	52321.189	NIST/VALD
6096.336	6096.163	Ne I	-0.300	134459.290	NIST/VALD
6103.676	6103.503	Fe II	-2.320	50143.489	NIST/VALD
6105.453	6105.280	Mn II	-0.500	83529.522	NIST/VALD
6122.608	6122.434	Mn II	0.950	82136.483	NIST/VALD
6122.984	6122.810	Mn II	0.080	82136.483	NIST/VALD
6123.592	6123.418	Mn II	-2.110	54942.486	NIST/VALD
6126.037	6125.863	Mn II	0.780	82144.600	NIST/VALD
6126.392	6126.218	Mn II	0.230	82144.600	NIST/VALD
6128.908	6128.734	Mn II	0.590	82151.290	NIST/VALD
6129.207	6129.033	Mn II	0.210	82151.290	NIST/VALD
6130.970	6130.796	Mn II	0.350	82155.981	NIST/VALD
6131.190	6131.016	Mn II	0.050	82155.981	NIST/VALD

Table 10 continued on next page

Table 10 (*continued*)

λ_{obs} (Å)	λ_{lab} (Å)	Species	$\log gf$	E_{low}	Ref.
6132.097	6131.923	Mn II	0.050	82158.392	NIST/VALD
6143.237	6143.063	Ne I	-0.100	134041.838	NIST/VALD
6145.785	6145.611	Fe II	-0.350	89444.458	NIST/VALD
6147.908	6147.734	Fe II	-2.800	31364.454	NIST/VALD
6149.405	6149.231	Fe II	-2.800	31368.453	NIST/VALD
6150.047	6149.873	Hg II	0.330	95714.001	NIST/VALD
6156.136	6155.961	O I	-1.360	86625.757	NIST/VALD
6156.155	6155.980	O I	-1.010	86625.757	NIST/VALD
6156.164	6155.989	O I	-1.120	86625.757	NIST/VALD
6156.912	6156.737	O I	-1.490	86627.777	NIST/VALD
6156.930	6156.755	O I	-0.900	86627.777	NIST/VALD
6156.945	6156.770	O I	-0.690	86627.777	NIST/VALD
6158.284	6158.109	Cr II	0.890	89325.907	NIST/VALD
6158.347	6158.172	O I	-1.000	86631.453	NIST/VALD
6158.355	6158.180	O I	-0.410	89511.404	NIST/VALD
6158.355	6158.180	Cr II	1.000	86631.453	NIST/VALD
6158.796	6158.621	Cr II	0.690	89172.659	NIST/VALD
6168.523	6168.348	Mn II	-1.960	55119.930	NIST/VALD
6175.310	6175.135	Fe II	-2.090	50187.824	NIST/VALD
6175.627	6175.452	Fe II	-1.980	62048.230	NIST/VALD
6179.553	6179.378	Fe II	-2.800	44915.056	NIST/VALD
6199.367	6199.191	Fe II	-2.940	44917.017	NIST/VALD
6215.124	6214.948	Fe II	-0.110	89625.937	NIST/VALD
6233.718	6233.541	Fe II	-2.830	44231.449	NIST/VALD
6238.552	6238.375	Fe II	-2.800	31364.454	NIST/VALD
6239.787	6239.610	Si II	0.180	103556.025	NIST/VALD
6239.837	6239.660	Si II	0.020	103556.156	NIST/VALD
6240.117	6239.940	Fe II	-3.600	31368.453	NIST/VALD
6241.116	6240.939	Mn II	-2.000	55369.961	NIST/VALD
6243.537	6243.360	Al II	0.660	105470.928	NIST/VALD
6247.531	6247.354	Fe II	-2.170	50078.965	NIST/VALD
6247.736	6247.559	Fe II	-2.400	31387.979	NIST/VALD

Table 10 continued on next page

Table 10 (*continued*)

λ_{obs} (Å)	λ_{lab} (Å)	Species	$\log gf$	E_{low}	Ref.
6249.084	6248.907	Fe II	-2.780	44449.216	NIST/VALD
6266.673	6266.495	Ne I	-0.360	134818.641	NIST/VALD
6267.275	6267.097	Mn II	-1.880	55369.961	NIST/VALD
6331.635	6331.455	Fe II	-0.400	89446.891	NIST/VALD
6332.135	6331.955	Fe II	-2.070	50142.810	NIST/VALD
6334.608	6334.428	Ne I	-0.310	134041.838	NIST/VALD
6346.917	6346.737	Mg II	0.030	93310.590	NIST/VALD
6347.142	6346.962	Mg II	-0.130	93311.112	NIST/VALD
6347.280	6347.100	Si II	0.150	65500.472	NIST/VALD
6357.342	6357.162	Fe II	0.240	87985.668	NIST/VALD
6362.650	6362.470	Fe II	-0.490	87985.668	NIST/VALD
6370.489	6370.308	Mn II	-1.570	55700.654	NIST/VALD
6371.541	6371.360	Si II	-0.080	65500.472	NIST/VALD
6371.899	6371.718	Fe II	-1.690	62171.625	NIST/VALD
6372.607	6372.426	Fe II	-0.320	88720.993	NIST/VALD
6375.978	6375.797	Fe II	-0.010	88189.068	NIST/VALD
6383.172	6382.991	Ne I	-0.230	134459.290	NIST/VALD
6383.911	6383.730	Fe II	-2.400	44784.787	NIST/VALD
6385.639	6385.458	Fe II	-2.700	44784.787	NIST/VALD
6402.430	6402.248	Ne I	0.350	134041.838	NIST/VALD
6405.261	6405.079	Fe II	-0.070	89624.335	NIST/VALD
6411.186	6411.004	Mn II	-1.450	66540.741	NIST/VALD
6414.440	6414.258	Fe II	-0.210	89119.451	NIST/VALD
6417.112	6416.930	Fe II	-2.900	31387.979	NIST/VALD
6425.905	6425.723	Fe II	-0.010	88853.537	NIST/VALD
6432.859	6432.677	Fe II	-3.500	23317.635	NIST/VALD
6434.002	6433.820	Fe II	-2.700	50157.476	NIST/VALD
6443.141	6442.958	Fe II	-2.700	44753.818	NIST/VALD
6446.520	6446.337	Mn II	0.340	98423.833	NIST/VALD
6446.591	6446.408	Fe II	-2.080	50187.824	NIST/VALD
6451.278	6451.095	Fe II	0.020	89333.971	NIST/VALD
6453.783	6453.600	O I	-1.290	86625.757	NIST/VALD

Table 10 continued on next page

Table 10 (*continued*)

λ_{obs} (Å)	λ_{lab} (Å)	Species	$\log gf$	E_{low}	Ref.
6454.623	6454.440	O I	-1.070	86627.777	NIST/VALD
6455.337	6455.154	Fe II	-0.350	88189.068	NIST/VALD
6456.163	6455.980	O I	-0.920	86631.453	NIST/VALD
6456.564	6456.381	Fe II	-2.200	31483.198	NIST/VALD
6457.058	6456.875	Ca II	0.150	68057.061	NIST/VALD
6457.058	6456.875	Ca II	0.050	68057.061	NIST/VALD
6457.458	6457.275	Mn II	-1.570	52385.713	NIST/VALD
6460.128	6459.945	P II	0.030	88196.735	NIST/VALD
6462.823	6462.640	Fe II	0.230	89124.267	NIST/VALD
6600.213	6600.026	Fe II	0.300	88853.537	NIST/VALD
6609.442	6609.255	Mn II	-2.010	55369.961	NIST/VALD
6615.134	6614.946	Fe II	-0.310	89624.335	NIST/VALD
6622.162	6621.974	Fe II	0.050	88853.537	NIST/VALD
6625.190	6625.002	Fe II	-0.440	89124.267	NIST/VALD
6627.424	6627.236	Fe II	-1.770	58666.197	NIST/VALD
6647.875	6647.687	Fe II	-0.500	87985.668	NIST/VALD
6660.709	6660.520	Si II	0.160	116978.384	NIST/VALD
6664.658	6664.469	Fe II	-0.440	89119.451	NIST/VALD
6672.069	6671.880	Si II	0.410	117178.064	NIST/VALD
6677.518	6677.329	Fe II	-1.880	58628.442	NIST/VALD
6678.340	6678.151	He I	0.329	171134.897	NIST
6678.466	6678.277	Ne I	-0.110	135888.715	NIST/VALD
6679.024	6678.835	Fe II	-0.490	88157.178	NIST/VALD
6682.572	6682.383	Mn II	-2.080	55700.654	NIST/VALD
6771.095	6770.903	Fe II	-0.360	90300.626	NIST/VALD
6792.731	6792.538	Fe II	-0.110	90487.827	NIST/VALD
6801.921	6801.728	Fe II	1.000	114103.255	NIST/VALD
6803.329	6803.136	Fe II	-0.280	90593.510	NIST/VALD
6811.557	6811.364	Fe II	0.830	109618.808	NIST/VALD
6817.474	6817.281	Fe II	1.110	109594.612	NIST/VALD
6818.643	6818.450	Si II	-0.520	103860.741	NIST/VALD
6820.179	6819.986	Fe II	0.960	109925.305	NIST/VALD

Table 10 continued on next page

Table 10 (*continued*)

λ_{obs} (Å)	λ_{lab} (Å)	Species	$\log gf$	E_{low}	Ref.
6828.757	6828.563	Fe II	0.130	90648.656	NIST/VALD
6829.994	6829.800	Si II	-0.260	103885.252	NIST/VALD
6841.857	6841.663	Fe II	0.440	90593.510	NIST/VALD
6851.623	6851.429	Fe II	-0.300	90640.587	NIST/VALD
6858.048	6857.854	Fe II	0.610	90487.827	NIST/VALD
6860.486	6860.291	Fe II	-0.320	90300.626	NIST/VALD
6862.706	6862.511	Fe II	0.580	90300.626	NIST/VALD

ALL AUTHORS AND AFFILIATIONS

R. MONIER¹,LESIA, UMR 8109, Observatoire de Paris et Université Pierre et Marie Curie Sorbonne Universités, place J. Janssen,
Meudon, France.E.GRIFFIN²,

Dominion Astrophysical Observatory, 5071 West Saanich Road, Victoria, BC, V9E 2E7, Canada

M. GEBRAN³,

Department of Physics and Astronomy, Notre Dame University-Louaize, PO Box 72, Zouk Mikael, Lebanon.

T. KILIÇOĞLU⁴,

Department of Astronomy and Space Sciences, Faculty of Science, Ankara University, 06100, Turkey.

T.MERLE⁵,Institut d'Astronomie et d'Astrophysique, Université Libre de Bruxelles, CP 226, Boulevard du Triomphe, 1050
Brussels, Belgium

AND

F. ROYER⁶.

GEPI, Observatoire de Paris, place J. Janssen, Meudon, France.